Vanessa Angst-Nicollier

Moisture Induced Stresses in Glulam

Effect of Cross Section Geometry and Screw Reinforcement

Thesis for the degree of Philosophiae Doctor

Trondheim, February 2012

Norwegian University of Science and Technology
Faculty of Engineering Science and Technology
Department of Structural Engineering

NTNU – Trondheim
Norwegian University of
Science and Technology

NTNU
Norwegian University of Science and Technology

Thesis for the degree of Philosophiae Doctor

Faculty of Engineering Science and Technology
Department of Structural Engineering

ISBN 978-82-471-3562-4 (printed ver.)
ISBN 978-82-471-3563-1 (electronic ver.)
ISSN 1503-8181

Doctoral theses at NTNU, 2012:139

Printed by NTNU-trykk

PREFACE

This doctoral thesis is submitted to the Norwegian University of Science and Technology (NTNU) for the degree Philosophiae Doctor (PhD). The work was carried out at the Department of Structural Engineering, Faculty of Engineering Science and Technology at NTNU in Trondheim, Norway.

Supervisor has been Professor Kjell Arne Malo.

The project started in January 2008 and completed for submission in February 2012, including 7 months of maternity leave and 7 months of part-time work (50%).

The author, Vanessa Angst, declares that this thesis and the work presented in it are her own and have been generated by her as the result of original research while in candidature for the degree of Philosophiae Doctor at NTNU. The thesis contains no material that was previously submitted for a degree at this university or any other institution.

ACKNOWLEDGEMENTS

This work has been funded by the Research Council of Norway through the KMB project *Moisture induced effects on screws and threaded bar connections in timber structures* (Grant no 186821/I10). It has moreover been supported by industrial partners, such as the Norwegian organization *Treindustrien* and the Norwegian company *Christiania Spigerverk AS* as well as the *Norwegian Public Road Administration*. Their financial contributions making the project possible are kindly acknowledged.

I would like to thank my supervisor, Professor Kjell Arne Malo, for encouraging me and giving me the opportunity to work on this PhD project, as well as for valuable discussions, critical manuscript readings and for taking care of administrative issues.

I am also grateful to all the people helping me in my struggle to obtain a fully functional climate chamber, in particular Kjell Ove Slutås for his initiative, Ove Loraas and Ole Aunrønning (from the Building and Material Technology group) for providing me other climate chambers as interim solutions. I would also like to thank the other PhD students at the Department of Structural Engineering for a pleasant social environment.

I would like to express my deepest gratitude to my husband, Ueli, for his support throughout the project, for his inspiring inputs to my research, and for reading my manuscripts. Without his encouragement and help, this thesis would not have been accomplished. Finally, I would like to thank my lovely daughter, Elin Hanna, for giving me so much joy and laughter, and also my unborn child, for unintentionally pushing me on finishing my thesis.

SUMMARY

It is well known that timber structures are affected by the climate to which they are exposed. Changes in relative humidity of the surroundings of a structural member such as a glulam beam lead to an inhomogeneous moisture distribution in the cross section. Owing to hygroexpansion being internally restrained, this results in moisture induced stresses perpendicular to grain. A cross section subjected to one-dimensional wetting exhibits compressive stresses at the border and tensile stresses in the centre, whereas in a drying case, the opposite applies. It was in the literature reported that the stresses established during wetting are generally larger than corresponding stresses during drying. Moreover, the tensile stresses were found to exceed the characteristic tensile strength of timber perpendicular to grain. This led to an increasing interest in moisture induced stresses in timber, which was also underpinned by the occurrence of several failures of timber structures during the last years, where tension perpendicular to grain was one of the most common failure causes.

This thesis presents a state of the art on moisture induced stresses in glulam, complemented with own findings. These are covered in detail in the appended papers. The first objective was to find a suitable model to describe moisture induced stresses, in particular with respect to mechanosorption. A review of existing models led to the conclusion that the selection of correct material parameters is more critical to obtain reliable results than the formulation of the mechanosorption model. A series of laboratory tests was thus performed in order to determine the parameters required for the model and to experimentally measure moisture induced stresses in glulam subjected to one-dimensional wetting/drying. Special attention was paid to using glulam from the same batch for all the experimental measurements in order to calibrate the numerical model reliably.

The results of the experiments confirmed that moisture induced stresses are larger during wetting than during drying, and that the tensile stresses could clearly exceed the characteristic tensile strength perpendicular to grain. Nevertheless, experimental approaches are only capable of determining average stresses (average over cross section height). Thus, in a subsequent step, a numerical model was used to calculate local moisture induced stresses. It was shown that the arising stresses depend highly on the annual ring configuration of the glulam cross section. Moreover, local stresses can be significantly larger than

average stresses. It was also shown that the stresses can be reduced by optimising the geometrical configuration of the cross section, namely by using laminates without piths.

Furthermore, the use of self-tapping screws as a measure to increase the load bearing capacity of glulam beams subjected to climate variations was studied. It was shown that this timber reinforcement method was able to significantly reduce the large tensile stresses arising during wetting in the cross section centre, while during drying, it increased only slightly the tensile stresses at the border. The numerical model was further used to study the effect of the screw distance, cross section width, and pith location in the laminates during wetting. It was found that all three factors considerably influence the stresses. The results indicated, however, that a significant reduction of tensile stresses is possible with practical screw distances.

TABLE OF CONTENTS

LIST OF PAPERS

The thesis includes the following appended papers. They are referred to by name and year.

1 Moisture induced stresses perpendicular to the grain in glulam: Review and evaluation of the relative importance of models and parameters

Vanessa Angst and Kjell A. Malo
Holzforschung 64 (2010) 609–617

2 The effect of climate variations on glulam – an experimental study

Vanessa Angst and Kjell A. Malo
European Journal of Wood and Wood Products (2012)
DOI 10.1007/s00107-012-0594-y

3 Moisture induced stresses in glulam cross sections during wetting exposures

Vanessa Angst and Kjell A. Malo
Submitted to Wood Science and Technology (2011)

4 Effect of self-tapping screws on moisture induced stresses in glulam

Vanessa Angst and Kjell A. Malo
Submitted to Engineering Structures (2012)

Declaration of authorship for papers 1-4

Vanessa Angst planned and conducted all the experiments, did the numerical simulations, evaluated the results, and wrote the appended papers. The co-author contributed with constructive criticism that increased the scientific quality of the publications.

SYMBOLS, INDICES AND ABBREVIATIONS

Symbol	Meaning	Dimension
α	Hygroexpansion coefficient	-
D	Diffusion coefficient	m^2/s
E	Modulus of elasticity	MPa
ε_c	Creep strain	-
ε_e	Elastic strain	-
ε_{ms}	Mechano-sorptive creep strain	-
ε_s	Linear shrinkage-swelling strain	-
ε_{mean}	Mean released strain	-
H	Cross section height	mm
k_{DOL}	Stress level at failure (ratio of failure load to the short-term strength)	-
k_{mod}	Modification factor for DOL and MC	-
L	Specimen length (in longitudinal direction)	mm
Ψ	Load combination factor	-
σ	Stress	MPa
S	Surface emission coefficient	m/s
t_F	Time to failure	days
u	Moisture content	%
u_{eq}	Equilibrium moisture content	%
u_{surf}	Surface moisture content	%
W	Cross section width	mm

Indices	Meaning
L	longitudinal direction
mean	mean value
R	radial direction
T	tangential direction

Abbreviation	Meaning
d	Days
DOL	Duration of load
EMC	Equilibrium moisture content
FSP	Fibre saturation point
GEV	Generalised extreme value distribution
MC	Moisture content
MiS	Moisture induced stresses
MOE	Modulus of elasticity
RH	Relative humidity

1 INTRODUCTION

1.1 Background

Timber is the oldest building material. It has been used since ancient time for structural purposes such as boat constructions, housings and bridges. Timber has been extensively used, due to its workability, its tradition and particularly due to its availability almost everywhere. Japan and Scandinavia are regions with a long tradition of timber construction, where even timber structures from the seventh and twelfth century, respectively, are still existing (Thelandersson 2003). Before modern structural materials became available, timber was the predominant material used in bridge construction. One of the oldest still existing timber bridges is the Chapel Bridge in Lucerne, Switzerland, built in 1333. These examples show that if timber structures are properly designed and maintained, they have excellent durability (Thelandersson 2003).

Today, timber as a structural material is used in a wide variety of applications, such as single family houses, large scale residential and industrial buildings, as well as bridges. Timber has several advantages compared to other building materials: It is environmentally friendly, easily recyclable and exhibits very low energy consumption during production (Thelandersson 2003). Moreover, timber has a high strength-to-weight ratio, which facilitates production, transport and erection and which contributes to a good performance of timber buildings during earthquakes (Karacabeyli and Popovski 2003). In addition, timber is aesthetically pleasing, thus offering great possibilities in architectural design.

Due to the fact that the maximum dimension of solid timber is naturally limited, engineered wood products were developed to extend the spans for timber structures. Glued laminated timber (glulam) was one of the first engineered wood products, which is produced by gluing together timber laminates to form larger members. Glulam is still highly competitive in modern, large-scale constructions, as it can be produced in almost any shape and size (Thelandersson 2003; Glulam handbook 2003).

The increasing environmental awareness and the trend towards using ecologically sound materials in construction lead to a growing popularity of timber. However, several failures of wooden roof structures that occurred in central and northern Europe in the last years negatively affected the image of timber as a construction

material. In the cases, where these failures led to fatalities and accordingly received large media attention, weaknesses related to the material timber itself were believed to be the cause (Frühwald et al. 2007). The truth is though that almost without exception, structural failures were due to human errors. Failure analyses showed that a majority of mistakes were related to incorrect assumptions or insufficient consideration of loads and actions. In many cases, the inadequate consideration of climatic effects led to intolerable effects for timber structures. The most common problem is cracks perpendicular to grain as arising from moisture induced stresses (Frühwald et al. 2007; Frese and Blass 2007).

In the past years, studies were performed to investigate the effect of climate variations on glulam members, e.g. (Aicher and Dill-Langer 1997; Jönsson 2005b). These have shown that significant moisture induced stresses perpendicular to grain develop, which increase the risk for cracking. There is a need for increasing the knowledge about moisture effects, in order to properly take them into account in design standards and thus in the design of safe timber structures.

1.2 Objectives

The objective of the thesis was to approach the problem of moisture induced stresses perpendicular to grain in glulam by means of the following tasks:

1. **Numerical model for moisture induced stresses**
   Review the literature and find a suitable model to describe moisture induced stresses, in particular with respect to mechanosorption

2. **Experiments to calibrate the numerical model**
   Experimentally measure moisture induced stresses in glulam specimens; measure the material parameters required for the numerical model

3. **Main parameters and local stresses**
   Use the experimental results and the model to identify the main parameters that determine moisture induced stresses; focus in particular on local stresses in addition to stresses averaged over the cross section height

4. **Reinforcement screws**
   Assess the suitability of self-tapping screws as means to mitigate cracking perpendicular to grain owing to moisture induced stresses

1.3 Limitations

In the experiments and numerical simulations only glulam made of Norway spruce (Picea Abies) is considered. The studied specimens are on a macro scale level, thus including various defects such as knots, fibre inclination, reaction wood and resin pockets. The property and the impact of these defects as well as of the microstructure of the wood are not treated. Effects from varying moisture contents resulting from varying RH levels are studied, while the effect of fluctuating temperature is disregarded, as well as possible hysteresis effects. Other effects, such as size and duration of load effects are addressed in the theoretical and review part, but are neglected in the experiments and simulations performed by the author. Similarly, time-dependent creep is ignored.

2 GLULAM AND SOME OF ITS PROPERTIES

2.1 Glulam manufacture

The dimension of structural timber sawn from logs is naturally limited. To overcome these limitations timber beams are glued together to form larger members, commonly referred to as glued laminated timber or simply glulam.

In principle, any wood species can be used for glulam production, but in practice mainly softwoods (spruce) are used, as hardwoods are often associated with difficulties in gluing. Laminates of a certain thickness are sawn from the log and dried to uniform moisture content, before being strength graded. The strength grading allows a glulam cross section to be built up of laminates with the same strength (homogeneous glulam), or with higher quality in the outer laminates, where stresses normally are highest (combined glulam). The laminates are joined lengthwise by means of finger-joints and cut to the required length. The laminates are then placed on top of each other, with their grain in the longitudinal direction of the member, and glued together to form the desired cross section. To reduce internal stresses the laminates are placed in such a way that the core sides are identically oriented throughout the cross section, while the outermost laminates are always turned with the core side outwards (Fig. 1).

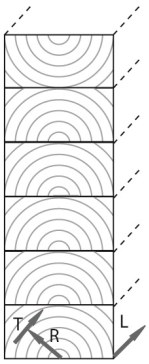

Fig. 1 Orientation of laminates in a glulam beam

The laminate package or glulam member is then lifted over to benches where the necessary pressure is applied. When pressure is applied, the laminates may be bent to produce cambered or curved forms. Theoretically, glulam can be manufactured in almost any desired shape and size. In practice, however, the size is limited for reasons related to transportation, size of the production area and open time of the adhesive. Glulam is suitable for a wide variety of uses, but owing to its high strength-to-weight ratio it is especially appropriate for the construction of halls with large spans. Further information about glulam can be found a.o. in the Glulam handbook (2003).

2.2 Moisture content and dimensional changes

The moisture content (MC) is defined as the weight of water contained in the wood relative to the weight of dry wood. Water contained in wood may be present in two forms, as free water (in the cell lumen) or as bound water (bound in cell walls). When wood is dried, free water is first lost. The moisture content, when the cell walls are saturated with water but no free water is present in the cell lumen, is called fibre saturation point (FSP). Generally, the fibre saturation point ranges from 25-35%, where 30% is a reasonable average for most practical purposes (Glass and Zelinka 2010).

The laminations used in glulam components are dried individually to a wood moisture content of about 12 % before gluing. Under different climatic conditions the moisture content of the glulam member will in time adjust itself to the surrounding relative humidity (RH) and to the temperature. The moisture content which is in equilibrium with the relative humidity and the temperature, is termed the equilibrium moisture content (EMC) and depends on whether it is reached as a result of desorption or adsorption. This phenomenon is known as hysteresis. As a consequence of seasonal changes in the climate, the moisture content in a structure will vary continuously.

Glulam, like other timber materials, exhibits dimensional changes as a result of moisture variations (below fibre saturation): Glulam shrinks when the moisture content decreases and swells when it increases. These dimensional changes or movements are not equal in all directions. Often tangential changes are about twice the radial changes, whereas longitudinal changes are negligible (Glass and Zelinka 2010). To quantify these movements, dimensional changes are recorded over a range of relative humidities or moisture contents. The linear relationship

between change in length *Δl* and change in moisture content *Δu* can be expressed with the following equation:

$\Delta l = \alpha \cdot \Delta u$, where α is the hygroexpansion coefficient. (1)

The present author has performed measurements and calculations concerning the hygroexpansion coefficient in tangential and radial direction, reported in Angst and Malo (2012a) and Appendix A. In the first reference, glulam specimens (Fig. 1) were seasoned in either dry (40% RH) or wet climate (90% RH) before being cut into slices along the height. The slices were exposed to wetting or drying, respectively, while the change in lengths and the moisture contents were measured. The relation between change in lengths and change in moisture contents resulted in effective hygroexpansion coefficients along the height of the slices. By means of a numerical model, the effective hygroexpansion coefficients could be divided in a tangential and a radial hygroexpansion coefficient. In contrast to the literature, the present author found different coefficients for the case of wetting and drying. Additional measurements and calculations of hygroexpansion coefficients reported in Appendix A revealed the same: Different coefficients were obtained for wetting and drying. Moreover, the individual coefficients were similar in both studies (Table 1), although these were determined on different specimens subjected to different climate variations. The results were in the range of literature values for the same type of glulam, or glulam lamination being Norway spruce (Picea abies), respectively. Table 1 shows that the coefficients obtained by different authors vary considerably although they were recorded on the same material. The relation between tangential and radial coefficient, however, is very similar, being approximately 2:1.

Table 1 Hygroexpansion coefficients for Norway spruce (Picea abies)

	Tangential direction	Radial direction
Present author (Angst and Malo 2012a)	0.32 / 0.26 wetting / drying	0.15 / 0.14 wetting / drying
Present author (Appendix A)	0.34 / 0.28 wetting / drying	0.17 / 0.14 wetting / drying
Jönsson (2005b)	0.22	0.11
Ormarsson (1999)	0.35	0.19
Dinwoodie (2000)	0.15	0.07

In order to minimize dimensional changes of glulam members in service, the members are dried to a moisture content close to the equilibrium moisture content likely to be encountered in service before assembly. Otherwise, hindered shrinkage deformations can occur which may, for example, cause tension perpendicular to grain and lead to a premature failure.

2.3 Strength and stiffness

Glulam components achieve in general greater strength and stiffness properties than corresponding dimensions of ordinary structural timber, because the variability in strength within the member is smaller. Strength reducing defects of solid wood are either removed during manufacture or more uniformly distributed in the finished glulam member so that each defect has less importance compared to solid wood. This can be explained by the so-called “lamination effect”, which means that the load sharing between laminations allows locally weak zones to redistribute stress to adjacent stronger regions (Glulam handbook 2003). The strength of ordinary structural timber, on the other hand, corresponds to the strength of the weakest cross section, usually at the location of a knot or similar weaknesses.

Strength and stiffness properties vary considerably with respect to the material direction. Due to the orientation of the wood fibres, strength and stiffness are much higher in the longitudinal direction than in the transverse direction. The properties differ also in the transverse direction, between radial and tangential direction. In engineering design, however, no distinction is made between tangential and radial direction, and thus only parameters parallel and perpendicular to the grain are provided. A glulam beam is composed of several laminates, each with a different annual ring pattern, and thus different material orientations (Fig. 1). Thereby, the origin of the material orientations is located in the pith of each laminate, i.e. the centre of the annual rings. This non-homogeneity of glulam results in irregular stress distributions within the cross section upon loading. A standard glulam cross section which is subjected to uniformly distributed tensile loading of 0.2 MPa in vertical direction reveals two issues (Aicher and Dill-Langer 1997): The horizontal distribution of vertical stresses at the lower edge of one board located in the centre of the cross section exhibits a pronounced stress peak near mid-width (Fig. 2). This peak is believed to result from the differences between tangential and radial stiffness and also from a so-called shear coupling effect. The vertical stress distribution along the centre-line (mid-width) shows an increase of the stress towards the gluelines (Fig. 2), due

to the breaking of the polar material symmetry at the interfaces of the glued laminations. The maximum stresses are approximately 2.5 times the applied uniform tensile stress on the cross section. A similar study involving glulam cross sections with different annual ring patterns obtained maximum stresses which were between 2.5 and 4.4 times the applied uniform tensile stress, depending on the geometrical configuration of the cross section (Aicher and Dill-Langer 2005). An analogous influence of the cross section configuration was also found in curved glulam beams which were subjected to an opening bending moment.

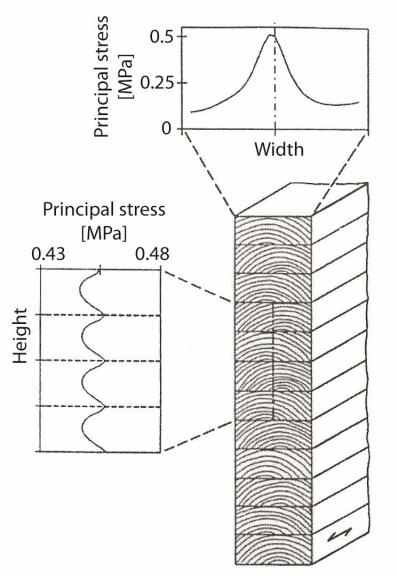

Fig. 2 Stress distributions in a glulam cross section due to uniaxial tensile loading in vertical direction (Aicher and Dill-Langer 1997)

In addition, the mechanical properties are also influenced by other effects, such as moisture content, duration of loading (DOL), and cross section size. The latter is commonly referred to as “size effect” or “volume effect” and means that large beams tend to have lower strength than small beams. Generally, this is explained by “Weibull’s weakest link theory”, a stochastic phenomenon, which states, that the probability of encountering a defect able to cause failure in a beam increases with an increase in the volume of the beam. However, this size or volume effect is believed to also be caused by a deterministic phenomenon, namely by stress

concentrations (Astrup et al. 2007). These stress concentrations, which cause lower strength, arise from the cylindrical orthotropic structure of glulam.

2.4 Tensile strength perpendicular to grain

Glulam has a very low tensile strength perpendicular to grain, which is also influenced by the different effects mentioned above. In the following, the different effects will be discussed specifically with regard to tensile strength perpendicular to grain, as this property is relevant for the present research. The main observations and results from literature concerning tensile strength of glulam perpendicular to grain will be presented.

Effect of MC level: Tensile strength increases with decreasing level of MC

Tensile tests performed on glulam specimens, which have been seasoned in different climates, show a clear effect of the MC level. The higher the MC in the glulam is, the lower is the corresponding tensile strength. Note, that in the present section only specimens with constant MC over the cross sections are regarded.

The following results are from Jönsson and Thelandersson (2003). They performed tensile tests perpendicular to grain on thin glulam specimens (*W*H*L* = 90*270*16 mm^3), which were seasoned in 40%, in 60%, or in 80% RH prior to testing. Figure 3 shows the mean ultimate tensile strength of specimens seasoned in 40%, 60% and 80% RH that correspond to equilibrium MC of approx. 9, 11, and 16%, respectively. It can be noticed that the strength in a dry stage (40% RH) is 60% higher than in a wet stage (80% RH).

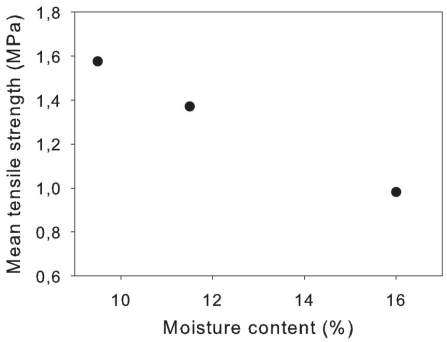

Fig. 3 Effect of moisture content on tensile strength perpendicular to grain (based on values from Jönsson and Thelandersson (2003))

Duration of load effect: Tensile strength decreases under long term loading

Timber or glulam experiences a significant loss of strength and stiffness under long term loading, which is commonly referred to as duration of load (DOL) effect. DOL is generally quantified by comparing the strength of specimens under long-term loading and standard short-term tests. Thereby, different specimens have to be used for these two tests, as the same specimen cannot be broken twice. To minimize this effect, matched samples are usually compared (Hoffmeyer 2003). The long-term tests are performed under constant or ramp loads until failure occurs. The stress level at failure, which is the relation between the long-term and short-term stress, denotes the DOL effect:

Stress level at failure: $$SL\left(t_F\right) = k_{DOL} = \frac{\sigma_{long-term}}{\sigma_{short-term}} \quad (2)$$

DOL tests performed on tension specimens (90 and 140 mm width) and curved glulam beams (90 and 140 mm width, 4-point bending tests) in constant climates (65% and 85% RH) showed, that the tensile strength is reduced under long term loading (Aicher et al. 1998; Gowda et al. 1998): Stress levels at failure (k_{DOL}) of tension specimens (90 and 140 mm) were 0.70 and 0.75, whereas they were 0.77 and 0.87 in the case of curved beams. Thus, the duration of load effect appears to be slightly less severe in curved beams. The associated times to failure were 22-24 days in the case of tension specimens and 4-14 days with curved beams.

Size or volume effect: Tensile strength increases with decreasing volume

Numerous short-term tensile tests performed on glulam specimens and on curved glulam beams (tested under 4-point bending) in constant climates reported in the literature show a clear size or volume effect: With increasing specimen size (or volume) the mean ultimate tensile strength decreases.

Figure 4 shows the volume (a) and the height (b) of tension specimens versus the mean ultimate tensile strength from three different literature sources (Aicher et al. 1998; Blass and Schmid 2001; Astrup et al. 2007). In prismatic glulam specimens under uniaxial tensile loading the height appears to be the dominant factor for the size effect.

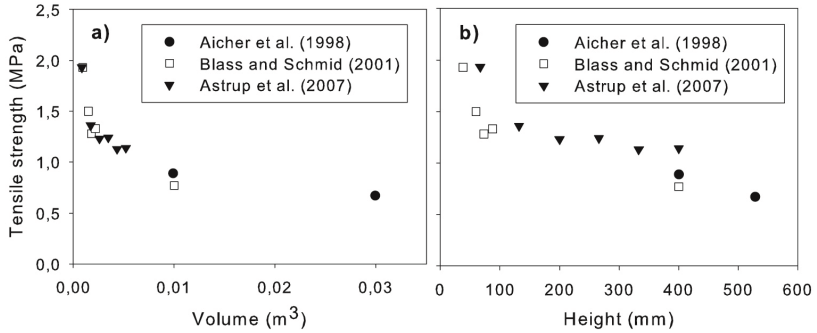

Fig. 4 Size effect in glulam specimens under tensile loading

Figure 5a shows the volume (of constant moment area) of curved glulam beams versus the mean short-term tensile strength under 4-point bending from two different literature sources (Ehlbeck and Kürth 1992; Aicher et al. 1998). Plotting the strength versus the beam height (Fig. 5b) reveals that in curved beams under bending the height is not the only factor controlling the size effect. In particular the data from Aicher et al. (1998) shows that the width and the length rather than the height affect the measured strength.

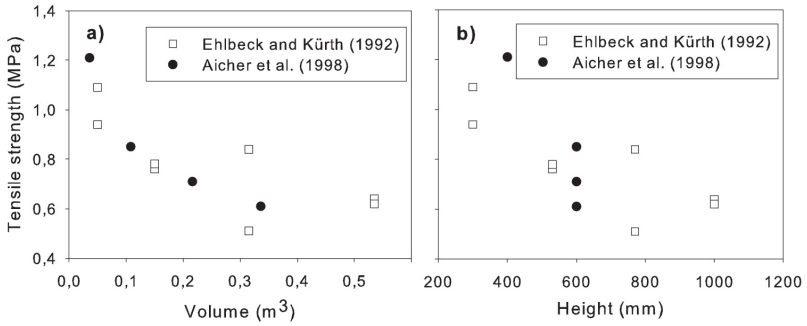

Fig. 5 Size effect in curved glulam beams under 4-point bending

The volume effect can be described as follows (adapted from the expression given in Eurocode 5 (2004)):

$$\left(\frac{V_0}{V}\right)^n \cdot f_{t,V0} = f_{t,V}\,, \tag{3}$$

where V_0 is a reference volume (m^3) having strength $f_{t,V0}$.

In the following, the exponent n for the volume effect was calculated based on the mean tensile strengths from the glulam specimens displayed in Fig. 4a. The reference volume was set to 0.01 m^3, as suggested in Eurocode 5 (2004). The resulting exponent was found to be 0.37 (Fig. 6a). Similarly, a height effect exponent can be calculated. In the present case, the exponent was found to be 0.4 for a reference height of 400 mm. The volume effect exponent calculated based on mean values from curved glulam beams is about 0.28. This relationship is displayed in Fig. 6b. Thus, this volume effect is of a slightly lower size in curved glulam beams than in tension specimens.

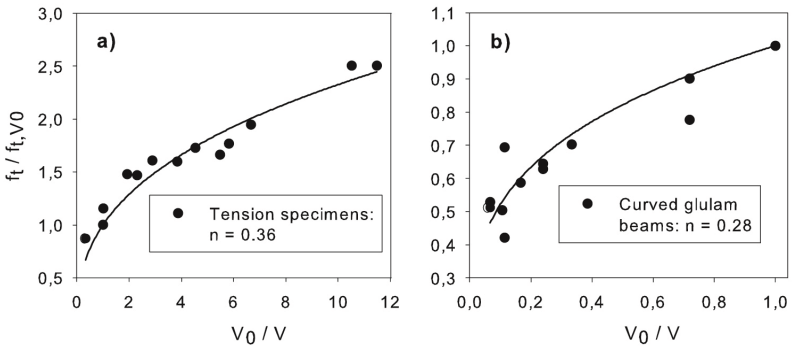

Fig. 6 Fitted exponent for the volume effect

Effect of geometrical configuration:

Tensile tests performed on glulam laminates or on thin slices of solid wood (spruce, *W*H*L* = 45*180*70 mm^3), respectively, revealed that the results are strongly influenced by the main annual ring pattern (Blass and Schmid 2001). The largest tensile strength was obtained when the annual rings were oriented mainly in radial direction. When the rings were oriented under 45 degree, the mean strength was 20% lower, and in tangential direction, the mean strength was 30% lower than in radial direction. However, when a pith was present within the tested wood slice, the mean strength was even 60% lower than the one in radial direction, independent of the annual ring orientation in this slice.

The geometrical configuration also influences the failure behaviour. When the pith is present within the failed laminate, the crack generally starts at the pith and evolves radially to the edges. This was observed both by Blass and Schmid (2001) in the case of tensile tests on wood slices, and by Jönsson (2005b) in the case of tensile tests on glulam specimens. When the pith is absent, failure starts in locations of stress concentrations. Jönsson observed that failure occurred in the vicinity of the glueline, where stress concentrations are present due to differences in the annual ring pattern between the laminates (compare Fig. 2). Similarly, in the case of the glulam beams tested in 4-point bending by Ehlbeck and Kürth (1992), failure started at the location with the highest tensile stress and continued along the laminate. Most of the cracks appeared in or in the vicinity of the glued joint. But as these showed wood fibres on the surface, it was assumed that not the glue was the cause for failure but the change in wood structure between the laminates.

2.5 Fracture perpendicular to grain

As mentioned above, glulam or wood in general has a very low tensile strength perpendicular to grain, but also a low resistance to crack propagation. In structural design, efforts are made to avoid tension perpendicular to grain, as it may lead to cracking, when the corresponding strength is exceeded. However, such stresses cannot always be avoided, and several timber failures due to fracture perpendicular to grain have occurred. In fact, according to different failure analyses of timber structures, tension failure perpendicular to grain is one of the most common failure modes (Frese and Blass 2007; Frühwald et al. 2007).

A variety of causes can lead to tensile stresses perpendicular to grain (Gustafsson 2003). Firstly, certain geometrical shapes of the structural member can imply tension perpendicular to grain upon loading of the structure (Fig. 7). **Curved glulam beams**, for example, which are subjected to a moment exhibit radial stresses. If the moment tries to "flatten" the beam the radial stresses will be tensile stresses (perpendicular to grain). Similarly, curved glulam beams under vertical, downward loading exhibit tensile stresses perpendicular to the grain within the curved part. Large **holes** in glulam or structural timber beams i.e. sudden changes in the cross section, impede the flow of forces. This leads to local tensile stresses near the holes upon loading. **Notches** in beam ends cause concentrated tensile stresses, which may lead to cracking even at low external loading.

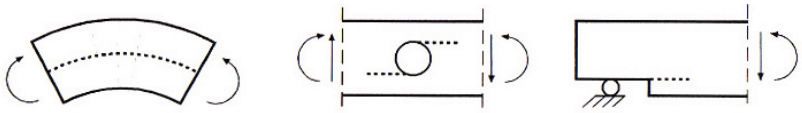

Fig. 7 Structural members exhibiting tensile stresses perpendicular to grain (Gustafsson 2003)

Eigenstresses are further causes for tension and thus fracture perpendicular to grain. A decrease in moisture content may give eigenstresses due to the different shrinkage in the tangential and the radial directions. The non-uniform moisture content in a structural member, as a result of seasonal climate changes, can lead to high compressive and tensile stresses perpendicular to grain, and thus produce cracking even without external load. This kind of eigenstresses will be discussed in detail in the next chapter.

Also the **non-homogeneity** of wood may induce high tensile stresses perpendicular to grain (Fig. 8). The annual ring pattern in a glulam cross section, for example, which is responsible for the local variations of material orientation, may result in cracking when a glulam specimen is loaded in compression perpendicular to grain.

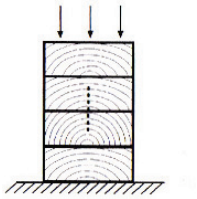

Fig. 8 Non-homogeneity of wood leading to tensile stresses perpendicular to grain (Gustafsson 2003)

There are of course also further cases of perpendicular to grain fracture, such as in mechanical and adhesive joints, but as these are not relevant in the present context, they are omitted.

3 MOISTURE INDUCED STRESSES

3.1 Introduction

The moisture content of glulam members in service varies with varying climate conditions of the surroundings. As moisture transport in timber or glulam is relatively slow, larger members generally exhibit nonuniform moisture content distributions across the cross section. These moisture gradients lead to internal stresses, which are often referred to as moisture induced stresses: The timber in the cross section cannot expand or shrink according to its actual moisture content, as it is restrained by adjacent timber exhibiting different moisture contents. In a wetting case, for instance, the moisture content increases in the outer parts of the cross section, giving rise to expansion. However, the expansion movement is restrained by the inner parts of the cross section (having lower moisture contents). In consequence of the restraint, compressive stresses arise in the outer parts, whereas tensile stresses arise in the centre of the cross section. In a drying case, the opposite effect takes place: The outer parts exhibit decreasing moisture contents, giving rise to shrinkage. Owing to the internal restraint, tensile stresses are created in the outer parts, and compressive stresses in the centre. Due to the fact, that no external stresses are present, the compressive and tensile stresses within the cross section are self-balancing. The moisture induced stresses can be tensile stresses in a perpendicular to grain direction and thus may cause cracks in the glulam member. Due to the low crack resistance in this direction, these cracks may evolve and cause failure of the whole member. According to the corresponding stress distribution in a wetting case, these cracks would start in the centre of the beam, while they would start on the surface in the drying case.

Moisture induced stresses can be evaluated by means of experiments or with numerical simulations. A typical case in practice is a long glulam beam (with $L >> W$ and H) that is covered on the top side. As climate changes are primarily induced from the lateral faces (e.g. rain, sun), moisture induced stresses are in this case generally assumed to result from a one-dimensional moisture transport perpendicular to grain.

3.2 Mechanosorption

Timber or glulam which is subjected to both stresses and varying climate conditions exhibit additional deformations – an effect called mechanosorption. Thereby, these stresses can be caused by an external load or by internal stresses, such as in the case of moisture induced stresses. Thus, wherever moisture induced stresses are present, mechanosorption takes place. Since mechanosorption is similar to pure creep, it is also referred to as mechano-sorptive creep. The difference is that pure creep is an effect of time, while mechanosorption is an effect of varying moisture contents.

The consequences of mechanosorption differ depending on whether the effect is a result of longitudinal stresses or transverse stresses (such as moisture induced stresses). Extensive work has been performed by different researchers to study the phenomenon of mechanosorption, e.g. (Grossman 1976; Hoffmeyer and Davidson 1989; Ranta-Maunus 1975; Mårtensson and Thelandersson 1990; Mårtensson 1994a, b). These studies were dealing mainly with longitudinal bending stresses due to external load. Typically, the deflection of a beam subjected to constant load and simultaneous moisture variations is monitored. Initially, an elastic deflection takes place, which, if moisture content and load are constant, is followed by a pure creep deflection. If the moisture content is varied instead, an increased deflection occurs, as a result of mechanosorption. This may lead to serviceability problems. However, in the case of transverse stresses due to swelling and shrinkage, which is relevant for the present research, mechanosorption is beneficial, as the additional deformations enable relaxation of internal stresses. An experimental study performed by Mårtensson and Svensson (1997) concluded, that under restrained conditions mechanosorption significantly reduces the stress level. This conclusion can be confirmed by the present author, who found considerable mechano-sorptive creep effects in glulam specimens under moisture induced stresses (Angst and Malo 2012a). Further experimental studies regarding mechanosorption perpendicular to grain found a.o. that the mechano-sorptive strain rate is larger during drying than during wetting (Mårtensson and Svensson 1997), and that mechanosorption is very similar in compression and tension (Svensson and Toratti 2002; Ranta-Maunus 1993). Generally, it was noticed, that mechanosorption is more significant in directions perpendicular to the grain than in longitudinal direction (Ranta-Maunus 1993).

Based on experimental results regarding mechanosorption, constitutive models have been formulated to describe the response of timber under stress and varying moisture contents (see section 3.5). Such models are indispensable for the simulation of moisture induced stresses.

3.3 Measurement of moisture induced stresses

For the measurement of moisture induced stresses the slicing technique is commonly used (Angst and Malo 2012a; Jönsson 2004; Svensson and Toratti 2002). A specimen which is under an internal stress state is cut into slices to release the internal stresses. The length of each slice is measured before and after cutting. An increase in length after cutting indicates compression stresses, and a decrease indicates tensile stresses.

The measurement procedure in detail is visualised in Fig. 9 (for the case of wetting) and explained in the following. Generally, the procedure is very similar among different experimental studies in the literature regarding moisture induced stresses. The timber or glulam specimens are prepared by seasoning them in a certain climate until a homogeneous moisture content is obtained throughout the cross section. Then, top, bottom, front and back faces of the specimen are sealed, before being exposed to a climate change (Fig. 9a). The sealing makes it possible to obtain a one-dimensional moisture transport perpendicular to the grain (only the lateral faces are exposed). After a certain time of climate exposure, the specimen exhibits differential dimensional changes (Fig. 9b). The specimen is then cut into slices along the height (Fig. 9c), while the released deformations along the height are measured. For the measurement of the released deformations different equipments can be used. The deformations can, for example, be measured by transducers positioned against the end of the specimens (Svensson and Toratti 2002) or by a contact free technique using either a digital camera (Jönsson and Svensson 2004) or a video extensometer (Angst and Malo 2012a). The contact free technique works as follows: Each slice in the specimen is marked with a dot along the upper and lower side. Before and after cutting the specimen into slices, the camera or the video extensometer records the location of the dots. The length between these dots is evaluated in both recordings, L_0 and L_1. The mean released strain over the measured length can then be calculated according to:

$$\varepsilon_{mean} = \frac{L_1 - L_0}{L_0} \tag{4}$$

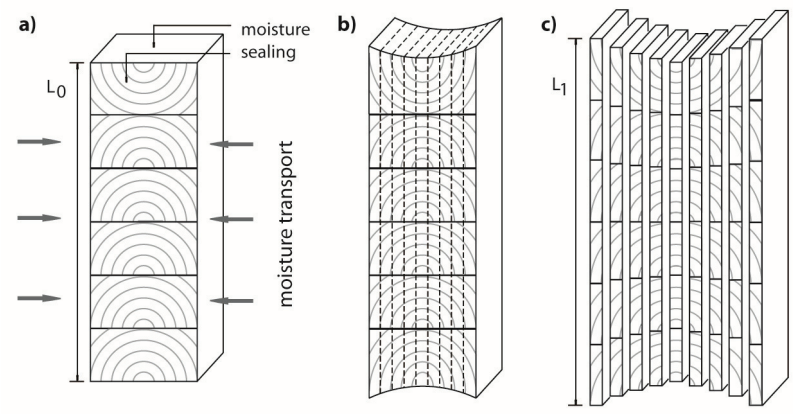

Fig. 9 Experimental procedure for evaluation of moisture induced stresses (wetting case)

Once the released deformations are known, the moisture induced stresses can be calculated. The mean moisture induced stresses correspond to the mean released deformations multiplied by the modulus of elasticity, according to:

$$\sigma_{mean} = E_{mean} \cdot \varepsilon_{mean} \tag{5}$$

Thus, with experiments, only mean moisture induced stresses can be obtained, i.e. one average value over the height for each slice. This gives an average stress distribution across the cross section. The procedure explained above does not permit the determination of local stresses in different points in the cross section.

The accuracy of moisture induced stresses determined by means of experiments depends on different factors. On the one hand, the accuracy of the measurement of the released deformations, which depends on the technique used, plays an important role. On the other hand, as apparent from Eq. (5), the selection of a correct modulus of elasticity (MOE), used for the calculation of stresses, is essential. The value for the MOE can either be selected from the literature or measured directly on the studied specimen. As literature values scatter considerably for the same type of timber or glulam (compare Table 4 in Angst and Malo (2010)), it is preferable to measure the modulus of elasticity on each slice of the specimen. Then again, the accuracy depends on the selected procedure for measuring the MOE. Furthermore, material parameters such as the MOE are highly influenced by the geometrical configuration of the specimen, on which the parameters are measured (Angst and Malo 2012a). This means that two different

specimens can give different MOE distributions and thus different stress distributions.

3.4 Experimental results

In the literature, experimental results concerning moisture induced stresses in glulam are scarce. The most known and often cited study is the one performed by Jönsson (2004). Jönsson measured the MC distribution, the released strains and modulus of elasticity in glulam specimens ($W*H*L$ = 90*270*16 mm^3) subjected to single and cyclic climate changes. With the obtained results, Jönsson calculated the average moisture induced stresses. The climate variations comprehended wetting from 40% to 80% RH, drying from 80% to 40% RH and moisture cycling between 40% and 80% RH, starting at 60% RH. A similar study was performed by the present author (Angst and Malo 2012a), investigating the average moisture induced stresses in glulam specimens ($W*H*L$ = 90*270*90 mm^3) subjected to wetting from 50% to 90% RH and drying from 90% to 50% RH. The average stresses after 12 and 21 days of climate exposure are displayed in Fig. 10, there "average" means stresses averaged over specimen height.

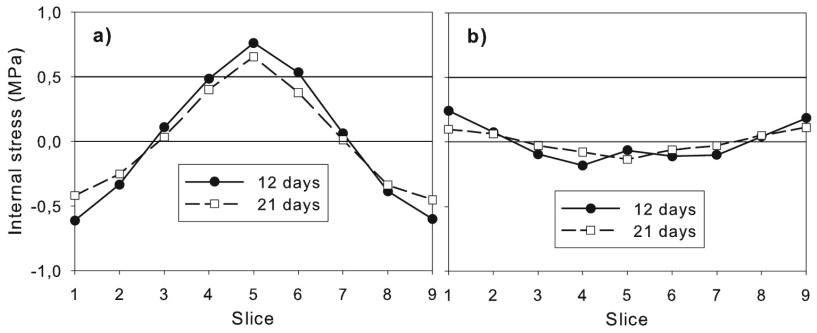

Fig. 10 Average moisture induced stresses after 12 and 21 days of a) wetting and b) drying and characteristic tensile strength (0.5 MPa) according to prEN 14080 (2011). This figure is a modification of Fig. 8 in Angst and Malo (2012a)

The conclusions from both studies concerning average stresses along slices were similar. During wetting (Fig. 10a), the tensile stresses arising in the centre of the specimen may clearly exceed 0.5 MPa, which is the characteristic tensile strength limit for glulam perpendicular to grain according to prEN 14080 (2011). Furthermore, the tensile and compressive stresses are always larger during wetting exposures compared to drying exposures (Fig. 10). Figure 11 shows the

absolute value of the stresses in the centre and at the border of the specimens during wetting and drying (average over specimen height). The figure includes results from Jönsson (2004), which are the stresses after 3, 11, and 38 d of climate exposure, and the results from Angst and Malo (2012a), which are the stresses after 5, 12, 21, and 38 d of exposure. The figure clearly reveals that stresses are larger during wetting than corresponding stresses during drying.

The results concerning cyclic climate changes performed by Jönsson (2004) and by the present author (Appendix B) show the same effect: After a wetting period the stresses are significantly larger than after a drying period. Thereby, no cumulative effect of repeated moisture cycling was observed.

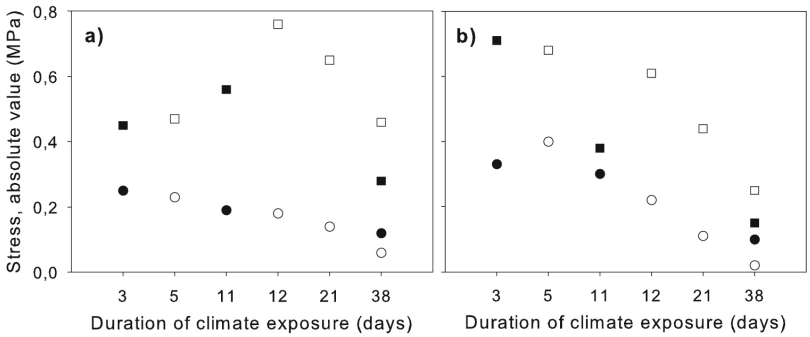

Fig. 11 Absolute moisture induced stresses during wetting and drying in a) the centre and b) at the border of the specimens (squares = wetting, circles = drying, black = Jönsson, white = Angst and Malo)

A further study investigated moisture induced stresses in a glulam laminate or in a board of Norway spruce (*W*H*L* = 120*40*20 mm^3) (Svensson and Toratti 2002). In contrast to the previously mentioned studies, the one-dimensional moisture transport occurred not along the width, but in the direction of the height. Accordingly, the specimens were cut along the width and not along the height. Thus, the moisture induced stresses were investigated mainly in tangential direction after wetting from 40% to 90% RH or drying from 90% to 40% RH during 1, 14, and 43 days. After 1 d the maximum average stresses were significantly larger during wetting (1 MPa) than during drying (0.5 MPa), which conforms well with the results from the previously mentioned studies. In the present case, the specimens were relatively small, especially in direction of the one-dimensional moisture transport (40 mm). As a result, the stresses during wetting and drying

were reversed already after 14 d. Interestingly, the reversed stresses were larger during drying than during wetting.

3.5 Modelling of moisture induced stresses

The calculation of moisture induced stresses by means of numerical simulations is well established. The commonly applied basic material model is based on a strain rate formulation. Generally, this formulation takes on the following form:

$$\dot{\boldsymbol{\varepsilon}} = \dot{\boldsymbol{\varepsilon}}_e + \dot{\boldsymbol{\varepsilon}}_s + \dot{\boldsymbol{\varepsilon}}_{ms} + \dot{\boldsymbol{\varepsilon}}_c \tag{6}$$

The total strain rate is the sum of the elastic strain rate, $\dot{\boldsymbol{\varepsilon}}_e$, the linear shrinkage-swelling strain rate, $\dot{\boldsymbol{\varepsilon}}_s$, the mechano-sorptive creep strain rate, $\dot{\boldsymbol{\varepsilon}}_{ms}$, and the creep strain rate, $\dot{\boldsymbol{\varepsilon}}_c$. The dot denotes derivative with respect to time. The model is most often one-dimensional, but in recent years several three-dimensional models have been applied, e.g. (Fortino et al. 2009; Gereke and Niemz 2010; Ormarsson et al. 1998).

Elastic strain:

The strain rate is commonly written as:

$$\dot{\boldsymbol{\varepsilon}}_e = C\dot{\boldsymbol{\sigma}} + \dot{C}\boldsymbol{\sigma} \tag{7}$$

Here $\boldsymbol{\sigma}$ is the stress vector and C the compliance matrix, which, in matrix notation, is as follows:

$$C = \begin{bmatrix} \frac{1}{E_L} & -\frac{\nu_{LR}}{E_R} & -\frac{\nu_{LT}}{E_T} & 0 & 0 & 0 \\ -\frac{\nu_{RL}}{E_L} & \frac{1}{E_R} & -\frac{\nu_{RT}}{E_T} & 0 & 0 & 0 \\ -\frac{\nu_{TL}}{E_L} & -\frac{\nu_{TR}}{E_R} & \frac{1}{E_T} & 0 & 0 & 0 \\ 0 & 0 & 0 & \frac{1}{G_{LR}} & 0 & 0 \\ 0 & 0 & 0 & 0 & \frac{1}{G_{LT}} & 0 \\ 0 & 0 & 0 & 0 & 0 & \frac{1}{G_{RT}} \end{bmatrix} \tag{8}$$

The characters, *E*, *G*, and ν, denote moduli of elasticity, shear moduli and Poisson's ratios, respectively. The indices, *L*, *R*, and *T* denote longitudinal, radial and tangential direction, respectively.

The last term in Eq. (7) implies that the material parameters, which are the moduli of elasticity *E*, the shear moduli *G* and Poisson's ratios ν, are functions of moisture content, and thus, time. Thus, the rate of the compliance matrix is needed. However, measurements of moduli of elasticity *E* in glulam specimens have shown that in the range of climate variations occurring in practice, the effect of MC is negligible (Angst and Malo 2012a). In the present work, the same assumption is made for the effect of MC on shear moduli *G* and on Poisson's ratios ν. In this case, the last term of Eq. (7) can be omitted and thus $\dot{\boldsymbol{\varepsilon}}_e$ becomes the elastic strain rate. For rather extreme climate variations, though, an effect of MC on modulus of elasticity could be observed, namely that the modulus of elasticity increases with decreasing MC (Appendix A).

Linear shrinkage-swelling strain:

The linear shrinkage-swelling strain rate is derived from the hygroexpansion coefficient vector $\boldsymbol{\alpha}$ and the rate of change of moisture content $\dot{u}$ to be

$$\dot{\boldsymbol{\varepsilon}}_s = \boldsymbol{\alpha} \cdot \dot{u} \tag{9}$$

The vector $\boldsymbol{\alpha}$ is defined as

$$\boldsymbol{\alpha} = \begin{bmatrix} \alpha_L & \alpha_R & \alpha_T & 0 & 0 & 0 \end{bmatrix}^T \tag{10}$$

Mechano-sorptive creep:

In the literature, various models have been proposed for mechano-sorptive creep. A review of these models is given in Hanhijärvi (2000). The proposed models include mainly Maxwell type and Kelvin type models, whereby the latter are usually more advanced comprising more model parameters. However, it has been shown that for the present application, which is modelling of moisture induced stresses in timber without external load, the type of selected model has a relatively small effect, while the selection of correct material parameters is much more important (Angst and Malo 2010). For the present research, the mechano-sorptive creep strain model, proposed a.o. by Ormarsson (1999) is used:

$$\dot{\boldsymbol{\varepsilon}}_{ms} = \boldsymbol{m} \cdot \boldsymbol{\sigma} \cdot \left| \dot{u} \right| \tag{11}$$

The matrix $\boldsymbol{m}$ is a mechanosorption property matrix defined as:

$$\boldsymbol{m} = \begin{bmatrix} m_L & -\mu_{RL} m_R & -\mu_{TL} m_T & 0 & 0 & 0 \\ -\mu_{LR} m_L & m_R & -\mu_{TR} m_T & 0 & 0 & 0 \\ -\mu_{LT} m_L & -\mu_{RT} m_R & m_T & 0 & 0 & 0 \\ 0 & 0 & 0 & m_{LR} & 0 & 0 \\ 0 & 0 & 0 & 0 & m_{LT} & 0 \\ 0 & 0 & 0 & 0 & 0 & m_{RT} \end{bmatrix} \tag{12}$$

where m are mechanosorption coefficients in the orthotropic directions and planes and μ are coupling coefficients.

Time-dependent creep:

In the literature, different models can be found to model time-dependent creep. A very simple way to include creep effects is to reduce the elastic modulus (Mårtensson and Svensson 1997). However, the effect of time-dependent creep at low moisture contents and temperatures is considered to be small compared with mechano-sorptive creep (Mårtensson and Svensson 1997; Toratti and Svensson 2000; Virta et al. 2006). As a result, this term is often neglected in the strain rate formulation presented in Eq. (6) (Ormarsson et al. 1998; Svensson and Toratti 2002; Häglund 2008; Gereke and Niemz 2010).

Moisture transport:

The strain rate formulation (Eq. 6) with its terms is a function of the moisture content change within the timber cross section. Generally, a moisture transport model based on Fick's second law of mass diffusion is used for the calculation of the moisture content, which, for the case of one-dimensional diffusion, can be written in the following form:

$$\frac{\partial u}{\partial t} = \frac{\partial}{\partial x}\left(D \frac{\partial u}{\partial x} \right) \tag{13}$$

For simplicity reasons, the diffusion coefficient D can be assumed to be equal in radial and tangential direction (Koponen 1983; Rosenkilde and Arfvidsson 1997), thus resulting in one value for the cross grain direction. The moisture flow through the timber surface is expressed with the following equation:

$$\left(D \frac{\partial u}{\partial x} \right) = S\left(u_{eq} - u_{surf}\left(t\right) \right) \tag{14}$$

The surface emission coefficient *S* takes into account the moisture transfer resistance at the surface, where the moisture flow is driven by the difference between the actual surface moisture content $u_{surf}(t)$ and the equilibrium moisture content u_{eq}, i.e. the moisture content reached at t = ∞ under exposure to a certain RH.

3.6 Numerical results

The basic material model (Eq. 6) presented above has been used in a wide range of applications by different researchers. It has, among others, been used to predict checking during timber drying (Salin 1992), to study the shape stability of timber (Ormarsson et al. 1998), or to model tangential swelling stresses in spruce (Virta et al. 2006).

In the following, results from the literature concerning moisture induced stresses in glulam, obtained by means of numerical simulations, are presented. Although the model formulation and the procedure are very similar among the different studies, the objectives differ. In some studies absolute stress values are prospected, whereas the influence of various parameters is investigated in other studies. In the following, the results will be grouped according to their specific objectives. Please note that only results concerning moisture induced stresses in glulam without external load are considered. The presence of an additional external load is discussed in a later chapter.

Effect of natural climate variations:

A study dealing with glulam beams (*W*H* = 90*270 mm^2), has shown that calculated moisture induced stresses using naturally varying indoor RH (calculated from measured outdoor RH) at different locations in Sweden during several years are almost independent of the location (Häglund 2008). The moisture variations at the different locations induced similar stress levels. Furthermore, as expected, the stress variability in time was found to be larger near the surface of the beam than in the centre of the beam. In the centre of the beam large tensile stresses did arise, which were around 1 MPa, thus significantly above 0.5 MPa (being the characteristic tensile strength according to prEN 14080 (2011)). These tensile stresses did arise during summer. The climate variations over all the seasons corresponded to a variation of the relative humidity between 40% and 90% RH. Neglecting the small RH frequencies in time, the main RH variation exhibited long

moisture cycles of half a year between 90% and 40% RH and half a year between 40% and 90% RH.

Effect of material and model parameters:

Variation of different input parameters significantly affects the resulting moisture induced stresses perpendicular to grain. The calculation of internal stresses by means of a numerical model, thereby varying the level of individual input parameters provides information about the relative effect of a single parameter. One of the strongest effects arises from the mass transfer coefficient, which governs the moisture transfer at the surface of the glulam. By lowering this coefficient through, for example, surface coating of the beam, stresses can significantly be reduced (Häglund 2010). Other considerable effects arise from the material parameters, whereby the influence of different hygroexpansion coefficients is stronger than that of different MOE's (Häglund 2010; Angst and Malo 2010). The selection of a certain mechanosorption model as well as the magnitude of the mechanosorption coefficients, however, were found to be less important with regard to moisture induced stresses perpendicular to grain without external load (Häglund 2010; Angst and Malo 2010).

These findings suggest that when calculating moisture induced stresses by means of a numerical model the emphasis should be put on selecting correct material parameters, due to their strong effect on the results. As the material parameters proposed in the literature scatter widely for the same material, measurement of all relevant parameters on the same batch of material is recommended in order to obtain reliable results. Moreover, the mechanosorption model parameters, which cannot or can only hardly be measured, may only be properly calibrated, when the material parameters are known for the actual case. For performing sensitivity analyses, however, literature data are useful.

Effect of geometrical configuration:

The geometrical configuration of a glulam specimen, which is the distribution of the pith locations among the laminates, significantly influences the stresses. It has a strong effect particularly on the local moisture induced stresses in the cross section, but also on the average stresses. In the vicinity of a pith, large local stresses arise, and when a pith is present within a laminate, also large average stresses are induced (Angst and Malo 2010, 2011; Gowda et al. 1998). A numerical study by the present author investigated the effect of 24 different geometrical configurations (manually recorded on glulam specimens) on moisture induced

stresses (Angst and Malo 2011). The ratio of local and average stresses was found to be in the range 2-7, depending on the geometrical configuration, in particular the presence or absence of piths within the laminates, but also the location of piths within the cross section. The studied wetting exposure (wetting from 50 to 90% RH) resulted in local tensile stresses, which exceeded the tensile strength of the material, and consequently could lead to small cracks in the cross section. It was concluded, that configurations containing piths were more vulnerable to crack formation compared to pith-free cross sections.

Effect of cross section width:

A numerical study performed by the present author (Angst and Malo 2011) investigated the effect of different glulam cross section widths (W = 90, 140, 215 mm) on moisture induced stresses. The average stresses were calculated for 5, 12, 21, and 38 d of wetting from 50 to 90% RH. In addition, also the development over time of average stresses (over cross section height) and local stresses (in selected points where due to the geometrical configuration high local stresses arise) were computed. The results showed that the wider a cross section was, the longer it took until large stresses arose, due to the facts that the arising tensile force is distributed over a larger internal part of the cross section and that more time is needed until the cross section centre is affected by a moisture content change. On the other hand, however, the large stresses were present for a longer period of time compared to smaller cross sections (because large moisture gradients are maintained longer). The highest average and local stresses were attained in the 140 mm wide cross section, followed by the 90 mm (8-12% lower), and the 215 mm wide cross section (14-15% lower). It was concluded, that wider cross sections are only prone to cracking when long wetting cycles (> 20 days) occur.

3.7 Summary

Moisture induced stresses can be determined with experiments and numerical simulations. While only average stresses (average over cross section height) can be obtained by means of experiments, numerical simulations, on the other hand, make it possible to also evaluate local stresses within the cross section. In the case of experiments, the accuracy of the obtained stresses depends on the accuracy of the measured parameters. In the case of numerical simulations, different parameter studies have shown that calculated results are strongly affected by the selected material parameters and by the used geometrical configuration of the

specimen. Thus, the accuracy of numerical results depends on the selection of correct parameters and configurations. Different investigations regarding moisture induced stresses in glulam under realistic climatic conditions have shown that significant tensile stresses develop, which may clearly exceed the characteristic tensile strength of glulam. Thus, cracks might be induced even without external loading. Furthermore, it was found that larger stresses develop during wetting than during drying.

4 SUPERPOSITION OF INTERNAL AND EXTERNAL STRESSES

4.1 Introduction

Often, internal stresses, such as moisture induced stresses, occur in combination with stresses from external loads. This is, for example, the case in structurally loaded members which exhibit tension perpendicular to grain due to their geometrical shape and which are at the same time subjected to climate changes. As previously presented (section 2.5), such members include curved glulam beams, beams with large holes and end-notched beams. Superposition of different stresses may lead to very non-uniform stress distributions with unfavourable stress concentrations. It can also result in large tensile stresses perpendicular to grain, which might exceed the low tensile strength of glulam in this direction and lead to cracking. When these cracks evolve in the longitudinal direction, failure of the beam might occur and in extreme cases even lead to failure of the whole structure.

4.2 Superposition of stresses in glulam

The stress distribution in a glulam beam or specimen exhibiting internal and external stresses is a combination of the non-uniform internal stress $\sigma_i(x)$ and the non-uniform stress $\sigma_e(x)$ imposed by the external loading. The latter is non-uniform, because the modulus of elasticity in loading direction varies over the cross section width *(x)* of the glulam beam or specimen. The modulus of elasticity is about two to three times larger in the central part of the cross section than in the outer parts due to the annual ring orientation of the laminates, with predominant radial directions in the central part. The combined stress can be expressed as follows (Jönsson and Thelandersson 2003):

Combined stress: $\sigma_c(x) = \sigma_e(x) + \sigma_i(x) = \frac{F_u}{A}\frac{E(x)}{\bar{E}} + \sigma_i(x)$, (15)

where F_u is the external load, $E(x)$ the varying modulus of elasticity over the cross section width, and $\bar{E}$ the average modulus of elasticity over the cross section.

Wetting:

In a wetting case, the superposition of internal moisture induced stresses and external stresses from tensile loading results in an unfavourable stress distribution with large tensile stresses in the cross section centre: As discussed in chapter 3, the internal stresses exhibit tensile stresses in the centre and compressive stresses at the border. The distribution of the external stresses depends directly on the variation of the modulus of elasticity (compare Eq. 15) and as the latter increases towards the cross section centre, the distribution exhibits a similar shape as the internal stresses. As a result, the combined stress takes on a distribution as schematically shown in Fig. 12a. The findings from the experimental study performed by the present author (Angst and Malo 2012a) and Eq. (15) were taken as a basis for drawing Fig. 12.

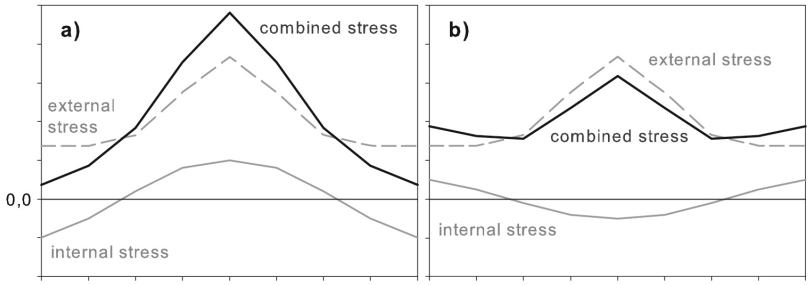

Fig. 12 Superposition of stresses over the cross section width, schematically shown for a) wetting and b) drying

Drying:

In a drying case, the superposition of stresses leads to a more uniform stress distribution. As shown in chapter 3, the internal moisture induced stresses exhibit compressive stresses in the centre and tensile stresses at the border of the cross section. The external stresses resulting from tensile loading exhibit in principle the same distribution as in the wetting case: The stress distribution is directly related to the variation of the MOE across the cross section width and exhibits thus the opposite shape as the internal stresses. When both stresses are combined, a distribution as schematically shown in Fig. 12b is obtained.

Parameters affecting the combined stress distribution:

The distributions from the superposition of stresses presented above (Fig. 12) are especially true for glulam specimens, exhibiting typical cross sections with annual ring patterns as shown in Fig. 1. In cross sections, built up with laminates having flat annual rings, for example, the MOE variation across the cross section width would be more uniform. This would result in more uniform external stress distributions and consequently in a more favourable superposed stress distribution in the wetting case.

4.3 Experimental results

Tensile strength perpendicular to grain:

The internal stress state in a glulam beam or a specimen, as for instance arising from moisture induced stresses, will affect the tensile strength perpendicular to grain that remains to take up externally caused stresses. In cases, where moisture induced stresses are very large, the residual tensile strength of the glulam may accordingly be very low. The internal stresses will not only affect the strength but also the failure behaviour of the beam.

An experimental study performed by Jönsson and Thelandersson (2003) investigated the (residual) tensile strength perpendicular to grain of glulam specimens, having internal stresses. Thin glulam specimens (*W*H*L* = 90*270*16 mm^3) were subjected to different climate histories, to create internal moisture induced stresses, before performing tensile tests perpendicular to grain. The climate histories involved a long wetting cycle from 40% to 80% RH, a long drying cycle from 80% to 40% RH, and short wetting-drying cycles (7 days interval) between 80% and 40% RH, starting at 60% RH.

The results showed, that, in the wetting case, the tensile strength perpendicular to grain was significantly lower than the strength of corresponding specimens seasoned in high humidity. After 5 days of wetting the mean ultimate strength started to be lower than the strength of specimens seasoned in 80% RH. After 24 days of wetting the strength was lowest, being 30% lower than the strength in 80% RH.
However, for the drying case, the results showed that the tensile strength perpendicular to grain was barely affected, i.e. it was of a similar magnitude as the strength of specimens seasoned in low humidity.

The results from specimens subjected to moisture cycling, revealed the following: If the specimen was in a wetting phase at test time, it behaved similar to the wetting case, and if the specimen was in a drying phase at test time, it behaved similar to the drying case. Thereby, the number of the cycles was not significant. The strength of cycling specimens in a wetting phase at test time was 11% lower than specimens seasoned in 60% RH, whereas specimens in a drying phase at test time exhibited 11% higher strength than specimens seasoned in 60% RH.

The failure behaviour of the glulam specimens during testing, observed by Jönsson and Thelandersson (2003), is in accordance with the combined stress distribution at failure, shown in Fig. 13: In the wetting case, cracking started in the centre (due to the large combined tensile stress of around 2 MPa there) and grew until final failure (non brittle). In the drying case, the ultimate failure started with a crack at the border of the specimen leading to brittle failure. The reason for the crack starting at the border was believed to be due to the annual ring orientation of the glulam. At the border of the cross section glulam consists mainly of tangential wood, which has lower strength properties than radial wood (in the cross section centre)(Dahl 2009).

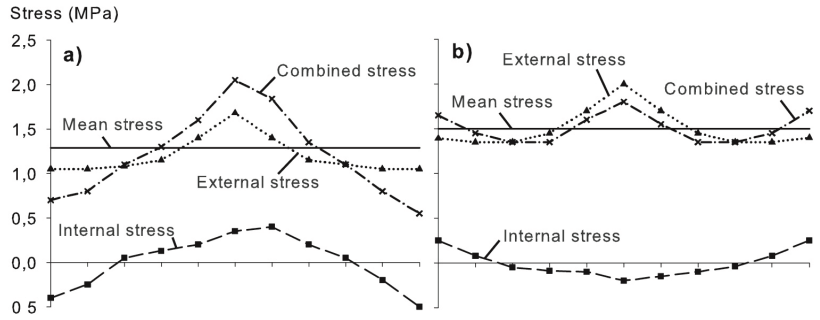

Fig. 13 Superposition of stresses at failure after 5 days of a) wetting and b) drying (Jönsson and Thelandersson 2003)

Another experimental study involved curved glulam beams (W = 140 mm), which were subjected to cyclic humidity (between 55% and 90% RH), before testing the short-term tension strength perpendicular to grain by a 4-point bending test (Gowda et al. 1998). The study showed similar results as the ones presented above: The maximum tensile strength of beams in a wetting phase was 12% lower than the tensile strength of beams seasoned in high humidity (85% RH).

Bending strength:

The bending strength of curved glulam beams appears to be similarly affected by internal moisture gradients. Jönsson (2005a) performed bending tests on curved glulam beams ($W*H$ = 90*280 mm^2), which had previously been subjected to wetting from 40% to 80% RH or drying from 80% to 40% RH. In the wetting case, the bending strength was reduced as compared with beams exhibiting constant moisture contents, i.e. being free from internal stresses: After 11 days of wetting exposure the bending strength was found to be lowest, being 40% lower than the bending strength of corresponding beams seasoned in 80% RH. In the drying case, the bending strength was found to be slightly higher than the bending strength of corresponding beams seasoned in 40% RH.

Another study investigated the bending strength of curved glulam beams (W = 140 mm), which had been subjected to cyclic humidity (between 55% and 90% RH) before being tested in a wetting phase (Gowda et al. 1998). The study showed similar results, although less pronounced. The bending strength was found to be 10% lower than the one of beams seasoned in high humidity (85% RH).

Duration of load:

Generally, duration of load effect is accelerated under simultaneous moisture changes and mechanical loading.

Experimental studies have been performed to investigate the DOL effects of glulam under varying climate changes (Gowda et al. 1998; Aicher et al. 1998). DOL effects in tension perpendicular to grain were investigated with prismatic specimens and curved beams. The prismatic glulam specimens ($W*H*L$ = 90*400*275 mm^3 and $W*H*L$ = 140*528*405 mm^3) were subjected to an axial tensile force perpendicular to grain during DOL test, whereas the curved glulam beams (W = 90 and 140 mm) were loaded in 4- point bending, both with stepwise increasing loads. During testing, the climate was varied between 55% and 90% RH with cycle lengths of 28 days. The results showed that the stress levels at failure were considerably lower under cyclic exposure than in constant climate (85% RH), namely by ca. 35% in the axially loaded tension specimens and by ca. 30% (W = 90 mm) and 13% (W = 140 mm) in the tests with curved beams, respectively. The mean stress levels at failure (k_{DOL}) were 0.45 and 0.50 in the case of small and large tension specimens, and 0.60 and 0.66 in the case of curved beams. The associated mean times to failure ranged from 15 to 28 days. As the major DOL

effect results from the climate variations, the wider cross sections (140 mm), which are less affected by climate changes, showed 10% less severe DOL effect compared to the smaller cross sections (90 mm). The failure of the beams occurred almost always when the climate was at a high RH-level (75% and 90% RH). Tensile stresses perpendicular to grain were found to be highest in the centre of the cross section (compare section 4.2), and as a result, failure of the beams took place with the appearance of a single major crack in the centre of the beams.

Other specimens were subjected to naturally varying climate in sheltered outdoor conditions instead of the cyclic climate changes mentioned above. In this case, it could be observed that the majority of the samples also failed during moist weather conditions. The studies concluded that the increased DOL effect in variable climate results from the super-imposed eigenstresses caused by the transient moisture gradients.

4.4 Numerical results

Different numerical studies have investigated how the tensile stresses perpendicular to grain in glulam are affected by simultaneous external and internal loading. The internal stresses, which result from varying climate changes, have shown to cause significant additional tensile stresses.

Zhou et al. (2009) investigated a simply supported glulam beam (W = 90 mm) under normal service load and climatic variations. While the stress perpendicular to grain induced by the service load alone was 0.3 MPa, the stress induced by load and daily MC variations between 11 and 13 % MC was 2.2 MPa. These stresses corresponded to maximum local stresses on the surface of the beam. This means that, in this case, the main contribution to the stresses perpendicular to grain resulted from the climate changes of the surroundings. Due to the large tensile stresses, there is a high risk for the glulam beam to crack. It should be noted, however, that only very short moisture cycles were applied and thus the moisture content varied only at the surface of the beam, whereby the large tensile stresses arose during drying.

Another study investigated a glulam cross section ($W*H$ = 90*396 mm^2) subjected to an externally applied tensile stress perpendicular to grain of 0.2 MPa and climate variations between 50 and 90% RH (Aicher and Dill-Langer 1997). The cycles which lasted 4 weeks yielded considerably higher stresses than cycles

lasting only 2 weeks. Generally, the stresses after wetting periods were significantly larger than after drying periods, which conforms well with other studies (Angst and Malo 2012a; Jönsson 2004). The maximum stresses in the cross section centre resulting from climate variations and external loading were about 1 MPa, while they were about 0.7 MPa at the border. The calculation of a fictive constant stress (Weibull stress) acting on the whole cross section width yielded stresses varying between 0.2 and 0.65 MPa, whereby the larger stresses occurred after wetting periods.

4.5 Summary

The superposition of internal and external stresses takes on a very different form depending on if the internal stresses are the result of wetting or drying exposure. In the case of wetting, the combination of stresses leads to high tensile stresses perpendicular to grain in the cross section centre. In the drying case, however, the combination of stresses results in a more uniform stress distribution over the cross section. As a consequence, the remaining tensile strength is reduced, if the glulam beam or specimen is in a wetting phase, whereas it is barely affected, if the glulam beam or specimen is in a drying phase. Thereby, it appears not to be important if the wetting or drying phase results from a single or a cyclic climate change. It can thus be concluded, that wetting is worse than drying with respect to the superposition of stresses and the remaining strength of the beam.

In a similar manner, the DOL effect of glulam specimens and curved beams is affected in a varying climate. The stress levels at failure are up to 35% lower compared to the ones in constant climates.

5 DEALING WITH MOISTURE INDUCED STRESSES

5.1 Introduction

As discussed in the previous sections, exposure to moisture variations can lead to significant stresses perpendicular to grain in timber structures and in particular in combination with external loads give rise to cracking or even problems regarding structural safety. Thus, the question arises in what way to consider moisture induced stresses in design calculations. At present (in European standards, e.g. Eurocode 5 (2004)), moisture conditions are considered together with duration of load effects as a strength reducing factor, k_{mod}. The standard defines 5 different load-duration classes and 3 different service classes (characterised by different climatic conditions). For each combination of a load-duration and a service class, a value for k_{mod} is proposed, that may range from 0.5 to 1.1. The design value X_d of a strength property can then be calculated according to Eurocode 5 (2004):

$$X_d = k_{\mathrm{mod}} \frac{X_k}{y_M}, \tag{16}$$

where X_k is the characteristic value of the strength property, and y_M is the partial factor for the material property.

In the following, different measures with respect to moisture induced stresses are presented and discussed.

5.2 Moisture induced stresses as an additional load

An approach, which is suggested by several researchers, is to consider moisture induced stresses as a load case instead of a strength reducing factor (Gowda et al. 1998; Ranta-Maunus 2003, 2001). Thus, the load caused by moisture gradients would be added to other loads, such as permanent (e.g. weight or structure itself) and dynamic (snow, wind, etc.) structural loads. These calculations would have to be done when timber is loaded in tension perpendicular to grain. In a similar way, moisture induced stresses would have to be added to mechanical stresses in the design of curved beams, for example. However, the question arises if the stresses are in fact additive. According to Ranta-Maunus (2003, 2001), the error made

when stress components are added could be tolerated, as the analysis of all effects simultaneously would be highly difficult to perform in structural design. Ranta-Maunus proposed a simple approach to consider moisture induced loads, by giving values for moisture stresses in design codes. These values would be based on experimental and calculated results, where a rough estimate could be 0.25 MPa for uncoated and 0.1 MPa for coated beams. These values could be reduced by a load combination factor, ψ, when combined with other stresses; however, the exact value of this factor is not clear. Generally, load combination factors account for the highly unlikely event that the extreme values of several variable loads coincide at the same time.

Häglund and Carlsson (2010) suggested a load combination factor for moisture induced stresses (MiS), when MiS and snow load were combined, with snow as the leading load. Based on daily measured snow depths and calculated MiS at four different locations in Sweden, a load combination factor of 0.2 for MiS was calculated.

Another study performed by Häglund and Carlsson (2008) dealt with extreme value analysis of moisture induced stresses. In accordance with building codes, a design value for the moisture induced stress was calculated as the 98^{th} percentile of its annual maximum distribution (obtained by fitting extreme values against the GEV distribution). The calculation was performed for a glulam beam of 90 mm width using indoor relative humidity conditions in Stockholm (which were determined from recorded outdoor climate data). The 98^{th} percentile of maximum annual surface stress was found to be 1.05 MPa.

Ranta-Maunus (2001) calculated moisture loads in uncoated glulam beams depending on climate variation when acting simultaneously with a mechanical load of 0.2 (0.5) MPa by means of an effective Weibull stress. The moisture loads were found to correspond to the following extra loads: 0.16 to 0.25 (0.23 to 0.31) MPa (cyclic variation between 55 and 90% RH), 0.15 (0.21) MPa (cyclic variation between 40 and 85% RH), 0.2 to 0.21 (0.23 to 0.25) MPa (single climate change from 76 to 90% RH), 0.32 to 0.35 (0.37 to 0.4) MPa (single climate change from 65 to 90% RH). It was concluded, that single fast climate changes were more severe than the test cycles analysed.

A similar study was performed by Aicher and Dill-Langer (1997). The researchers found that climate variations between 50% and 90% RH cause additional tensile stress levels up to 0.32 to 0.52 MPa when acting simultaneously with a tensile stress of 0.2 MPa.

However, the latter study as well as other studies investigating moisture gradients in glulam (Angst and Malo 2012a; Jönsson 2004; Angst and Malo 2011) have shown that moisture induced stresses can easily be in the range of the characteristic tensile strength perpendicular to grain of glulam. Thus, these stresses might in principle be treated as an additional load. Considering design calculations according to the European standard for a case with both external and moisture loads, it will however be hard to fulfill the requirements for the limit state (as the characteristic strength is already reached by the moisture load).

5.3 Coating of glulam beams

A possibility to avoid or to limit moisture gradients and thus moisture induced stresses is to apply a coating on the surface of the beam which is exposed to weather conditions.

Generally, glulam can be surface-treated using the same products and methods as ordinary timber. In order to protect outdoor structures of glulam or timber, which are subjected to large moisture content variations, surface finishes can be applied. These protect the surfaces from weathering and affect the rate at which absorption and desorption occur. To ensure durability, surface treatment has to be maintained, whereby the maintenance intervals depend on the placing of the structure and the type of surface treatment (Glulam handbook 2003).

The surface finishes used for outdoor timber can be divided into two groups: Penetrating and film-forming finishes, whereby the latter are generally more durable. Penetrating finishes can penetrate the wood cell walls. They include transparent or colored water-repellent preservatives (WRPs), oil-based semitransparent stains and oils that do not form a film (paraffin oil). Most often, these are applied by brush. The film-forming finishes, ranked according to their effectiveness (from least to most), include varnish, waterborne latex stains (acrylic polymers), and paints (solvent-borne alkyds, waterborne latex). Paints are film-forming coatings giving the most protection against weathering, by a.o. retarding penetration of moisture. The film-forming finishes are usually applied by brush, sprayer or roller (Sam Williams 2010).

Surface finishes provide protection against weathering, but they do not prevent decay against fungal attacks, for example. For certain structural components or for certain exposures additional protection may be required. In such cases, chemical preservatives or surface finishes combined with chemical preservatives can be applied. Wood preservatives can be divided into two groups: Oil-type

preservatives (e.g. creosote, pentachlorophenol), and waterborne preservatives (e.g. ACC, ACZA, CCA, Boron), whereby the latter can be combined with surface treatments. The oil-type preservatives, which are applied without surface treatment, provide a.o. protection from weathering. Creosote and pentachlorophenol solutions are well suited for outdoor structures, but, for reasons of workers' safety, need to be used with great care. Generally, wood preservatives can be applied by pressure-treatment, which is more effective, or by non-pressure processes. In both cases, studies have shown that small amounts of preservative components are released into the environment (Lebow 2010).

Studies dealing with coating of timber in the literature mainly compare different surface treatment systems with respect to their effect on the average moisture content of the wood. However, studies investigating the effect of coating on moisture induced stresses are scarce.

Comparison of different surface treatments

One experimental study investigated the effectiveness of four surface treatments during 2 years of weathering (Roux et al. 1988). The treatments included: impregnating stain, film-forming stain, pigmented acrylic latex paint, and pigmented alkyd paint. The latter two treatments were found to be most durable as they were mostly intact after 2 years of weathering, whereas the treatments with stains started to show damages after 9 months. In addition, also the moisture exchange damping efficiency was determined. This factor, being 0% for uncoated wood, was highest (77%) for alkyd paint, and between 37 and 47% for the other treatments. This factor was higher in the beginning, but decreased rapidly as the surface finishes (stains) started to develop cracks.

Another study investigated a solvent-borne alkyd coating and two waterborne acrylic coatings with different layer thickness (2 and 4 layers) applied on defect-free spruce (de Meijer and Militz 2000). The samples were exposed to liquid water and the average moisture content over time was measured. After 1700 hours the uncoated sample exhibited the largest increase in moisture content (20 – 30%), followed by the two waterborne acrylic coatings (17-23%), and the solvent-borne coating (15 – 18%). The study also investigated the diffusion properties in coated and uncoated samples and concluded that moisture content profiles in coated wood could best be modelled by adapting the moisture flux at the surface according to the coating and using the diffusion coefficient of uncoated wood.

Further studies comparing the effect of different paint systems, however generally in other contexts, can be found in the literature review by Fredriksson (2010).

Effect of coating on moisture induced stresses

A numerical study performed by Häglund (2010) investigated the effect of paint on the moisture induced tensile stress of glulam subjected to outdoor climate variations. The effect of the paint was taken into account by reducing the mass transfer coefficient (surface emission coefficient): Guideline values for the water vapour resistance for paint (alkyd paint and acrylic plastic) were taken as a basis and converted to a mass transfer coefficient (here 1/50 of the value for uncoated glulam). The results of the parametric study showed that the mass transfer coefficient had a significant effect on stresses, and – as expected – by lowering this coefficient, the stress levels could be considerably reduced.

Another numerical study (Fragiacomo et al. 2011) investigated the effectiveness of different coatings; alkyd oil paint, PVC lacquer, and vinyl paint. Again, the effect of the coatings was taken into account by reducing the surface emission coefficient. The maximum tensile stresses perpendicular to grain and the yearly variations of average moisture content (in a depth of 10 mm) were calculated for glulam cross sections exposed to different European climates during 1 and 10 years. The MC variations were found to be largest in uncoated glulam, followed by alkyd oil painted glulam (51% lower), PVC lacquered glulam (93% lower), and vinyl painted glulam (99% lower). The maximum stress in alkyd oil painted glulam was 13 – 16 % and in PVC lacquered glulam <0.1 % of the stress value calculated for uncoated glulam. Thus, it was concluded that the application of a protective coating was an effective measure to reduce moisture variations and, therefore, moisture induced stresses and cracking. However, the stress level in uncoated glulam seems very high (between 4 and 6.7 MPa) compared to the results of other studies. Also only stresses at the surface or close to the surface were regarded, and large tensile stresses in the centre of the cross section, which especially develop during wetting, were not considered. Furthermore, it is not clear, where the surface emission coefficients for the different coatings were taken from as no references were given in the paper.

An experimental study dealing with duration of load effects in curved glulam beams, investigated a.o. the effect of surface treatment with alkyd paint on glulam beams subjected to cyclic RH variations between 40 and 85% RH (Ranta-Maunus 1998). The results showed that in painted beams, the DOL effect resulted

almost only from the wood material getting weaker due to accumulating damage, thus being similar to the DOL effect of uncoated beams subjected to constant RH. In uncoated beams subjected to cyclic RH variations, however, the DOL effect was more severe, as the DOL effect resulted from both material getting weaker and from changed stress distributions caused by creep and hygroexpansion. Calculations of moisture loads showed that a good surface coating (here with alkyd paint) would decrease the moisture load from 0.15 to 0.05 MPa, which is a reduction by ca. 70%.

The few studies reviewed above suggest that coating is very effective in keeping moisture ingress low and thus lead to low moisture induced stresses. However, this requires an undamaged coating for the entire service life. Small damages such as cracks on the treated surface will probably affect the effectiveness of the coating, which has also been shown by the study performed by Roux et al. (1988). If coatings are to reduce moisture induced stresses to ensure structural safety, it is thus critical that they remain crack-free and undamaged. Degradation of coatings might, however, remain unnoticed by owners or their repair or replacement might take time and lead to temporarily exposed timber. In this case, arising moisture induced stresses could be a severe safety issue.

5.4 Reinforcement perpendicular to grain

Another approach to deal with moisture induced stresses is to enhance the low strength perpendicular to grain of glulam by reinforcement. Effective reinforcement can be achieved by gluing and/or nailing plywood to the sides of the beam or by gluing in rods or threaded bolts perpendicular to the beam. The use of self-tapping screws as reinforcement has several advantages compared to other reinforcement methods. Screws do not change the appearance of the beam, as they are drilled inside, and are thus invisible from the outside of the beam. Moreover, the increased bending and torsion capacities of the screws enable them to be used without pre-drilling the holes, which makes them more time efficient. The use of reinforcement can have major advantages: It can increase the mechanical properties, which in turn allows to reduce the dimension of the wooden member and also to introduce lower wood grades.

Furthermore, different experimental studies investigating the performance of screw reinforcements have shown that with a reinforcement the ductility is enhanced. One of these studies (Blass and Bejtka 2003) investigated the efficiency of self-tapping scews used as a reinforcement in structural details where stresses

perpendicular to grain occur. These included notched beam supports and beams with holes. Reinforced beams subjected to bending reached higher ultimate loads and showed a ductile failure compared to non-reinforced specimens, which failed in a brittle way.

Trautz and Koj (2008) investigated the load bearing and deformation characteristics of reinforced glulam beams. They performed bending tests on glulam beams reinforced with self-tapping screws positioned as tension struts under an angle of 45°. The reinforced specimens showed an increased stiffness compared with non-reinforced specimens. While non-reinforced specimens failed due to extensive delamination, the reinforced specimens exhibited a local failure perpendicular to the beam axis. Thus, the screw reinforcement provided a diminution of delamination during failure. Further, the coaction of scattered defects in different laminates was reduced due to the reinforcement.

Jönsson (2005a) investigated the load carrying capacity of curved glulam beams ($W*H$ = 90*280 mm^2) reinforced with self-tapping screws perpendicular to grain by means of a 4-point bending test. The beams were seasoned in 40% RH or 80% RH. The unreinforced beams failed predominantly in tension perpendicular to grain, whereas the reinforced beams failed in shear, but exhibited also a brittle failure mode. The stiffness of reinforced beams was the same as for the unreinforced beams, but the strength, however, was increased by 40-50%. After failure, the unreinforced beams were reinforced and tested again and reached 10-20% higher strength. The stiffness was in the same order of magnitude, while the deformation capacity was approximately doubled.
Other unreinforced beams were subjected to drying from 80 to 40% RH or wetting from 40 to 80% RH before being tested in 4-point bending. After failure, these beams were reinforced and tested again. In the wetting case, the strength was increased by 30%, while in the drying case, there was no increase in strength.

The present author (Angst and Malo 2012b) studied the effect of self-tapping screws on moisture induced stresses arising in glulam ($W*H$ = 90*270 mm^2) exposed to wetting from 50 to 90% RH and drying from 90 to 50% RH. The study was performed by means of both experiments and numerical simulations. The large tensile stresses perpendicular to grain (average stresses), which arise in the cross section centre during wetting exposure, were found to be significantly reduced by the screw reinforcement. Compared to unreinforced glulam beams, a reduction by ca. 30 to 70% could be achieved depending on screw distance. Moreover, the (average) tensile stresses arising between the screws (in

longitudinal beam direction) were found to strongly depend on geometric properties of the beam (cross section width, geometrical configuration). For drying exposure, the results showed that the screw reinforcement had a negative effect, by slightly increasing the tensile stresses at the cross section border. However, as these stresses were considerably lower than stresses during wetting, the positive effect of the reinforcing screw for wetting exposures is believed to predominate. For rather extreme climate variations, though, the negative effect of the reinforcing screw during drying exposure was more pronounced (Appendix A).

5.5 Summary

Three different approaches to deal with moisture induced stresses have been discussed. First, moisture induced stresses could be considered as a load case in design calculations. As suggested by several authors, this is a more transparent approach than the common practice of taking moisture effects into account by a strength reducing factor. However, both experimental and numerical studies – including results from the present thesis – have shown that moisture induced stresses can easily reach the level of the characteristic tensile strength of glulam perpendicular to grain. Thus, in order to increase the capacity to bear external structural loads or to mitigate cracking, additional measures have to be taken. One possibility is to apply a coating on the beam surface. This reduces moisture ingress and keeps thus moisture induced stresses low. The few existing studies in this field have shown that this is a very effective measure. However, the long-term effectiveness of coatings, especially when cracks develop on the treated surface, is not known. A further method to deal with moisture induced stresses is the use of reinforcement, which acts by enhancing the low tensile strength of glulam perpendicular to grain. An economic reinforcement type is the use of self-tapping screws, which was found to increase both load bearing capacity and ductility of beams. However, the performance of screw reinforced glulam beams in varying climates has not been sufficiently studied and is thus not well-understood.

6 CONCLUSIONS AND FUTURE WORK

6.1 Summary and conclusions

The present study provides a deeper knowledge about the effect of climate variations in glulam members. The development of moisture induced stresses is studied, as well as the different parameters affecting the calculation and the stress levels. Moisture induced stresses can be obtained either through experiments or by means of numerical simulations, the latter being more common in the literature due to the smaller amount of work and equipment.

In **paper I** (Angst and Malo 2010) a review of the parameters and mathematical models commonly applied for numerical simulations of moisture induced stresses in glulam was presented. Models and parameters from the literature were compared and the relative influence of these on calculated moisture induced stresses was evaluated. It was concluded that geometrical properties as well as material parameters had a significantly stronger effect on the simulation results than the selected mathematical formulations of mechanosorption.

Based on the results from **paper I**, an experimental study was performed in **paper II** (Angst and Malo 2012a), with the objective of obtaining a comprehensive set of parameters suitable for calibration of numerical models. Glulam specimens were subjected to one-dimensional wetting and drying perpendicular to grain, before material parameters and moisture induced stresses were determined. The study revealed that the material parameters, which comprised the moduli of elasticity and the hygroexpansion coefficients (both measured on slices cut along the cross section height), were strongly affected by the geometrical configuration (pith locations) of the specimens. Thus, this also affects the level of the calculated internal stresses. Furthermore, the experiments confirmed previous studies, namely that moisture induced stresses, which developed during wetting were significantly larger than corresponding stresses during drying. In the wetting case, the measured tensile stresses clearly exceeded the characteristic tensile strength of glulam. Thus, although mechano-sorptive creep effects were found to strongly reduce the internal stresses, the remaining stresses were still of a considerable magnitude.

Based on the findings and the measured parameters from **paper II**, a numerical study was performed in **paper III** (Angst and Malo 2011), where various glulam

cross sections subjected to wetting were investigated. Wetting exposures were selected, because they are known to result in significantly larger stresses than corresponding drying exposures. The main parameters were the cross section width and its geometrical configuration (based on 24 visually recorded cross section configurations). The study concluded that local moisture induced stresses were significantly larger than average stresses (average over cross section height). The local stresses were found to strongly depend on the annual ring pattern of the laminates in the glulam cross section. Especially the presence or absence of piths within the laminates, but also the location of piths within the cross section mainly affected the magnitude of local stresses. It was concluded, that in some cases the local tensile stresses could lead to cracking in the cross section even without external load and thus reduce the load bearing capacity of the member. Finally, the comparison of different cross section widths revealed that the wider a cross section was, the longer it took until large stresses arose.

Based on the results from **paper II** and **paper III**, the use of screw reinforcement was studied in **paper IV** (Angst and Malo 2012b), by means of both experiments and numerical simulations. The model parameters for modelling reinforced specimens during wetting were found to correspond to the ones applied for modelling unreinforced specimens (**paper III**), due to the observation that both specimens exhibit similar mechano-sorptive creep behaviour. The large tensile stresses arising during wetting were found to be significantly reduced by a screw reinforcement in the cross section centre. With screw distances from 70 to 210 mm, stress reductions by 70 to 30% were achieved (compared to unreinforced glulam beams). Moreover, the study revealed that the tensile stresses arising between the reinforcing screws were not only depending on screw distance, but to a large extent also on cross section width and annual ring pattern of the laminates. During drying, the tensile stresses at the cross section border were found to be slightly increased due to the additional restraint caused by the screw. However, as the overall stresses during drying were in general significantly lower than during wetting, the advantages using a screw during wetting were believed to outweigh the disadvantages during drying.

6.2 Future research work

Based on the state of the art of moisture induced stresses in glulam as well as on the new findings summarised above, the following research topics are believed to be of major importance:

- Coating: Coating of glulam beams seems to be a possible measure against large moisture induced stresses. However, experimental measurements investigating the effect of a specific coating on the moisture induced stress level are lacking. Similarly, the long term efficiency of different coatings and the behaviour during their degradation are currently not well understood.

- Reinforcement: Another measure to deal with moisture induced stresses is the use of reinforcement perpendicular to grain. One method is to use self-tapping screws, which has shown satisfying results in constant climates. The performance of screw reinforcement in climatic variations, however, is at present not well understood.

- Impact of cracking: How do the cracks, which may be induced by high local moisture induced stresses, affect the glulam member, especially its load bearing capacity?

- Geometrical configuration: Results of the present thesis have indicated that moisture induced stresses can be reduced by optimising cross section design (orientation of laminates, piths, etc.). Further research work is required in this regard.

7 REFERENCES

Aicher S, Dill-Langer G (1997) Climate induced stresses perpendicular to the grain in glulam. Otto-Graf-Journal 8:209-231

Aicher S, Dill-Langer G (2005) Effect of lamination anisotropy and lay-up in glued-laminated timbers. Journal of Structural Engineering 131:1095-1103

Aicher S, Dill-Langer G, Ranta-Maunus A (1998) Duration of load effect in tension perpendicular to the grain of glulam in different climates. Holz als Roh- und Werkstoff 56 (5):295-305

Angst V, Malo KA (2010) Moisture induced stresses perpendicular to the grain in glulam: Review and evaluation of the relative importance of models and parameters. Holzforschung 64:609-617

Angst V, Malo KA (2011) Moisture induced stresses in glulam cross sections during wetting exposures. Submitted to Wood Science and Technology

Angst V, Malo KA (2012a) The effect of climate variations on glulam - an experimental study. European Journal of Wood and Wood Products DOI 10.1007/s00107-012-0594-y

Angst V, Malo KA (2012b) Effect of self-tapping screws on moisture induced stresses in glulam. Submitted to Engineering Structures

Astrup T, Clorius CO, Damkilde L, Hoffmeyer P (2007) Size effect of glulam beams in tension perpendicular to grain. Wood Science and Technology 41:361-372

Blass HJ, Bejtka I (2003) Querzugverstärkungen in gefährdeten Bereichen mit selbstbohrenden Holzschrauben (in German). Kurzberichte aus der Bauforschung, vol 44.

Blass HJ, Schmid M (2001) Querzugfestigkeit von Vollholz und Brettschichtholz (in German). Holz als Roh- und Werkstoff 58:456-466

Dahl KB (2009) Mechanical properties of clear wood from Norway spruce. PhD Thesis, Department of Structural Engineering, Norwegian University of Science and Technology, Trondheim

de Meijer M, Militz H (2000) Moisture transport in coated wood. Part 1: Analysis of sorption rates and moisture content profiles in spruce during liquid water uptake. Holz als Roh- und Werkstoff 58:354-362

Dinwoodie JM (2000) Timber - Its nature and behaviour (2nd ed.). E & FN SPON, London and New York

Ehlbeck J, Kürth J (1992) Einfluss des querzugbeanspruchten Volumens auf die Tragfähigkeit gekrümmter Träger und Satteldachträger aus Brettschichtholz (in German). Holz als Roh- und Werkstoff 50:33-40

Eurocode 5 (2004) Design of timber structures - Part 1-1: General - Common rules and rules for buildings. European committee for standardization, Brussels

Fortino S, Mirianon F, Toratti T (2009) A 3D moisture-stress FEM analysis for time dependent problems in timber structures. Mechanics of Time-Dependent Materials 13:333-356

Fragiacomo M, Fortino S, Tononi D, Usardi I, Toratti T (2011) Moisture-induced stresses perpendicular to grain in cross-sections of timber members exposed to different climates. Engineering Structures 33:3071-3078

Fredriksson M (2010) A critical literature review of moisture and temperature conditions in wood exposed outdoors above ground. Division of Building Materials, Lund Institute of Technology, Report TVBM-3152 edn., Lund, Sweden

Frese M, Blass HJ (2007) Failure analysis on timber structures in Germany - a contribution to COST action E55. Paper presented at the First Workshop May 2007, Graz University of Technology, Austria

Frühwald E, Serrano E, Toratti T, Emilsson A, Thelandersson S (2007) Design of safe timber structures - How can we learn from structural failures in concrete, steel and timber? Division of Structural Engineering, Lund Institute of Technology, Report TVBK-3053 edn., Lund, Sweden

Gereke T, Niemz P (2010) Moisture-induced stresses in spruce cross-laminates. Engineering Structures 32:600-606

Glass SV, Zelinka SL (2010) Moisture Relations and Physical Properties of Wood. In: Wood Handbook - Wood as an Engineering Material (Centennial ed.). Forest Products Laboratory, Department of Agriculture, Forest Service, Madison, Wisconsin

Glulam handbook (2003) Svenskt Limträ AB, Stockholm, available from http://www.svensktlimtra.se/en/signin/signin.asp

Gowda S, Kortesmaa M, Ranta-Maunus A (1998) Duration of load effect on curved glulam beams - Part 2: Long term load tests and analysis. VTT Publications 334

Grossman PUA (1976) Requirements for a model that exhibits mechano-sorptive behaviour. Wood Science and Technology 10:163-168

Gustafsson PJ (2003) Fracture perpendicular to grain - structural applications. In: Timber engineering. Thelandersson S, Larsen HJ (eds), John Wiley & Sons Ltd, Chichester, England, pp 103-130

Hanhijärvi A (2000) Advances in the knowledge of the influence of moisture changes on the long-term mechanical performance of timber structures. Materials and Structures 33:43-49

Hoffmeyer P (2003) Strength under long-term loading. In: Timber engineering. Thelandersson S, Larsen HJ (eds), John Wiley & Sons Ltd, Chichester, England, pp 131-152

Hoffmeyer P, Davidson RW (1989) Mechano-sorptive creep mechanism of wood in compression and bending. Wood Science and Technology 23:215-227

Häglund M (2008) Varying moisture content and eigen-stresses in timber elements. Wood Material Science and Engineering 1-2:38-45

Häglund M (2010) Parameter influence on moisture induced eigen-stresses in timber. European Journal of Wood and Wood products 68:397-406

Häglund M, Carlsson F (2008) Extreme value analysis of moisture induced eigenstresses in timber. Paper presented at the World Conference on Timber Engineering (WCTE), Miyazaki, Japan

Häglund M, Carlsson F (2010) Load combination of moisture induced eigenstresses in timber. Paper presented at the World Conference on Timber Engineering (WCTE), Trentino, Italy

Jönsson J (2004) Internal stresses in the cross-grain direction in glulam induced by climate variations. Holzforschung 58:154-159

Jönsson J (2005a) Load-carrying capacity of curved glulam beams reinforced with self-tapping screws. Holz als Roh- und Werkstoff 63:342-346

Jönsson J (2005b) Moisture induced stresses in timber structures. PhD Thesis, Division of Structural Engineering, Lund Institute of Technology, Sweden

Jönsson J, Svensson S (2004) A contact free measurement method to determine internal stress states in glulam. Holzforschung 58:148-153

Jönsson J, Thelandersson S (2003) The effect of moisture gradients on tensile strength perpendicular to grain in glulam. Holz als Roh- und Werkstoff 61 (5):342-348

Karacabeyli E, Popovski M (2003) Design for earthquake resistance. In: Timber engineering. Thelandersson S, Larsen HJ (eds), John Wiley & Sons Ltd, Chichester, England, pp 267-299

Koponen H (1983) Diffusion and surface emission coefficients of birch, pine and spruce and their dependence on wood properties. Paperi ja puu 65 (10):619-624

Lebow ST (2010) Wood Preservation. In: Wood Handbook - Wood as an Engineering Material (Centennial ed.). Forest Products Laboratory, Department of Agriculture, Forest Service, Madison, Wisconsin

Mårtensson A (1994a) Creep behavior of structural timber under varying humidity conditions. Journal of Structural Engineering 120 (9):2565-2582

Mårtensson A (1994b) Mechano-sorptive effects in wooden material. Wood Science and Technology 28:437-449

Mårtensson A, Svensson S (1997) Stress-strain relationship of drying wood - Part 1: Development of a constitutive model. Holzforschung 51:472-478

Mårtensson A, Thelandersson S (1990) Effect of moisture and mechanical loading on wooden materials. Wood Science and Technology 24:247-261

Ormarsson S (1999) Numerical analysis of moisture-related distortions in sawn timber. PhD Thesis, Department of Structural Mechanics, Chalmers University of Technology, Göteborg

Ormarsson S, Dahlblom O, Petersson H (1998) A numerical study of the shape stability of sawn timber subjected to moisture variation - Part 1: Theory. Wood Science and Technology 32:325-334

prEN 14080 (2011) Timber structures - Glued laminated timber and glued solid timber. European committee for standardization, Brussels

Ranta-Maunus A (1975) The viscoelasticity of wood at varying moisture content. Wood Science and Technology 9:189-205

Ranta-Maunus A (1993) Rheological behaviour of wood in directions perpendicular to the grain. Materials and Structures 26:362-369

Ranta-Maunus A (1998) The effect of weather changes and surface coating on the load bearing capacity of curved glulam structures. Paper presented at the World Conference on Timber Engineering (WCTE), Montreux, Switzerland

Ranta-Maunus A (2001) Moisture Gradient as Loading of Curved Timber Beams. Paper presented at the IABSE Conference: Innovative Wooden Structures and Bridges, Lahti, Finland

Ranta-Maunus A (2003) Effects of climate and climate variations on strength. In: Timber engineering. Thelandersson S, Larsen HJ (eds), John Wiley & Sons Ltd, Chichester, England, pp 153-167

Rosenkilde A, Arfvidsson J (1997) Measurement and evaluation of moisture transport coefficients during drying of wood. Holzforschung 51 (4):372-380

Roux M-L, Wozniak E, Miller ER, Boxall J, Böttcher P, Kropf F, Sell J (1988) Natural weathering of various surface coatings on five species at four European sites. Holz als Roh- und Werkstoff 46:165-170

Salin J-G (1992) Numerical prediction of checking during timber drying and a new mechano-sorptive creep model. Holz als Roh- und Werkstoff 50:195-200

Sam Williams R (2010) Finishing of Wood. In: Wood Handbook - Wood as an Engineering Material (Centennial ed.). Forest Products Laboratory, Department of Agriculture, Forest Service, Madison, Wisconsin

Svensson S, Toratti T (2002) Mechanical response of wood perpendicular to grain when subjected to changes of humidity. Wood Science and Technology 36:145-156

Thelandersson S (2003) Timber engineering - general introduction. In: Timber engineering. Thelandersson S, Larsen HJ (eds), John Wiley & Sons Ltd, Chichester, England, pp 1-11

Trautz M, Koj C (2008) Mit Schrauben bewehren (in German). Bautechnik 85:190-196

Virta J, Koponen S, Absetz I (2006) Measurement of swelling stresses in spruce (Picea abies) samples. Building and Environment 41:1014-1018

Zhou HZ, Zhu EC, Fortino S, Toratti T (2009) Modelling the hygrothermal stress in curved glulam beams. Accepted for publication in Journal of Strain Analysis 45:129-140

Paper I

Moisture induced stresses perpendicular to the grain in glulam: Review and evaluation of the relative importance of models and parameters

Vanessa Angst and Kjell A. Malo

Holzforschung 64 (2010) 609–617

Holzforschung, Vol. 64, pp. 609–617, 2010 • Copyright © by Walter de Gruyter • Berlin • New York. DOI 10.1515/HF.2010.089

Moisture induced stresses perpendicular to the grain in glulam: Review and evaluation of the relative importance of models and parameters

Vanessa Angst* and Kjell A. Malo

Department of Structural Engineering, NTNU Norwegian University of Science and Technology, Trondheim, Norway

*Corresponding author.
Department of Structural Engineering, NTNU Norwegian University of Science and Technology, Richard Birkelandsvei 1A, N-7491 Trondheim, Norway
E-mail: vanessa.angst-nicollier@ntnu.no

Abstract

Stresses perpendicular to the grain arising from moisture changes might cause cracks and thereby severely affect the load bearing capacity and serviceability of timber structures. The present paper reviews parameters and mathematical models commonly applied for numerical simulation of moisture-induced stresses in glulam members. The basis of the calculations is a hygro-mechanical model coupled with a moisture transport model. Several models and ranges of parameters reported in the literature are compared and the significance of the parameter selection is evaluated. It was found that geometrical properties as well as material parameters have a significantly stronger effect on the outcome of the simulations than the selection of a certain numerical formulation of mechanosorption.

Keywords: glulam; mechanosorption; moisture-induced stresses; numerical simulation.

Introduction

Timber structures are usually subjected to climatic changes of the surrounding environment. As a result of varying relative humidity (RH) in the ambient air, moisture gradients occur in the timber elements and induce stresses. Stresses perpendicular to the grain might cause cracks to develop in the longitudinal direction and thus severely affect the load-bearing capacity and serviceability of timber members. Indeed, tension perpendicular to the grain is the most common failure mode (Frese and Blass 2007; Frühwald et al. 2007).

The increased cross-section sizes and the higher share of engineered and highly stressed connections, which have been utilized in past decades, make the structures more vulnerable to crack development. To be able to investigate crack problems related to moisture-induced stresses (MiS), moisture-related models are needed together with engineering tools such as the finite element method and design standards. However, models taking into account the effects of moisture are not common in engineering standards. In fact, the knowledge about such models and their application is moderate in the engineering community.

Extensive work on the numerical simulation of MiS has been undertaken by many researchers. Usually, constitutive relations between stress, strain, and moisture changes are used to describe the physical and mechanical behavior of timber exposed to climatic changes. It is well known that there is a strong interaction between mechanical response and moisture variations, which is usually referred to as mechanosorptive creep. Over the years, several formulations have been proposed to describe mechanosorptive creep, most of which are restricted to one dimension. In recent years a few two-dimensional (2D) and three-dimensional (3D) models have also been developed.

The main purpose of the present study is to review some models and parameters reported in the literature to evaluate the relative influence of these various mathematical models and material parameters on calculated MiS. Thus, the present paper contributes to a basis for the selection of both an appropriate model and material parameters for evaluation of MiS in glulam members under service life conditions. In the present case, numerical simulations of MiS have been performed and the results obtained by different models and parameters have been compared.

The approach adopted is as follows: a constitutive model for the computation of drying and wetting stresses perpendicular to the grain in glulam is chosen. As a first step, the transient moisture distribution in the timber is determined by a moisture transport model. Based on this distribution, the MiS can be computed using a hygro-mechanical model. For the stress calculation, different mechanosorption models and material parameters are applied, and then compared with respect to stress development versus time to evaluate the effect of various input parameters. Both one-dimensional (1D) and 2D analyses have been performed.

Theory

Moisture transport model

The most common approach to describe moisture transport in wood is to use Fick's second law of mass diffusion

$$\frac{\partial u}{\partial t} = \frac{\partial}{\partial x}\left(D\frac{\partial u}{\partial x}\right) \quad (1)$$

where u is the moisture content (MC, mass of water/mass of dry wood) and D [$m^2\ s^{-1}$] is the corresponding diffusion coefficient. Although the concept of an effective diffusion coefficient is not able to describe the several parallel transport processes actually taking place in wood, it is commonly used for engineering purposes and gives reasonably accurate results below fiber saturation (Häglund 2007).

There are two different approaches to describe the moisture transport through the surface of the wood. The first type of boundary condition assumes that the MC in the outermost wood layer, u_{surf}, is equal to the equilibrium MC (EMC) corresponding to the RH in the air, u_{eq}:

$$u_{surf} = u_{eq} \quad (2)$$

Changes in the external climate thus affect the state of moisture in the outermost wood layer without any delay. By contrast, the second type of boundary condition takes into account the moisture transfer resistance at the surface, where the flux of moisture is driven by the difference between the surface MC and the EMC:

$$\left(D\frac{\partial u}{\partial x}\right) = S(u_{eq}\text{-}u_{surf}) \quad (3)$$

where S [$m\ s^{-1}$] is the surface emission factor. As the resistance decreases, the surface emission factor increases and the second boundary condition (3) approaches the first boundary condition (2). For the case of water ingress, Shi (2007) found the moisture transfer resistance to be very low and thus suggested that the first type of boundary condition is suitable for modeling absorption processes. In desorption, however, the weight loss of wood specimens was experimentally found to be delayed and thus Shi suggested that the behavior can be described by means of the surface emission coefficient according to Eq. (3).

The values for the diffusion and the surface emission coefficients depend among others on the methods applied for their measurement or determination (Comstock 1963; Cai and Avramidis 1997). Hence, a wide range of values is reported in the literature. Some diffusion coefficients for spruce wood in the cross-grain direction are presented in Figure 1. When different values were proposed for both transversal directions (Koponen 1984), these values are averaged herein. It seems that diffusion coefficients in both transversal directions are the same at low MCs (Koponen 1983; Rosenkilde and Arfvidsson 1997) and very similar at higher MCs. The figure shows that diffusion coefficients in the cross-grain direction scatter widely, particularly above 15% MC, where the scatter is up to one order of magnitude. Furthermore, it shows that diffusion coefficients are usually found to be dependent on MC. Table 1 shows some reported surface emission coefficients for spruce wood in the cross-grain direction. Apparently, the values scatter over two orders of magnitude.

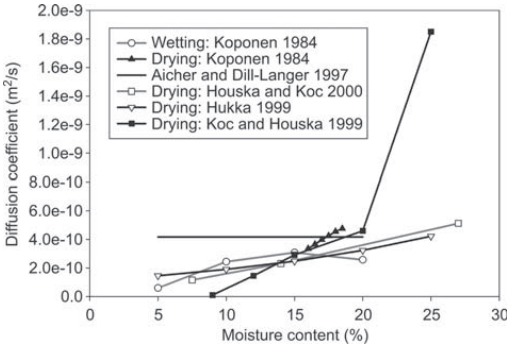

Figure 1 Diffusion coefficients for spruce in the cross-grain direction (at 20±2°C).

Table 1 Surface emission coefficients of spruce at 20±2°C.

Surface emission coefficients ($m\ s^{-1}$)	References
2.2×10^{-8}	Aicher and Dill-Langer 1997
8.36×10^{-8}	Houska and Koc 2000
1.05×10^{-6}	Koc and Houska 2002
12.4×10^{-8}–22×10^{-8}	Koponen 1985

Hygro-mechanical model

The most common approach to describe the hygro-mechanical behavior of timber is by means of a strain rate formulation (Mårtensson 1994a; Aicher and Dill-Langer 1997; Hanhijärvi 2000a).

$$\dot{\varepsilon} = \dot{\varepsilon}_e + \dot{\varepsilon}_s + \dot{\varepsilon}_{ms} + \dot{\varepsilon}_c \quad (4)$$

Here $\dot{\varepsilon}$ is the total strain rate, $\dot{\varepsilon}_e = \dot{\sigma}/E$ the elastic, $\dot{\varepsilon}_s = \alpha\dot{u}$ the linear shrinkage-swelling, $\dot{\varepsilon}_{ms}$ the mechanosorptive creep, and $\dot{\varepsilon}_c$ is the time-dependent creep strain rate. Parameters σ, E, α, and u are the stress, the elastic modulus, the hygro-expansion coefficient, and the MC, respectively.

Mechanosorptive creep In the literature, different models are proposed for mechanosorptive creep; these models describe the simultaneous effect of mechanical and moisture loading on wood. A general review about the different types of models is given in Hanhijärvi (2000a). Initially, models were formulated for the mechanosorptive effects on timber beams in the grain direction, which result in increased deflections (Leicester 1971; Ranta-Maunus 1975; Mårtensson 1994a,b). Later, a closely related research area was the numerical simulation of timber drying, where creep perpendicular to the grain is important, because it enables relaxation of drying stresses (Salin 1992; Mårtensson and Svensson 1997a,b; Hanhijärvi 2000b; Häglund 2008).

Some mechanosorptive creep models proposed in the literature are listed in Table 2 for the numerical simulation of

Table 2 Mechanosorptive creep models from the literature.

	Models	Parameters for spruce	References
Maxwell type models			
1a	$\begin{bmatrix}\dot{\varepsilon}^{r}_{ms}\\ \dot{\varepsilon}^{t}_{ms}\\ \dot{\gamma}^{rt}_{ms}\end{bmatrix}=\begin{bmatrix} m_r & -\mu_{tr}m_t & 0\\ -\mu_{rt}m_r & m_t & 0\\ 0 & 0 & m_{rt}\end{bmatrix}\begin{bmatrix}\sigma_r\\ \sigma_t\\ \tau_{rt}\end{bmatrix}\lvert\dot{u}\rvert$	m_r=0.15 MPa^{-1}, m_t=0.2 MPa^{-1}, m_{rt}=0.8 MPa^{-1}, μ_{rt}=1, μ_{tr}=0.75	Ormarsson 1999
1b	$\dot{\varepsilon}_{ms}=\sigma\left(m\lvert\dot{u}\rvert-\beta\dot{u}\right)$	m=0.085 MPa^{-1}, β=0.045 MPa^{-1} (parameters from Häglund)	Aicher and Dill-Langer 1997; Häglund 2008
Kelvin type models			
2a	For wetting: $\dot{\varepsilon}_{ms}=m\left(\sigma-E_{ms}\varepsilon_{ms}\right)\dot{u}$ General form[b]: $\dot{\varepsilon}_{ms}=m\left(\sigma-E_{ms}\varepsilon_{ms}\right)\lvert\dot{u}\rvert$	m=0.2 MPa^{-1}, E_{ms}=69 MPa (parameters and model from Virta et al. for wetting)	Salin 1992; Virta et al. 2006[a]
2b	$\begin{bmatrix}\dot{\varepsilon}^{r}_{ms}\\ \dot{\varepsilon}^{t}_{ms}\\ \dot{\gamma}^{rt}_{ms}\end{bmatrix}=\begin{bmatrix} \kappa_r & -\mu_{tr}\kappa_t & 0\\ -\mu_{rt}\kappa_r & \kappa_t & 0\\ 0 & 0 & \kappa_{rt}\end{bmatrix}\begin{bmatrix}\sigma_r\\ \sigma_t\\ \tau_{rt}\end{bmatrix}\lvert\dot{\varepsilon}^{t}_{s}\rvert-\frac{1}{s_{\max}}\begin{bmatrix}\beta_r & 0 & 0\\ 0 & \beta_t & 0\\ 0 & 0 & \beta_{rt}\end{bmatrix}\begin{bmatrix}\varepsilon^{r}-\varepsilon^{r}_{s}\\ \varepsilon^{t}-\varepsilon^{t}_{s}\\ \gamma^{rt}\end{bmatrix}\lvert\dot{\varepsilon}^{t}_{s}\rvert$	κ_t=0.7 MPa^{-1}, κ_r=0.3 MPa^{-1}, κ_{rt}=2.5 MPa^{-1}, μ_{rt}=1, μ_{tr}=0.38, $s_{\max}$~0.06, β_{rt}=0, β_{t1}=2, β_{t2}=4, β_{r1}=1.8, β_{r2}=3.8 (index 1: for drying, index 2: for wetting)	Mårtensson and Svensson 1997b

Note: The free shrinkage rate in tangential direction, $\dot{\varepsilon}^{t}_{s}$, is used in all directions.
Note: In the original reference the strain rates are expressed as functions of free shrinkage and not time.

Terms: $\dot{\varepsilon}_{ms}$, mechanosorptive creep strain rate; σ, τ, stress; $\dot{u}$, moisture content rate; m, μ, β, κ, mechano-sorptive creep parameters; E_{ms}, retardation coefficient of mechanosorptive creep; $\dot{\varepsilon}_{s}$, linear shrinkage-swelling strain rate; ε, γ, total strain; $s_{\max}$, value of the total shrinkage from green to dry condition.
[a] Note that the model by Virta et al. (2006) is not as presented in the original reference. The authors of the present paper assume that there was a (typing) error in the model and that it actually should be the same model as Salin (1992).
[b] To perform both wetting and drying analyses with the model by Virta et al. (2006), which was developed for wetting analyses only, the general form is used.

timber drying or wetting. Maxwell-type models are common. However, several researchers have remarked that this type of model gives unsatisfactory results for timber under-loading, because recovery cannot be described when unloading takes place. Consequently, new and more advanced Kelvin-type models were proposed, which are able to describe recovery (Salin 1992; Mårtensson and Svensson 1997a,b; Hanhijärvi 2000b; Svensson and Mårtensson 2002; Svensson and Toratti 2002). In Table 2, only the two most straightforward Kelvin-type models are presented, with corresponding parameters. Apart from the models of Ormarsson (1999) and by Mårtensson and Svensson (1997b), the models are restricted to one dimension. Models that did not provide parameters for spruce were not considered in the present review.

Time-dependent creep Different approaches were proposed to account for time-dependent creep. A good fitting of experimental creep behavior can be obtained by rheological models (Hanhijärvi 2000b). Simpler mathematical expressions are sometimes preferred (Aicher and Dill-Langer 1997). A successful mathematical description of creep in timber, under constant RH and temperature, is the power law (Ranta-Maunus 1993). Another simple way to include creep effects is to reduce the elastic modulus, so that a larger immediate increase in strain is obtained (Mårtensson and Svensson 1997a; Jönsson 2005). This is also the approach in Eurocode 5, where the reduction depends on the climatic environment and can be up to 30% of the mean modulus of elasticity (MOE) (Eurocode 2004).

However, there is agreement that the effect of time-dependent creep at low MCs and temperatures is small compared with mechanosorptive creep (Mårtensson and Svensson 1997a; Toratti and Svensson 2000; Virta et al. 2006). The former is therefore often ignored (e.g., Ormarsson et al. 1998; Svensson and Toratti 2002; Häglund 2008). By contrast, in some of the hygro-mechanical models that explicitly omit time-dependent creep, the input values for the MOE were lower than corresponding data of the literature. Often, a constant MOE, taken at fiber saturation point, has been chosen, instead of an MC dependent MOE. This means that time-dependent creep is in fact not neglected in these models, but implicitly taken into account by using low MOE values.

Calculations

In this study, MiS perpendicular to the grain in glulam was calculated by means of a hygro-mechanical model coupled with a moisture transport model. The influence on the result-

ing stresses was investigated based on several mechanosorption models and varying parameters. The calculations were run on Comsol Multiphysics (2007), a commercial finite element program, which relies on quadratic Lagrangian elements. The setup and the basic condition were chosen according to the experimental tests performed by Jönsson (2004), who investigated glulam specimens ($90\times270\times16$ mm^3, quality L40) which were conditioned in 40 or 80% RH. To ensure a 1D moisture transport perpendicular to the grain, the specimens in these experiments were sealed on four sides before being subjected to wetting from 40 to 80% RH or drying from 80 to 40% RH. Afterwards, the specimens were cut into small slices and the MC, the released strain, and the elastic modulus of each slice were measured and the MC distribution and the MiS were plotted. A schematic representation of Jönsson's experiments is shown in Figure 2.

Whereas the moisture transport model neglects the annual ring orientation of the glulam specimen, the hygro-mechanical model takes it into account by two different approaches for the 1D- and 2D-model (Figure 2). The first approach is in accordance with the work of Häglund (2009), who successfully modeled Jönsson's experiments based on the 1D-model. Häglund calculated an effective MOE and hygro-expansion coefficient for each slice of the glulam specimen with an estimated average angle θ between the x-axis and the tangent to the annual rings for each slice, according to:

$$E_{eff}=\frac{E_R E_T G_{RT}}{E_T G_{RT} m^2\cdot(m^2-n^2\nu_{RT})+E_R G_{RT} n^2\cdot(n^2-m^2\nu_{TR})+E_R E_T m^2 n^2} \quad (5)$$

$$\alpha_{eff}=\alpha_R\cdot m^2+\alpha_T\cdot n^2 \quad (6)$$

where $m=\cos\theta$ and $n=\sin\theta$. In the 1D-model (Figure 2), the MOE and the hygro-expansion coefficient are thus modeled as a function over the cross-section width based on the effective values reported by Häglund. It should be noted that the MOE is not a function of MC; this statement is in agreement with Jönsson (2004), who did not find significant differences when measuring the MOE in specimens conditioned in 40 or 80% RH. The 1D-model is nevertheless implemented in two dimensions as it is not possible to directly run a 1D-stress-strain analysis with Comsol Multiphysics. However, by setting the Poisson ratio equal zero, the stresses in the y-direction become a function of the strains in the y-direction only, and thus, it can be regarded as a 1D-model.

By contrast, the 2D model (Figure 2) takes into account the annual ring orientation of every laminate by defining a local cylindrical coordinate system in each laminate. The origin of the local coordinate systems is located in the pith of a laminate.

Selection of model parameters for the moisture transport model

The selection of the diffusion coefficient in the computations of the moisture distribution is a challenge. In the literature, a wide range of values is proposed (Figure 1) and, as Figure 3 illustrates, the value of this parameter has a strong effect on the resulting MC distribution. The results from the moisture transport model are decisive for the accuracy of the subsequent hygro-mechanical model; hence a diffusion coefficient giving the best fit to the experimental results from Jönsson (2004) is chosen (Table 3). A value fitted to experimental results is more appropriate than data taken from the literature, because the concept of an effective diffusion coefficient is only a very simplified mathematical description of several transport processes actually taking place parallel in the wood during moisture changes (Hukka 1999).

As mentioned above, no distinction is made between radial and tangential directions in the present moisture transport model. Different types of boundary conditions are considered, based on varying MC. The wetting process is modeled according to Eq. (2), whereas a boundary condition according to Eq. (3) is applied for the drying analysis. In the present case, wetting was best modeled with a constant diffusion coefficient, whereas for drying this coefficient is linearly dependent on the MC. The selected parameters are in the range of literature data (Figure 1) and are summarized in Table 3.

In Figure 4, the MC distribution in glulam specimens (initially conditioned at 40 or 80% RH) are compared. The comparisons are made after a single climate change obtained

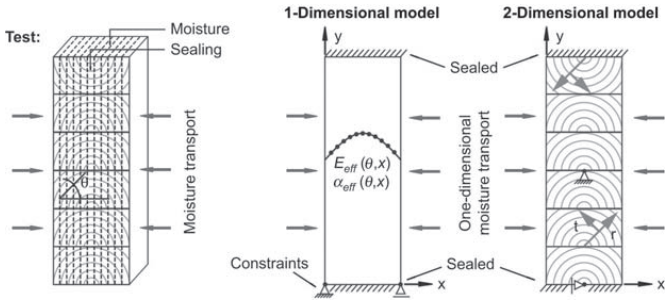

Figure 2 Schematic representation of the experimental setup from Jönsson (2004) and the two approaches used for the hygro-mechanical model.

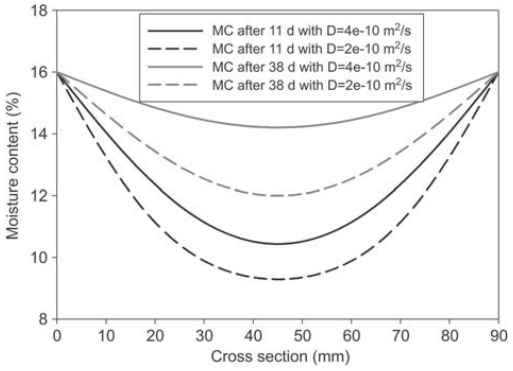

Figure 3 Moisture content distribution in glulam after 11 and 38 days of wetting from 9 to 16% MC, calculated using boundary conditions according to Eq. (2) and different diffusion coefficients based on Figure 1.

Table 3 Parameters for moisture transport models.

Analysis	Boundary condition/parameters
Wetting:	Boundary condition according to Eq. (2):
40→80% RH	u_0=0.09, u_{eq}=0.16, D=3e-10 m^2 s^{-1}
Drying:	Boundary condition according to Eq. (3):
80→40% RH	u_0=0.16, u_{eq}=0.08, S=5e-8 m s^{-1}
	D=2.857e-11* (u)-1.57e-10 m^2 s^{-1}
	(which corresponds to: D=1e-10 for u=0.09, and D=3e-10 for u=0.16)

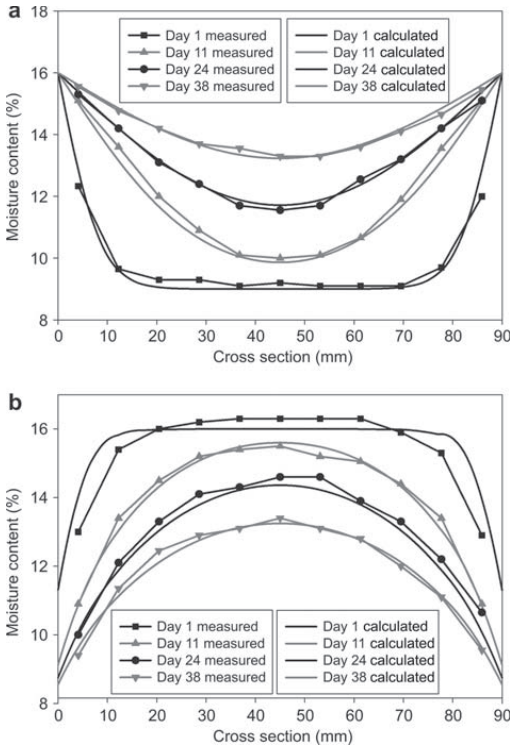

Figure 4 Comparison of measured and calculated moisture content distributions after 1, 11, 24, and 38 days of (a) wetting from 40 to 80% RH and (b) drying from 80 to 40% RH.

from measurements (Jönsson 2004) and from calculations based on the diffusion analysis. The selected parameters give reasonable results.

Selection of model parameters for the 1D-hygro-mechanical model

The hygro-mechanical model requires selection of various parameters, such as stiffness parameters and hygro-expansion coefficients, as well as that of appropriate mechano-sorption and time-dependent creep models. In the following, time-dependent creep will be omitted, an approach which is in accordance with several researchers, Häglund (2008).

Different mechanosorption models were compared with the 1D formulation (Figure 2). This was done by calculations of the MiS developing in a glulam cross-section over time, for a wetting, a drying, and a cycling case. The stiffness parameters and hygro-expansion coefficients were kept constant across the various models. The values for stiffness and hygro-expansion parameters in transversal directions [necessary for the calculation of the effective values by means of Eqs. (5) and (6)] were chosen according to Häglund (2009). The mechanosorption models which are compared, are the four models presented in Table 2 (two Maxwell- and two Kelvin-type models) with proposed parameters for spruce. To be able to apply the 2D-models of Ormarsson (1999) and Mårtensson and Svensson (1997b), the models were ''transformed'' into 1D-models based on the same principle as for the stiffness parameters; effective parameters were calculated from the values defined in transversal direction by Eqs. (5) and (6).

Selection of model parameters for the 2D-hygro-mechanical model

A sensitivity analysis was performed with 2D-formulation (Figure 2) for investigation of the influence of material parameters and geometrical configuration on calculated MiS. Values for hygro-expansion coefficients and stiffness moduli for spruce wood published in the literature were used (see Table 4). With regard to geometrical configuration, three different pith locations, shown in Figure 5, were studied. The pith locations were selected by visual evaluations of glulam cross-sections and are thus realistic. The mechanosorption model for the calculation was the one proposed by Ormarsson (1999) with corresponding parameters (Table 2). In the various configurations, the MiS developing in a glulam cross-section (in the center of the third laminate, indicated by the broken line in Figure 5) over time were calculated for both a wetting and a drying case. The parameters in the

Table 4 Parameter studies with 2D-models.

Variation	Legend	Configurations/parameters	References
Pith locations	Ref	On the bottom of the lamella	–
	A	In the center of the lamella	–
	B	Below the lamella	–
Hygro-expansion coefficients	Ref	α_r=0.11, α_t=0.22	Jönsson 2005
	C	α_r=0.19, α_t=0.35	Ormarsson 1999
	D	α_r=0.07, α_t=0.15	Dinwoodie 2004
Stiffness parameters	Ref	E_r=467 MPa, E_t=216 MPa, G_{rt}=42 MPa (E_l=97 MPa and ν_{rt}=0.55 are not varied)	Häglund 2008
	E	E_r=710 MPa, E_t=430 MPa, G_{rt}=23 MPa	Dinwoodie 2004
	F	E_r=2200*(0.3-u)+400 [MPa] E_t=1300*(0.3-u)+220 [MPa] G_{rt}=72*(0.3-u)+25 [MPa]	Ormarsson 1999

reference configuration, as well as the variations of parameters, are summarized in Table 4.

Results and discussion

In the following, stresses calculated by different hygro-mechanical models with different parameters are presented and discussed. The hygro-mechanical models are all based on the same moisture transport model.

Results obtained with the 1D-hygro-mechanical model

The MiS values, which develop in the center and on the border of a glulam cross-section during wetting from 40 to 80% RH, or drying from 80 to 40% RH, are plotted in Figure 6. It is obvious that the shape of the stress curves obtained with different types of mechanosorption models is similar. From theory, a decreasing stress rate is expected for the Kelvin-type models. In the present case, this effect is slightly apparent after 30–40 days when the Kelvin-curves exhibit somewhat smaller slopes. However, when the stresses are largest at the beginning of the analysis (5–10 days), Maxwell- and Kelvin-type models behave similarly for the following reason: the first term in the equation is the same in both types of models and is strongly dominated by the stress ($m\sigma$). In the same manner, the results of the cycling analysis (plotted in Figure 7), which involved 11 days of drying and wetting cycles each, show that there is no significant difference between the stresses obtained with the different models.

The only observable deviation is the stress shift obtained with Maxwell-model 1b. This is as a result of a term ($\beta\Delta u$)

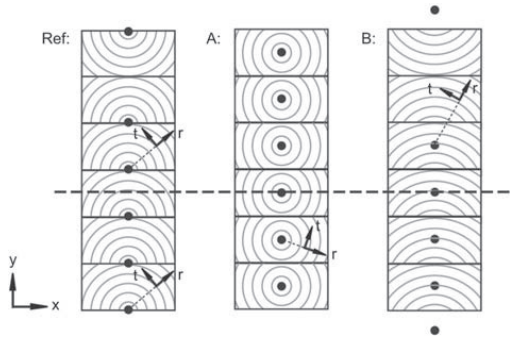

Figure 5 Different pith locations studied in the model (note that in case B, the piths are outside the laminates).

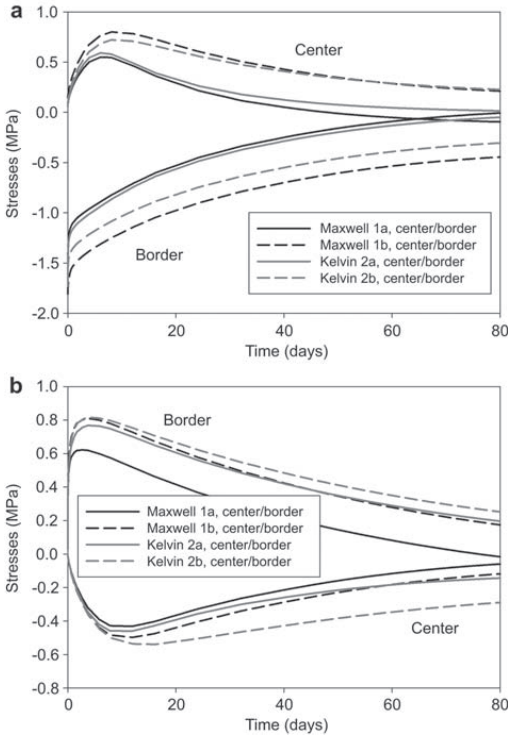

Figure 6 Internal stresses developing during (a) wetting and (b) drying using different mechanosorption models.

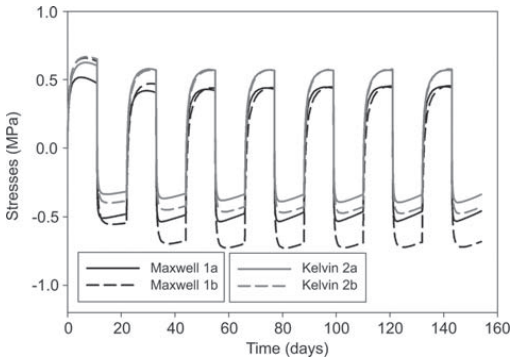

Figure 7 Internal stresses developing during cycling using different mechanosorption models.

included into the model, which depends on the direction of the MC change. Thus, all the compared mechanosorption models can be used for the present type of analysis, namely glulam subjected to climatic changes of the surrounding environment without external load. It might also be worth noticing that the dimensions of the cross-section together with the external moisture variations affect the magnitude of the established moisture gradient, which in turn largely determines the internal stresses. Thin cross-sections are not likely to exhibit as large MiS as wider cross-sections. In realistic cases, however, the level of stresses is likely to be the reason for a very similar behavior of Kelvin- and Maxwell-models (where the first term in the Kelvin-model is dominant). The parameters need to be adjusted to get the correct stress level for a certain application.

Results obtained with the 2D-hygro-mechanical model

Figure 8 presents the results from the calculated MiS which develop in the glulam cross-section during wetting from 40 to 80% RH, or drying from 80 to 40% RH, obtained with different configurations according to Table 4. The mechanosorption model with corresponding parameters proposed by Ormarsson (1999) (Table 2) was used for the calculations. In the plots, the stresses in the *y*-direction developing in the center of the third laminate are depicted (see also Figure 5). The vertical *y*-stress is computed from the local radial and tangential components.

Effect of pith location Figure 8a,b demonstrates the effect of the pith locations on the stresses. When the point at which the stresses are examined lies in a pith (case A), the local stresses are 4.0–4.5 times larger than the lowest stresses at that point (case B). However, when the average stresses over the height of the cross-section are examined, the effect of the pith location is smaller (2.6–2.8 times larger in case A). These results are in agreement with an analysis performed by Gowda et al. (1998) in 1D, which illustrates the sensitivity of the stress distribution owing to the annual ring orientation in the cross-section: the closer the pith is located to the lamina, the higher the stresses are.

Effect of hygro-expansion coefficients Figure 8c,d shows that the value for the hygro-expansion coefficient determines the maximum stress level which is reached after 7–11 days of climate change. At this time, the ratio between chosen hygro-expansion coefficients for the different scenarios, C and D, acts like a scaling factor for the obtained stresses. For instance, α_r and α_t for case C (high values) are on average 2.5 times larger than for case D (low values), and the maximum stresses in the center of the cross-section are in the same range. The same effect can also be observed, when the average stresses over the height of the cross-section are considered, which is in contrast to the pith locations.

Effect of stiffness parameters Figure 8e,f illustrates how the stresses are affected by different stiffness parameters. By using the stiffness values dependent on the MC (case F), as proposed by Ormarsson (1999), the maximum stresses in the center of the cross-section become up to 1.4 times larger than the stresses obtained with the constant stiffness values proposed by Häglund (2009) (case ref.). Moreover, this also affects the shape of the curve in the shown stress-versus-time plots. The influence of varying stiffness parameters on the stresses is the same when looking at local or averaged (over the sample height) values. These results are in agreement with a 1D parameter study; e.g., Häglund (2009) demonstrated that 50% higher or lower stresses can be obtained, depending on the selected value for the MOE or the hygro-expansion coefficient.

Conclusions

The present study highlights some considerations related to modeling of MiS in glulam under service life conditions (including single and cyclic climate changes with RH values below 100% and exhibiting pronounced moisture gradients across the cross-section).

The stress distributions calculated by a hygro-mechanical model are strongly affected by the input parameters. In the present study, the selected pith locations and the hygro-expansion coefficients show the strongest effect, followed by the stiffness parameters. The selection of the mathematical model describing mechanosorption, however, does not appear to be decisive for the results. More emphasis should be put on geometrical configuration and material characteristics rather than mathematical formulations. For modeling MiS in glulam members under service life conditions, Kelvin-type models for mechanosorptive creep offer no significant benefits over the mathematically simpler Maxwell-type models.

In fact, Kelvin-type models requires more parameters and increases computation time. Accounting for the strong influence of material parameters (diffusion coefficient, hygro-expansion parameters, stiffness parameters), calibration of mechanosorption model parameters can be done properly

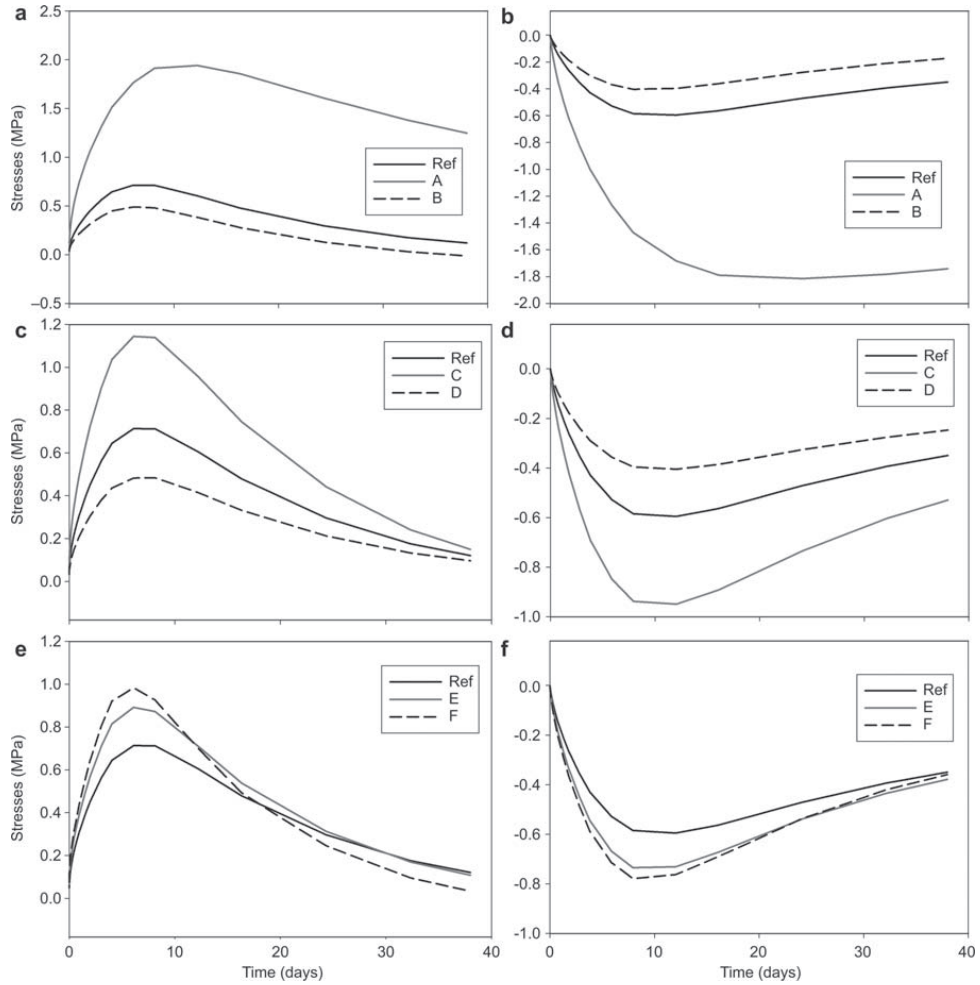

Figure 8 Stresses developing during (a) wetting and (b) drying using different pith locations, (c) wetting and (d) drying using different hygro-expansion coefficients, (e) wetting and (f) drying using different stiffness parameters.

when the material parameters are known for the actual case. Considering the large scatter in literature data, it is evident that measurement of all the relevant material parameters is necessary. Nevertheless, literature values are useful for performing sensitivity analyses or qualitative investigations.

References

Aicher, S., Dill-Langer, G. (1997) Climate induced stresses perpendicular to the grain in glulam. Otto-Graf-J. 8:209–231.

Cai, L., Avramidis, S. (1997) A study on the separation of diffusion and surface emission coefficients in wood. Dry. Technol. 15:1457–1473.

COMSOL Multiphysics (2007) Version 3.4. User manuals.

Comstock, G.L. (1963) Moisture diffusion coefficients in wood as calculated from adsorption, desorption, and steady state data. Forest Prod. J. 13:97–103.

Dinwoodie, J.M. Timber – its Nature and Behaviour. Taylor & Francis e-Library, London and New York, 2004.

Eurocode (2004) Eurocode 5. Design of Timber Structures – Part 1-1: General – Common Rules and Rules for Buildings.

Frese, M., Blass, H.J. (2007) Failure Analysis on Timber Structures in Germany – a Contribution to COST Action E55. First Workshop May 2007, Graz University of Technology, Austria.

Frühwald, E., Serrano, E., Toratti, T., Emilsson, A., Thelandersson, S. (2007) Design of Safe Timber Structures – How can we Learn from Structural Failures in Concrete, Steel and Timber? Report TVBK-3053. Lund Institute of Technology, Sweden.

Gowda, S., Kortesmaa, M., Ranta-Maunus, A. (1998) Duration of load effect on curved glulam beams – Part 2: Long term load tests and analysis. VTT Publ. 334.

Hanhijärvi, A. (2000a) Advances in the knowledge of the influence of moisture changes on the long-term mechanical performance of timber structures. Mater. Struct. 33:43–49.

Hanhijärvi, A. (2000b) Deformation properties of Finnish spruce and pine wood in tangential and radial directions in association to high temperature drying – Part IV. Modelling. Holz Roh Werkst. 58:211–216.

Houska, M., Koc, P. (2000) Sorptive stress estimation: an important key to the mechano-sorptive effect in wood. Mech. Time-Depend. Mat. 4:81–98.

Hukka, A. (1999) The effective diffusion coefficient and mass transfer coefficient of nordic softwoods as calculated from direct drying experiments. Holzforschung 53:534–540.

Häglund, M. (2007) Moisture content penetration in wood elements under varying boundary conditions. Wood Sci. Technol. 41:477–490.

Häglund, M. (2008) Varying moisture content and eigen-stresses in timber elements. Wood Mater. Sci. Eng. 3:38–45.

Häglund, M. (2009) Moisture Induced Stress Perpendicular to Grain in Timber Structures. Doctoral Thesis Report TVBK-1036. Lund Institute of Technology, Sweden.

Jönsson, J. (2004) Internal stresses in the cross-grain direction in glulam induced by climate variations. Holzforschung 58:154–159.

Jönsson, J. (2005) Moisture Induced Stresses in Timber Structures. Doctoral Thesis Report TVBK-1031 Lund Institute of Technology, Sweden.

Koc, P., Houska, M. (2002) Characterization of the sorptive properties of spruce wood by the inverse identification method. Holz Roh Werkst. 60:265–270.

Koponen, H. (1983) Diffusion and surface emission coefficients of birch, pine and spruce and their dependence on wood properties. Pap. Puu-Pap. Tim. 65:619–624.

Koponen, H. (1984) Dependences of moisture diffusion coefficients of wood and wooden panels on moisture content and wood properties. Pap. Puu-Pap. Tim. 66:740–745.

Koponen, H. (1985) Dependences of moisture transfer coefficients on moisture diffusion coefficients and wood properties. Pap. Puu-Pap. Tim. 6–7:363–368.

Leicester, R.H. (1971) A rheological model for mechano-sorptive deflections of beams. Wood Sci. Technol. 5:211–220.

Mårtensson, A. (1994a) Creep behavior of structural timber under varying humidity conditions. J. Struct. Eng. 120:2565–2582.

Mårtensson, A. (1994b) Mechano-sorptive effects in wooden material. Wood Sci. Technol. 28:437–449.

Mårtensson, A., Svensson, S. (1997a) Stress-strain relationship of drying wood – Part 1: Development of a constitutive model. Holzforschung 51:472–478.

Mårtensson, A., Svensson, S. (1997b) Stress-strain relationship of drying wood – Part 2: Verification of a one-dimensional model and development of a two-dimensional model. Holzforschung 51:565–570.

Ormarsson, S. (1999) Numerical Analysis of Moisture-related Distortions in Sawn Timber. Doctoral Thesis Publ. 99:7. Chalmers University of Technology, Göteborg, Sweden.

Ormarsson, S., Dahlblom, O., Petersson, H. (1998) A numerical study of the shape stability of sawn timber subjected to moisture variation – Part 1: Theory. Wood Sci. Technol. 32:325–334.

Ranta-Maunus, A. (1975) The viscoelasticity of wood at varying moisture content. Wood Sci. Technol. 9:189–205.

Ranta-Maunus, A. (1993) Rheological behaviour of wood in directions perpendicular to the grain. Mater. Struct. 26:362–369.

Rosenkilde, A., Arfvidsson, J. (1997) Measurement and evaluation of moisture transport coefficients during drying of wood. Holzforschung 51:372–380.

Salin, J.-G. (1992) Numerical prediction of checking during timber drying and a new mechano-sorptive creep model. Holz Roh Werkst. 50:195–200.

Shi, S.Q. (2007) Diffusion model based on Fick's second law for the moisture absorption process in wood fiber-based composites: is it suitable or not? Wood Sci. Technol. 41:645–658.

Svensson, S., Mårtensson, A. (2002) Simulation of drying stresses in wood – Part II: Convective air drying of sawn timber. Holz Roh Werkst. 60:72–80.

Svensson, S., Toratti, T. (2002) Mechanical response of wood perpendicular to grain when subjected to changes of humidity. Wood Sci. Technol. 36:145–156.

Toratti, T., Svensson, S. (2000) Mechano-sorptive experiments perpendicular to grain under tensile and compressive loads. Wood Sci. Technol. 34:317–326.

Virta, J., Koponen, S., Absetz, I. (2006) Measurement of swelling stresses in spruce (*Picea abies*) samples. Build. Environ. 41:1014–1018.

Received October 21, 2009. Accepted April 13, 2010.
Previously published online July 12, 2010.

Paper II

The effect of climate variations on glulam – an experimental study
Vanessa Angst and Kjell A. Malo
European Journal of Wood and Wood Products (2012)
DOI 10.1007/s00107-012-0594-y

Is not included due to copyright

PAPER III

Moisture induced stresses in glulam cross sections during wetting exposures

Vanessa Angst and Kjell A. Malo

Submitted to Wood Science and Technology (2011)

MOISTURE INDUCED STRESSES IN GLULAM CROSS SECTIONS DURING WETTING EXPOSURES

Vanessa Angst • Kjell Arne Malo
submitted to Wood Science and Technology (2011)

Abstract

Moisture induced stresses resulting from climate variations of the environment can induce cracks in timber members and thus affect the safety and serviceability. The present study highlights – by means of numerical simulations – the distribution and development over time of moisture induced stresses in various glulam cross sections during wetting. The results show that local stresses may be significantly larger than average stresses, the extent of which strongly depends on the geometrical configuration of the glulam laminates. Suggestions are made on the design of glulam cross sections to minimize the arising local stresses. Furthermore, the studied wetting exposure results in local tensile stresses which exceed the tensile strength of the material. In smaller cross sections this is the case within few days, while more time is required in wider cross sections.

1 INTRODUCTION

Safety and serviceability of timber structures are affected by climate variations of the surroundings. The varying relative humidity (RH) induces stresses perpendicular to grain in timber members. These stresses can be compressive or tensile stresses and are commonly referred to as moisture induced stresses (MiS). The tensile stresses are especially critical, as the tensile strength of timber perpendicular to grain is very low, and thus, if the latter is exceeded, cracks may occur. These cracks can evolve in the longitudinal direction and reduce the load-bearing capacity of individual timber members significantly. In the worst case, this can lead to failure of the structure. As a matter of fact, tension perpendicular to

grain is the most common failure mode of timber structures (Frese and Blass 2007; Frühwald et al. 2007)

Several experimental and numerical studies have shown that considerable MiS arise in timber under normal service conditions (Svensson and Toratti 2002; Aicher and Dill-Langer 1997; Häglund 2008; Jönsson and Svensson 2004; Jönsson 2004). The authors observed tensile stresses perpendicular to grain, which were similar to or even exceeded the tensile strength of the corresponding timber material. However, most of the studies dealing with MiS in glulam concern only mean stresses and do not consider that local stresses may even be larger. A further study, which investigated the combination of moisture induced and mechanical stresses, found the tensile capacity of the timber to be reduced by climate exposure (Jönsson and Thelandersson 2003). In evaluation of timber structures, it is therefore important to take MiS into account. One approach is to consider stresses induced by moisture gradients as loads and to take these MiS into account together with mechanical stresses (Ranta-Maunus 2003).

The main purpose of the present study is to quantify average and local MiS in different glulam cross sections subjected to wetting. The influence of various geometrical configurations (pith location distribution in the cross section) on local stresses is investigated. Also the effect of different cross section widths on average and maximum local stresses is investigated. The study is performed by means of numerical simulations, where the required material parameters are based on a previous experimental study by the present authors (Angst and Malo 2012). The calculated MiS are compared with ultimate stress values found in the literature.

2 NUMERICAL SIMULATIONS

The present paper considers timber (glulam) cross sections with the lateral faces exposed to wetting and top, bottom, front and back faces sealed, thus leading to one-dimensional moisture transport perpendicular to grain. As a basis for the geometry a glulam cross section with height 270 mm, consisting of 6 laminates, and various widths is used. Each laminate exhibits a different annual ring pattern, which, in the numerical simulations is taken into account by defining local cylindrical coordinate systems in each laminate. The origins of these coordinate systems are defined by the locations of the pith in the corresponding laminates. This allows modeling of orthotropic material properties in the radial and

tangential direction of the annual rings. Numerical simulations of MiS developing in glulam cross sections are performed by using a moisture transport model coupled with a hygro-mechanical model.

2.1 Moisture transport model

A one-dimensional moisture transport model based on Fick's second law of mass diffusion is used for the calculation of the moisture content (MC) *u* (mass of water per mass of dry wood) according to:

$$\frac{\partial u}{\partial t} = \frac{\partial}{\partial x}\left(D \frac{\partial u}{\partial x} \right) \tag{1}$$

The diffusion coefficient *D* [m^2/s] is assumed to be equal in radial and tangential direction, thus resulting in one value for the cross grain direction. The moisture flow at the timber surface is expressed with the following equation:

$$\left(D \frac{\partial u}{\partial x} \right) = S\left(u_{eq} - u_{surf}\left(t\right) \right) \tag{2}$$

The surface emission factor *S* [m/s] takes into account the moisture transfer resistance at the surface, where the moisture flow is driven by the difference between the actual surface MC $u_{surf}\,(t)$ and the equilibrium MC u_{eq}.

2.2 Hygro-mechanical model

A two-dimensional orthotropic hygro-mechanical model is used for the calculation of internal stresses resulting from MC changes. The model assumes the total strain rate vector $\dot{\boldsymbol{\varepsilon}}$ to be the sum of the elastic strain rate vector $\dot{\boldsymbol{\varepsilon}}_e$, the linear shrinkage-swelling strain rate vector $\dot{\boldsymbol{\varepsilon}}_s$, and the mechano-sorptive creep strain rate vector $\dot{\boldsymbol{\varepsilon}}_{ms}$:

$$\dot{\boldsymbol{\varepsilon}} = \dot{\boldsymbol{\varepsilon}}_e + \dot{\boldsymbol{\varepsilon}}_s + \dot{\boldsymbol{\varepsilon}}_{ms} \tag{3}$$

The dot denotes derivative with respect to time. For the present numerical model, the modulus of elasticity *E,* the shear modulus *G* and the Poisson's ratio *v* are assumed to be independent of MC. This is based on experimental results, where the effect of MC on *E* was found to be negligible (Angst and Malo 2012).

The elastic strain rate vector is defined as:

$$\dot{\boldsymbol{\varepsilon}}_e = \mathbf{C} \cdot \dot{\boldsymbol{\sigma}} \tag{4}$$

Here $\boldsymbol{\sigma}$ is the stress vector and $\mathbf{C}$ the compliance matrix, which, in matrix notation, is as follows:

$$\mathbf{C} = \begin{bmatrix} \frac{1}{E_R} & \frac{-\nu_{TR}}{E_T} & 0 \\ \frac{-\nu_{RT}}{E_R} & \frac{1}{E_T} & 0 \\ 0 & 0 & \frac{1}{G_{RT}} \end{bmatrix} \tag{5}$$

Here, indices *R* and *T* denote radial and tangential direction, respectively. The linear shrinkage-swelling strain rate vector is defined as:

$$\dot{\boldsymbol{\varepsilon}}_s = \boldsymbol{\alpha} \cdot \dot{u} \tag{6}$$

where $\dot{u}$ represents the MC rate and $\boldsymbol{\alpha}$ the hygroexpansion coefficient vector, according to:

$$\boldsymbol{\alpha} = \begin{bmatrix} \alpha_R & \alpha_T & 0 \end{bmatrix}^T \tag{7}$$

In the literature, various models have been proposed for mechano-sorptive creep. However, when modeling MiS in timber without external load, the type of selected model has a relatively small effect, while the selection of correct material parameters is much more important (Angst and Malo 2010). In the present study, the mechano-sorptive creep strain model, proposed a.o. by Ormarsson (1999) is used:

$$\dot{\boldsymbol{\varepsilon}}_{ms} = \mathbf{m} \cdot \boldsymbol{\sigma} \left| \dot{u} \right| \tag{8}$$

The matrix $\mathbf{m}$ is a mechano-sorption property matrix defined as:

$$\mathbf{m} = \begin{bmatrix} m_R & -\mu_{TR} m_T & 0 \\ -\mu_{RT} m_R & m_T & 0 \\ 0 & 0 & m_{RT} \end{bmatrix} \tag{9}$$

where m_R, m_T, m_{RT} are mechano-sorption coefficients in the orthotropic directions and planes and μ_{TR}, μ_{RT} are coupling coefficients.

It can be noticed that time-dependent creep is neglected in the strain rate formulation presented in Eq. 3. This is a common practice (Ormarsson et al. 1998; Svensson and Toratti 2002; Häglund 2008; Gereke and Niemz 2010), as the effect of time-dependent creep at low MCs and temperatures is considered to be small compared with mechano-sorptive creep (Mårtensson and Svensson 1997; Toratti and Svensson 2000; Virta et al. 2006).
The numerical simulations of the present study were performed in Comsol Multiphysics (2008), a commercial finite element program, by using Lagrange elements (quadratic).

2.3 Material and model parameters

The input parameters for the present numerical simulations (Table 1) are based on the experimental study reported in Angst and Malo (2012). In this study, glulam specimens were subjected to wetting, while MCs, restrained strains, released strains, moduli of elasticity and hygroexpansion coefficients were measured. Also, the geometrical configuration of 24 specimen cross sections was determined by measuring the location of the pith in each laminate (x- and y-coordinates).

The parameters needed for the moisture transport model include a.o. the initial MC, $u_{surf}\ (t_0)$, and the equilibrium MC, u_{eq}. These were measured in glulam specimens during wetting. The diffusion and the surface emission coefficients, D and S, were obtained by fitting modeled to measured MC distributions (Fig. 1), with the parameters given in Table 1.

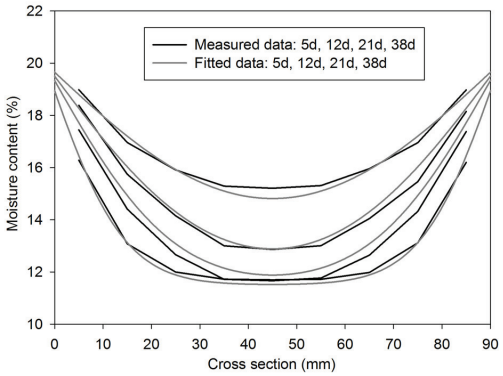

Fig. 1 Moisture content distribution after 5, 12, 21, and 38 days of wetting (from 50% to 90% RH): Measured (average of 5 parallel specimens) and fitted data

The parameters needed for the stress-strain model include the hygroexpansion coefficients and the stiffness parameters. These have been determined in Angst and Malo (2012) and are shown in Table 1. Note that the stiffness parameters correspond to the parameters, which Häglund (2008) successfully fitted to similar experimental results from literature (Jönsson and Svensson 2004).

The parameters needed for the mechano-sorption model include the mechano-sorption and the coupling coefficients (Eq. 9). These coefficients have not been measured, but, as all the other required material parameters are known, they can be estimated. In a first step, the mechano-sorption model parameters proposed by Ormarsson (1999) were applied, then, they were changed – by keeping the ratio between them constant – until calculated stresses agreed well with measured stresses. In the present case, a satisfying fit was obtained with the parameters presented in Table 1. Note that these parameters are reduced by 50% as compared to the ones published by Ormarsson, which have been defined and applied for drying analyses. The lower mechano-sorption parameters for the present wetting analyses might be explained by the fact that mechano-sorptive strain is smaller during wetting than during drying (Mårtensson and Svensson 1997; Ranta-Maunus 1993). Figure 2 shows that, with the parameters given in Table 1, the calculated (fitted) stresses agree well with the stresses from measurements. Note that the plotted stresses are the stresses in y-direction (in direction of the specimen height, see sketch in Table 2).

Table 1 Parameters used for the numerical simulations

Model part	Parameters	Parameters from
Diffusion model	$u_{surf}\ (t_0)$ = 11.5%, u_{eq} = 20%	Experiments (Angst and Malo 2012)
	S = 10e-8 ms^{-1}, D = 2e-10 m^2s^{-1}	Fitting
Stress-strain model:		
Hygroexpansion coefficients	α_R = 1.5e-3, α_T = 3.2e-3	Experiments and fitting (Angst and Malo 2012)
Stiffness parameters	E_R = 467 MPa, E_T = 216 MPa, ν_{RT} = 0.5, G_{RT} = 42 MPa	Experiments and fitting (Angst and Malo 2012; Häglund 2008)
Mechano-sorption model	m_R = 0.07 MPa^{-1}, m_T = 0.1 MPa^{-1}, m_{RT} = 0.4 MPa^{-1}, μ_{RT} = 1, μ_{TR} = 0.75	Fitting

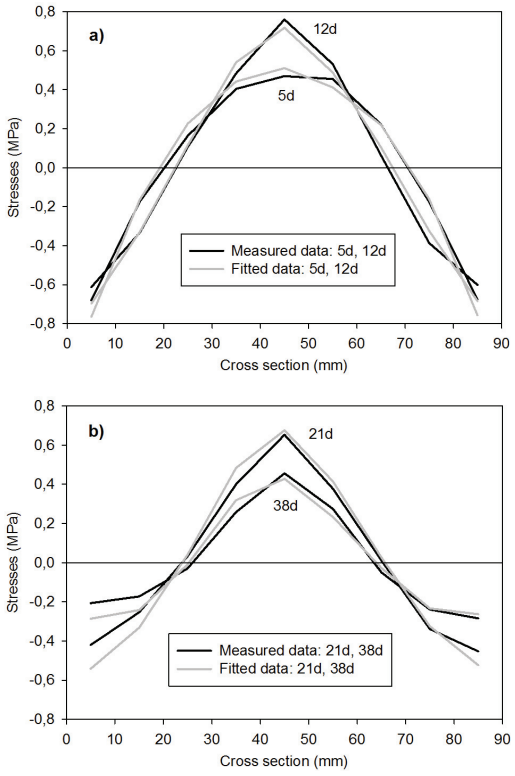

Fig. 2 Stress distribution after a) 5 and 12 days of wetting and b) 21 and 38 days of wetting (from 50% to 90% RH): Measured (average of 5 parallel specimens) and fitted data

2.4 Geometry of modeled cases

Various geometrical configurations are studied both with respect to cross section width as well as pith locations within the laminates. In the experimental study, the geometrical configuration of 24 specimen cross sections was recorded. On this basis, one typical configuration was selected as a reference configuration (see Table 2). This configuration is free from piths with exception of the lowest laminate that contains a pith at the very border (laminate no. 1, see Table 2), which is common due to the sawing procedure. In some cases, however, piths may well be present within the laminate. It has been demonstrated that the pith locations significantly affect the stresses (Aicher and Dill-Langer 2005; Angst and Malo 2010; 2012). To take into account the effect of piths within the laminates, additional cases will also be modeled as described below.

Table 2 Geometrical configurations used for the numerical simulations

Reference configuration		Example of a configuration with piths within certain laminates	
Coordinates (mm) of the pith location in each laminate: 6) x = 44, y = 221 5) x = 37, y = 227 4) x = 40, y = 186 3) x = 51, y = 142 2) x = 50, y = 98 1) x = 48, y = 0	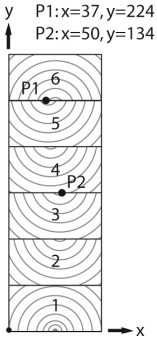	Coordinates (mm) of the pith location in each laminate: 6) x = 54, y = 275 5) x = 37, y = 227 4) x = 60, y = 142 3) x = 35, y = 138 2) x = 54, y = 96 1) x = 36, y = -8	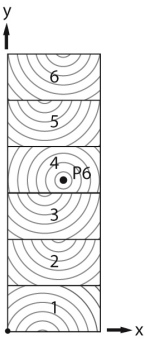
P1 and P2 are locations in the cross section, where large local stresses arise (see Fig. 3)			

2.4.1 Average and local stresses in a cross section of 90 mm width

A first series of analyses aims at studying average and local stresses in a cross section of fixed width (90 mm) but with varying pith geometry. The stresses are calculated after 12 d of wetting from 50% to 90% RH, because the experimentally measured stresses were largest at this time (Angst and Malo 2012). Whereas in the experiments, only estimation of average stresses is possible, numerical

simulations permit to calculate local stresses for every mesh node of the modeled cross section. From this, the maximum and minimum stresses are evaluated as a function of x-coordinate, thus yielding a profile of maximum and minimum stresses through the cross section. In addition, also the average over the cross section height is calculated as a function of x-coordinate. Note that here, stress always means stress in y-direction.

This analysis is performed for the reference cross section as well as for all of the 24 cross section geometries evaluated in the experimental study. This covers also some of the untypical cross sections that have piths within the laminates, an example of which is shown in Table 2.

2.4.2 Stress distribution in different cross section widths

A second series of analyses is performed to study the effect of different cross section widths. The MC and the stresses are calculated for cross sections of 90 mm, 140 mm, and 215 mm width after 5, 12, 21, and 38 d of wetting. Cross section 215 mm is the largest standard dimension commercially available in Norway. According to the glulam producer (personal communication) the sawing pattern of the timber log is basically the same for the build-up of each of these cross sections. Thus, the same reference configuration according to Table 2 is applied for all cross sections. The larger cross sections 140 and 215 mm are modeled, by enlarging the 90 mm wide cross section laterally. The calculated stresses are average stresses over the cross section height (as a function of x-coordinate).

2.4.3 Stress development over time in cross sections of different widths

Further analyses are concerned with the development of stresses over time. The stresses are calculated in selected points of cross sections of various widths in the range 90 mm – 215 mm during 180 d of wetting. These selected points correspond to points where – in the reference geometrical configuration of the cross section – high local stresses arise (P1 and P2, see Table 2). In addition, also the development of the average stress in the cross section center is evaluated.

3 RESULTS

3.1 Average and local stresses in a cross section of 90 mm width

Figure 3 shows the average stress compared to maximum and minimum local stress distributions (in y-direction) in a cross section with the reference geometrical configuration. The shaded area, which is limited by the maximum and the minimum stresses, highlights the large range of stresses present at a certain x-coordinate in the cross section. In the center parts of this typical cross section the maximum tensile stresses can be up to 2 MPa (indicated by P1), which is about 2.5 times the average stress in the center.

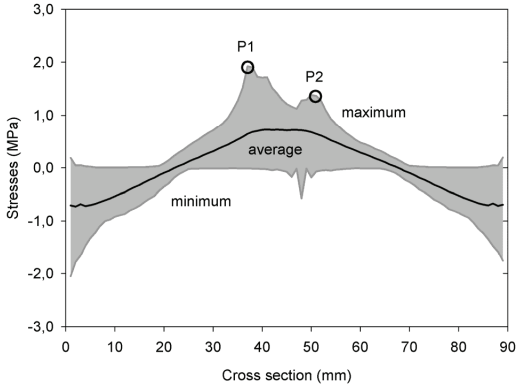

Fig. 3 Modeled stress range after 12 days of wetting in the reference cross section

Figure 4 shows the effect of different geometrical cross section configurations on local stresses. In addition to the stress distribution of the reference cross section (shown as light grey shaded area), also the maximum stresses obtained from 24 different cross section geometries are shown (by the upper envelope of all 24 cross sections). It can be noticed that the range of local stresses is clearly increased compared to Fig. 3, and that several significant peaks (indicated by P3-P6) are present. These peaks result from geometrical configurations where the pith is located within a laminate. There the maximum tensile stress value can be almost up to 5.5 MPa.

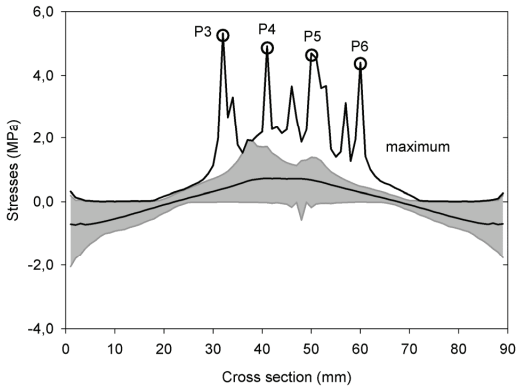

Fig. 4 Modeled stress range after 12 days of wetting obtained from 24 different geometrical configurations (upper envelope) compared to the stress range obtained with the reference configuration (light grey shaded area)

3.2 Stress distribution in cross sections of different widths

Figure 5a shows the calculated MC distribution after 5, 12, 21, and 38 d of wetting in a 90 mm, 140 mm, and a 215 mm wide cross section. As expected, the distributions are symmetric with respect to the cross section centers. The arising MC gradients depend to a large extent only on the initial climatic condition in the specimen and the external climate change, and thus, they are basically the same for all three studied specimen widths. However, the time at which the largest MC gradient occurs and the period in time during which a certain gradient is maintained differs for different specimen widths. The internal stresses (Fig. 5b), are directly related to the MC gradients, whereby large gradients result in large tensile stresses in the specimen center. The time at which the maximum internal stress in the specimen center arises, depends on the cross section width in an analogous manner as the MC distributions. In larger cross sections, the maximum stresses appear later in time, but in return they are present for a longer time period compared with smaller cross section sizes.

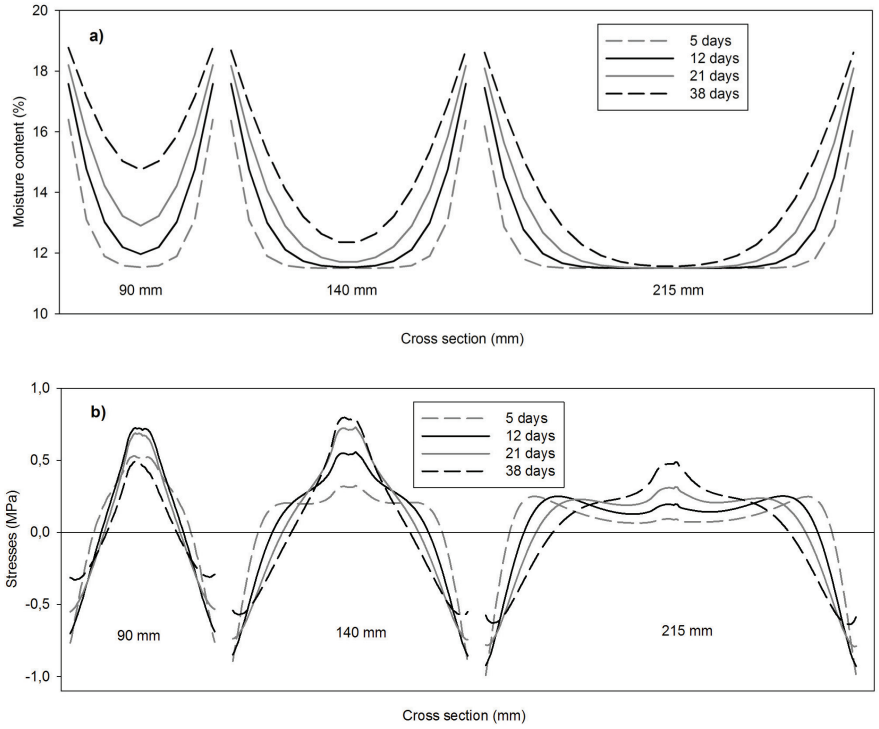

Fig. 5 Modeled a) moisture content and b) stress distribution during wetting in glulam cross sections of width 90 mm, 140 mm, and 215 mm (based on the reference configuration)

3.3 Stress development over time in cross sections of different widths

Figure 6a shows the development of the maximum tensile stresses during 180 d of wetting at two different locations in 90 mm, 140 mm, and 215 mm wide cross sections. The locations correspond to the points P1 and P2 shown for the 90 mm wide cross section in Fig. 3 and Table 2. Figure 6b displays the development of the average tensile stress (over the specimen height) in the cross section center. Figure 6b includes also the average stress development in 120 mm, 160 mm, and 180 mm wide cross sections. The figures show that the stress-time-curves differ for the three studied cross section widths. In the smallest cross section (90 mm

wide) the stresses increase rapidly and when the peak is reached, they decrease rapidly again. The larger the cross section, the slower the increase and decrease in stress, and the later is the peak stress reached. In addition, the time during which the peak stress is maintained gets longer with increasing cross section width. Interestingly, the peak stresses shown in Fig. 6a and 6b are largest in the 140 mm wide cross section.

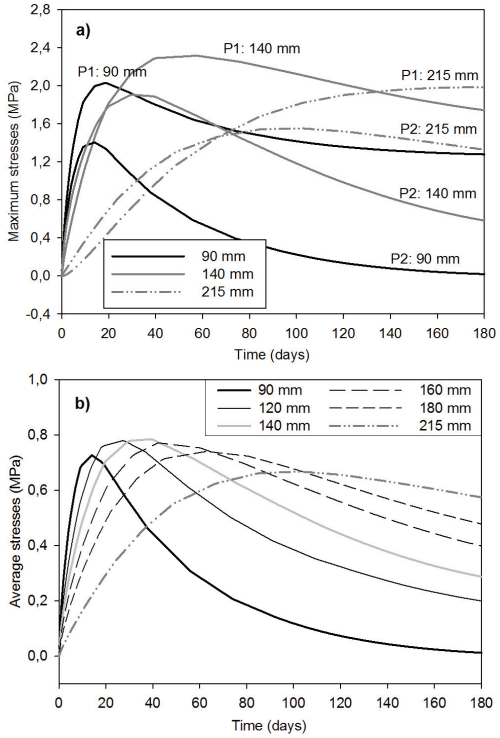

Fig. 6 Development over time of a) maximum local stresses (in selected points of the cross sections) and of b) average stresses in the cross section center

4 DISCUSSION

4.1 The effect of different cross section dimensions

It is apparent that the stress distributions plotted in Fig. 5b differ between different cross section widths. In the smallest studied cross section (90 mm), the stresses increase gradually towards the center for all wetting periods. In the wider cross sections, after a gradual increase in the outer zone, the stresses flatten out and show a further increase towards the very cross section center. This can be explained by two overlapping effects: MC gradients and varying modulus of elasticity. In the wider cross sections, the central parts are initially unaffected by wetting (Fig. 5a) and thus, no large moisture induced stresses occur. The stress increase in the very center can be explained by the modulus of elasticity, which, owing to the annual ring pattern, increases towards the center (Angst and Malo 2012).

The results concerning average stress development over time (Fig. 6b) show that the tensile stresses are largest in the 140 mm wide cross section. This can be explained by the balance of forces, which requires that internal stresses are in equilibrium. The size of the cross section area which exhibits compressive stresses is similar in all the studied cross sections (Fig. 5b). However, the size of the area, which takes up the tensile forces, is larger the wider the cross section, thus resulting in smaller stresses. In smaller cross sections (90 mm) the inner parts are affected earlier by the MC change, which results in smaller MC gradients and thus smaller stresses. The results in Fig. 6b suggest that 140 mm wide cross sections are unfavorable with respect to MiS. The stress peaks reached in 120 mm and 160 mm are, however, only slightly lower.

The present results concerning large cross sections are in accordance with a parametric study performed by Häglund (2010), where the tensile stresses in the center of 215 mm wide cross sections were found to be significantly lower than in 90 mm wide cross sections. However, different geometrical configurations were applied for the different cross sections.

4.2 Tensile stresses versus tensile strength of glulam perpendicular to grain

In this section the tensile stresses obtained by means of numerical simulations, as depicted in Figs. 3-6, are compared with tensile strength values from the literature.

Figure 7 shows the development of average stresses (in the cross section center) over time in cross sections of different widths (reference configuration) and tensile strength limits from the literature. The strength limits L1 (Astrup et al. 2007) and L2 (Jönsson and Thelandersson 2003) correspond to the ultimate strength of glulam specimens loaded in tension perpendicular to grain until failure. The dashed lines and the error bars in Fig. 7 represent mean values and standard deviations, respectively, of L1 ($\overline{x}$ = 1.13 MPa, s = 0.31 MPa) and L2 ($\overline{x}$ = 1.37 MPa, s = 0.23 MPa). These two literature strength limits are suitable for comparison with the average stresses obtained in the present study, as they were measured on specimens with similar height dimension and MC. The MC was around 12% and thus corresponds to the MC in the center of the specimen of the present study when the largest stresses arise (Fig. 5). Figure 7 suggests that it is unlikely for the stresses to exceed the strength limits. On the other hand, the stresses clearly exceed the characteristic tensile strength perpendicular to grain according to prEN 14080 (2011) (denoted "EN" in Fig. 7). Nevertheless, the strength of a cross section which exhibits MiS is reduced compared to a cross section without internal stresses. This was experimentally shown by Jönsson and Thelandersson (2003), who performed tensile tests on glulam specimens, after different days of wetting from 40% to 80% RH. In the present case, the difference between the strength limits and the maximum average stresses corresponds to the remaining strength of the cross section. As an example, the remaining strength of the 90 mm wide cross section is between 0.5 and 0.74 MPa after 24 d of wetting. This agrees well with the mean ultimate tensile strength of 0.65 MPa measured in glulam specimens after 24 d of wetting by Jönsson and Thelandersson (2003).

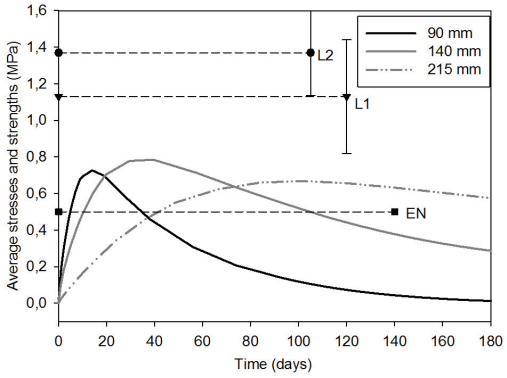

Fig. 7 Development of average stresses and tensile strength limits from literature with corresponding standard deviation (error bar), L1: Astrup et al. (2007), L2: Jönsson and Thelandersson (2003), EN: prEN 14080 (2011)

In the following, local stresses are compared with local tensile strength limits. Local tensile strength limits (in y-direction) were calculated for each x-coordinate where the maximum local stress arises, based on the annual ring configuration in the corresponding point, using Hankinson's equation:

$$f_{t,\theta} = \frac{f_{t,R} \cdot f_{t,T}}{f_{t,R} \cdot \sin^2 \theta + f_{t,T} \cdot \cos^2 \theta} \tag{10}$$

where θ is the angle between the radial direction of the wood and the y-direction of the specimen. The standard deviation was calculated in the same manner. The mean values for the tensile strength in radial and tangential direction, $f_{t,R}$ and $f_{t,T}$, as well as the standard deviations were taken from Blass and Schmid (2001): $f_{t,R}$ = 2.55 ± 0.485 MPa, and $f_{t,T}$ = 1.80 ± 0.423 MPa. Blass and Schmid performed tensile tests in different directions perpendicular to grain (radial, tangential) on thin solid timber slices made of spruce (MC = 12.5%).

Figure 8a shows a certain point in time, when the peak maximum stress is reached. This point in time differs between the various cross sections, being 19 d (90 mm), 57 d (140 mm) and 178 d (215 mm). As can be noticed, only the inner part of the cross section, especially the stress peak, exhibits tensile stresses which may be above limit values. At the peak the stresses are likely to exceed the tensile strength with a probability of 55% (215 mm), 62% (90 mm) and 80% (140 mm) depending on the cross section. The probabilities correspond to the area under

the probability density function of the local tensile strength (assumed as normally distributed), integrated from -∞ to the value of the stress peak. Note that the fluctuation of the strength limit in Fig. 8a, calculated with Hankinson's equation (Eq. 10), arises from the different locations of the maximum stress points with different annual ring patterns in each.

Figure 8b shows the maximum local stresses obtained with different geometrical configurations and corresponding strength limit. As apparent, the stress peaks, which arise close to a pith clearly exceed the strength limit. Moreover, the tensile strength measured on solid timber slices including a pith was found to be reduced compared to slices without pith (Blass and Schmid 2001). To sum up, small local cracks may arise, especially close to or at stress peaks.

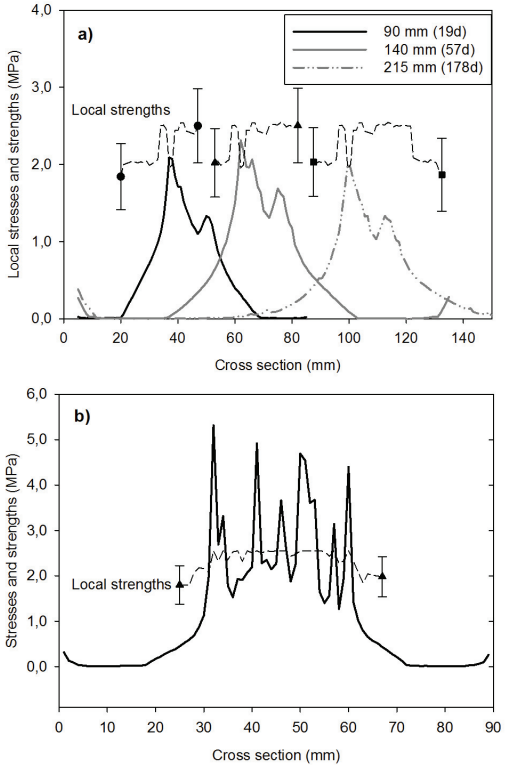

Fig. 8 Maximum local stresses at specific point in time and tensile strength limits from literature in cross sections of a) different widths (reference configuration) and b) obtained from 24 different geometrical configurations. The corresponding standard deviation (error bar) is only indicated at the border for reason of clarity

4.3 The effect of the geometrical configuration of glulam cross sections

The results concerning average and local stresses in a glulam cross section (Fig. 3, Fig. 4) have shown that the internal local stresses are strongly affected by the geometrical configuration of a glulam member. Configurations, where the pith is present within a laminate, exhibit high local stresses which significantly exceed the tensile strength limits presented above. This means that geometrical configurations that contain piths are probably more vulnerable to crack formation than pith-free cross sections.

From a practical perspective, high local stresses might thus be reduced by optimizing the procedure for production of glulam beams. Figure 9 depicts the sawing pattern commonly used for cutting laminates from logs (personal communication with glulam producer). While laminates A, cut from the log center, typically contain a pith at the border, laminates B are pith-free. A systematic investigation of geometrical configurations has shown that the cross section depicted in Fig. 9b, where type B laminates are glued face-to-face, exhibits the lowest MiS. Another way of optimizing glulam production could be to adapt the sawing pattern so that the pith is removed by cutting a thin central slice of the log as illustrated by the gray shaded area in Fig. 9c. This would allow using pith-free lamellas and at the same time keeping the material loss on a low level.

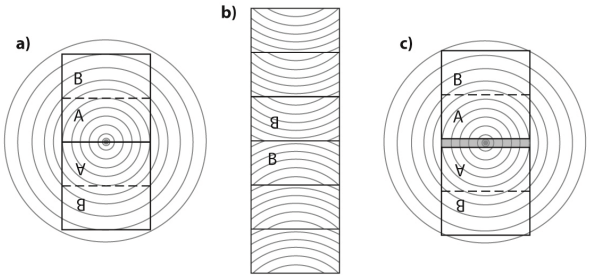

Fig. 9 Sawing pattern and cross section design

5 Conclusions

By means of numerical modeling, the present study highlights the distribution and development over time of MiS that arise in glulam cross sections during one-dimensional wetting.

The results have shown that owing to the annual ring pattern of the laminates in glulam cross sections, local stresses are significantly higher than average stresses (average over cross section height). The ratio of local and average stresses depends strongly on the cross section geometry and was in the present cases found to be in the range 2–7. These pronounced differences arise from different geometrical configurations, in particular the presence or absence of piths within the laminates; also the location of piths within the cross section affects the magnitude of local stresses. Based on the present numerical model, suggestions were made how optimized production of cross sections could improve their behavior and reduce MiS.

Similarly to the stresses, also the strength perpendicular to grain differs between average and locally evaluated strengths.

The results concerning local MiS have shown that these may lead to small cracks in the cross section even without external load. These cracks can reduce the load bearing capacity of the member. They will – in the case of wetting – initiate in the central part of the timber member and thus not be visible from the outside. The comparison of different cross section widths has shown that the wider a cross section is, the longer it takes until large stresses arise. Thus, wider cross sections appear only to be prone to cracking when very long wetting cycles occur. Measures such as coatings, which reduce moisture transport, or reinforcement perpendicular to grain, which increases the tensile strength of timber members, might be used to reduce the risk of cracking due to tension perpendicular to grain.

Acknowledgements

The authors acknowledge the support of the work from Norwegian Timber Industry, Norwegian Road Authorities and Christiania Spigerverk AS and Norwegian Research Council under KMB project grant 186821/I10. Specimens are delivered by Moelven Limtre AS and personal communication regarding production issues is highly acknowledged.

Conflict of interest

The authors declare that they have no conflict of interest.

REFERENCES

Aicher S, Dill-Langer G (1997) Climate induced stresses perpendicular to the grain in glulam. Otto-Graf-Journal 8:209-231

Aicher S, Dill-Langer G (2005) Effect of lamination anisotropy and lay-up in glued-laminated timbers. J Struct Eng-ASCE 131:1095-1103

Angst V, Malo KA (2010) Moisture induced stresses perpendicular to the grain in glulam: Review and evaluation of the relative importance of models and parameters. Holzforschung 64:609-617

Angst V, Malo KA (2012) The effect of climate variations on glulam - an experimental study. Eur. J. Wood Prod. DOI 10.1007/s00107-012-0594-y

Astrup T, Clorius CO, Damkilde L, Hoffmeyer P (2007) Size effect of glulam beams in tension perpendicular to grain. Wood Sci. Technol. 41:361-372

Blass HJ, Schmid M (2001) Querzugfestigkeit von Vollholz und Brettschichtholz. Holz Roh Werkst. 58:456-466

Comsol Multiphysics (2008) User manuals.

Frese M, Blass HJ (2007) Failure analysis on timber structures in Germany - a contribution to COST action E55. Paper presented at the First Workshop May 2007, Graz University of Technology, Austria

Frühwald E, Serrano E, Toratti T, Emilsson A, Thelandersson S (2007) Design of safe timber structures - How can we learn from structural failures in concrete, steel and timber? Division of Structural Engineering, Lund Institute of Technology, Report TVBK-3053 edn., Lund, Sweden

Gereke T, Niemz P (2010) Moisture-induced stresses in spruce cross-laminates. Eng. Struct. 32:600-606

Häglund M (2008) Varying moisture content and eigen-stresses in timber elements. Wood Mater. Sci. Eng. 1-2:38-45

Häglund M (2010) Parameter influence on moisture induced eigen-stresses in timber. Eur. J. Wood Prod. 68:397-406

Jönsson J (2004) Internal stresses in the cross-grain direction in glulam induced by climate variations. Holzforschung 58:154-159

Jönsson J, Svensson S (2004) A contact free measurement method to determine internal stress states in glulam. Holzforschung 58:148-153

Jönsson J, Thelandersson S (2003) The effect of moisture gradients on tensile strength perpendicular to grain in glulam. Holz Roh Werkst. 61 (5):342-348

Mårtensson A, Svensson S (1997) Stress-strain relationship of drying wood - Part 1: Development of a constitutive model. Holzforschung 51:472-478

Ormarsson S (1999) Numerical analysis of moisture-related distortions in sawn timber. Dissertation, Chalmers University of Technology, Göteborg

Ormarsson S, Dahlblom O, Petersson H (1998) A numerical study of the shape stability of sawn timber subjected to moisture variation - Part 1: Theory. Wood Sci. Technol. 32:325-334

prEN 14080 (2011). Timber structures - Glued laminated timber and glued solid timber. European committee for standardization, Brussels

Ranta-Maunus A (1993) Rheological behaviour of wood in directions perpendicular to the grain. Mater. Struct. 26:362-369

Ranta-Maunus A (2003) Effects of climate and climate variations on strength. In: Thelandersson S, Larsen HJ (eds) Timber Engineering. John Wiley & Sons Ltd., Chichester, England, pp 153-167

Svensson S, Toratti T (2002) Mechanical response of wood perpendicular to grain when subjected to changes of humidity. Wood Sci. Technol. 36:145-156

Toratti T, Svensson S (2000) Mechano-sorptive experiments perpendicular to grain under tensile and compressive loads. Wood Sci. Technol. 34:317-326

Virta J, Koponen S, Absetz I (2006) Measurement of swelling stresses in spruce (Picea abies) samples. Build. Environ. 41:1014-1018

PAPER IV

Effect of self-tapping screws on moisture induced stresses in glulam
Vanessa Angst and Kjell A. Malo
Submitted to Engineering Structures (2012)

Is not included due to copyright

APPENDIX A

Additional test results:
Glulam specimens subjected to wetting from 40 to ~100% RH
and drying from ~92 to 40% RH

APPENDIX A

Additional test results: Glulam specimens subjected to wetting from 40 to ~100% RH and drying from ~92 to 40% RH

Test program

In this appendix, additional test results on reinforced (using a SPAX screw) and unreinforced glulam specimens ($W*H*L$ = 90*270*90 mm^3) subjected to rather extreme wetting and drying exposure (one-dimensional) are presented and discussed. On the whole, the experiments correspond to previous studies performed by the present author (Angst and Malo 2012a, b) on glulam specimens subjected to wetting from 50 to 90% RH and drying from 90 to 50% RH. The main differences are the climate variation, which was more extreme in the present case, and the fact that only one point in time (12 d) was tested during climate exposure. The specimens used for the wetting analysis were seasoned in a climate chamber with 40% RH and subsequently placed in a box with water saturated air (~100% RH) for climate exposure. The specimens used for the drying analysis were seasoned in ~92% RH (climate chamber) and subsequently exposed to 40% RH (climate chamber). The RH's of the present study were selected to represent more extreme climate changes than the ones commonly measured in sheltered, unheated timber structures in Nordic countries (Ranta-Maunus 2003). The test program is summarised in Table A.1.

The experimental procedure for determining restrained strains, released strains, moisture contents (MC), moduli of elasticity (MOE) and hygroexpansion coefficients is described in detail in Angst and Malo (2012a). For the slightly adapted procedure in the case of screw reinforced specimens it is referred to Angst and Malo (2012b). However, in the present study, 3 of the 6 reinforced specimens in the wetting case (marked with * in Table A.1) were smaller than the others. After inserting the reinforcement screw, these specimens (with an original length of L = 90 mm) were diminished by removing a 22.5 mm thick slice from both the front and the back side, resulting in a reinforced specimen with L = 45 mm (in longitudinal direction). The objective with these specimens, in the

following named “reinforced s”, was to be able to perform the measurements closer to the screw.

Table A.1 Test program

Test series (measurements)	Seasoned in	Exposed to	Parallel specimens	Testing time
Restrained strain,	40% RH	~100% RH	3 unreinforced / 2×3=6* reinforced	12 d
released strain, MC	~92% RH	40% RH	3 unreinforced / 3 reinforced	12 d
Modulus of	40% RH	~100% RH	3	12 d
elasticity	~92% RH	40% RH	3	12d
Hygroexpansion	40% RH	~100% RH	3	At increasing
coefficient	~92% RH	40% RH	3	time intervals

* 3 are with smaller specimens, see text for explanations

Results and discussion

In the following the results from the present experiments are presented and discussed. Except for the moisture content, the results were assumed to be symmetric, thus the values from the same distance from the cross section centre (slices 1/9, slices 2/8, slices 3/7, slices 4/6) obtained from the cutting procedure described in Angst and Malo (2012a) were considered together. In this way, the mean values and the standard deviations were based on 6 measured values per slice.

Fig. A.1 shows the **moisture content** in the different slices of the reinforced and unreinforced specimens after 12 d of wetting and 12 d of drying. As expected, the distribution is symmetric. The standard deviation is minimal in the cross section centre (slice 5) and largest at the border of the cross section (slices 1 and 9), where the MC is very sensitive to changes in the surrounding climate. Such small changes are to be expected in the used climate chambers and even more in the saturated box used for the 100% RH.

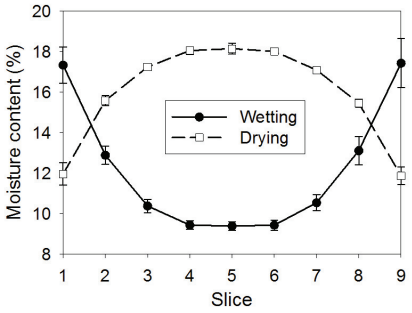

Fig. A.1 Mean moisture content distribution in wetting and drying specimens (whiskers = standard deviation)

Fig. A.2 shows the **restrained swelling and shrinkage strains**, which were measured on the front surface of the reinforced and unreinforced specimens after climate exposure. Although the standard deviation between parallel specimens is considerable, especially in the drying case, the effect of the screw is clearly visible. The screw prevents to a certain degree the glulam from swelling and shrinking. When comparing both reinforced specimens in the wetting case (reinforced / reinforced s), it can be noticed, that the effect is more pronounced the closer to the screw the strains are measured (as expected). However, the difference between both reinforced specimens is rather small, due to the fact that the effect of the screw decreases rapidly with increasing distance to the screw (Angst and Malo 2012b).

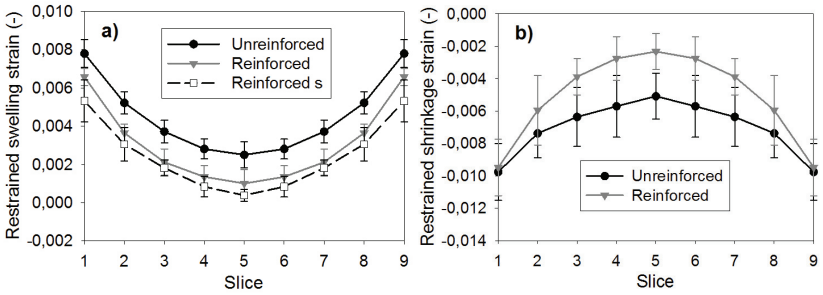

Fig. A.2 Mean restrained strains after a) 12 d of wetting and b) 12 d of drying (whiskers = standard deviation)

Fig. A.3 shows the **released strain** distribution of unreinforced and reinforced specimens. These strains together with the measured MOE values are in the following used to calculate the internal stresses. In reinforced specimens the released strains could not be evaluated in the cross section centre (slices 4, 5, 6) due to the presence of the screw.

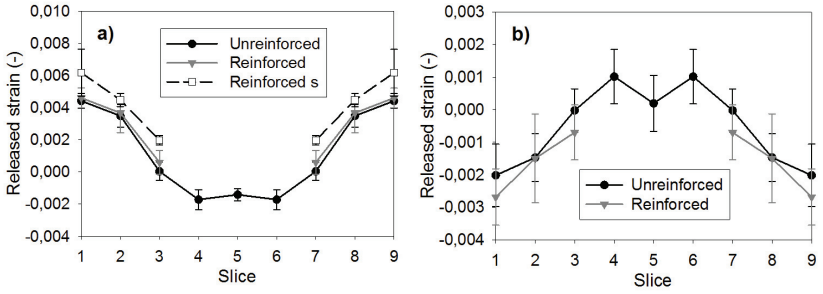

Fig. A.3 Mean released strains after a) wetting and b) drying (whiskers = standard deviation)

Fig. A.4 shows the distribution of the **effective MOE** (average in direction of the specimen height (or the slice length)) measured in wetting and drying specimens after 12 d of climate exposure. As expected, the values increase towards the cross section centre, due to the annual ring orientation: In the centre, mostly radial wood is present, exhibiting a MOE about twice the size of the MOE of tangential wood, which is primarily present at the cross section border (Dinwoodie 2000). The scatter between individual specimens is generally low, except for the central slices.

The figure suggests that the MOE values are affected by moisture: MOE increases with decreasing MC, which is according to usual assumption (Dinwoodie 2000). At the cross section border, the drying specimens exhibit lower MC values (~12%) than wetting specimens (~17%) and accordingly higher MOE values. In the cross section centre, the opposite is the case: The centre slices of drying specimens exhibit higher MC values (~18%) than wetting specimens (~9.5%), which correspondingly result in lower MOE values. These observations are in contrast to the findings in the previous study (Angst and Malo 2012a), where the effect of moisture was found negligible compared to the effect of geometrical configuration. One reason for this discrepancy could be the larger MC variations involved in the present case, which increase such effects. However, the effect of geometrical configuration, which was found to be pronounced in the previous

study, was not evaluated in the present case, thus the ratio between both effects (MC and geometrical configuration) is not known for the present study.

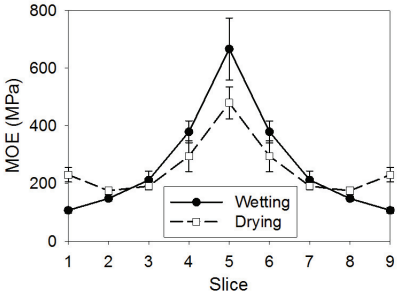

Fig. A.4 Mean effective modulus of elasticity after 12 d of wetting and drying (whiskers = standard deviation)

Fig. A.5 presents the **internal stresses**, calculated by means of the released strains (Fig. A.3) and the MOE's (Fig. A.4). Note that the mean values and the standard deviations are based on 6 measured strain and 3 measured MOE values per slice. In the figure also the characteristic tensile strength of glulam perpendicular to grain is depicted, which is 0.5 MPa according to prEN 14080 (2011). In the wetting case (Fig. A.5a) the internal tensile stresses in unreinforced specimens (ca. 1.0 MPa) clearly exceed the characteristic tensile strength. With a reinforcement in the specimen centre these stresses could be significantly decreased (Angst and Malo 2012b). However, the reinforcing screw causes larger stresses at the cross section border (slices 1/9), which – in the wetting case – concern compressive stresses and are thus not considered problematic, while – in the drying case – they concern tensile stresses. As can be noticed these tensile stresses exceed the characteristic tensile strength in reinforced specimens as opposed to the case in unreinforced specimens (Fig. A.5b). Thus, the reinforcing screw has a positive effect in wetting cases by reducing internal tensile stresses, while in drying cases, it increases tensile stresses at the border (owing to a more pronounced internal restraint). However, the present climate variations are rather large and for smaller, more realistic variations the tensile stresses during drying in reinforced specimens were not found to exceed the characteristic tensile strength (Angst and Malo 2012b).

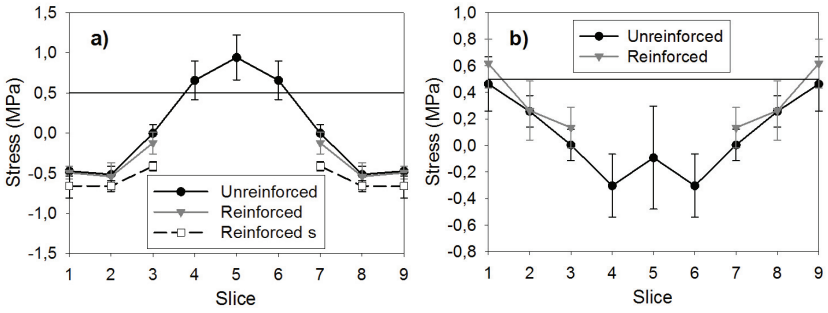

Fig. A.5 Mean internal stress distribution after 12 d of a) wetting and b) drying (whiskers = standard deviation)

Fig. A.6 shows the **free swelling and shrinkage strains** in the various slices of the specimen at different moisture contents. These hygroscopic strains correspond to the amount a slice expands or shrinks when it is not restrained during exposure to climate variations. Linear regression lines were fitted through the data points, whereby the slopes of the lines represent the effective hygroexpansion coefficients α in direction of the specimen height (or slice length). The expansion or shrinkage is smallest in the cross section centre (slice 5) and increases towards the cross section border (slices 2/8, 1/9), which is due to the annual ring orientation. The movement in the outer slices is determined by the hygroexpansion coefficient in tangential direction, which is about twice the size of the coefficient in radial direction, the latter being determinant for the inner slices.

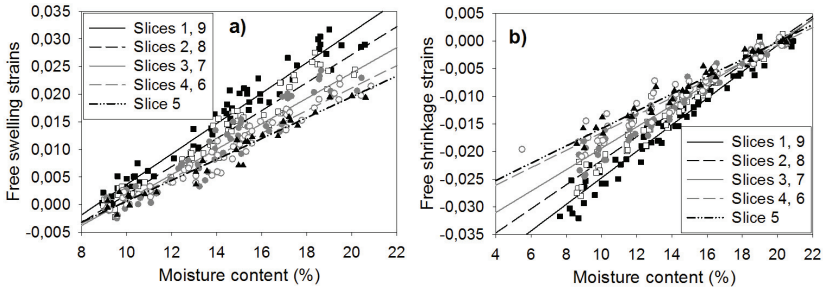

Fig. A.6 Hygroscopic strains during a) wetting and b) drying

The **hygroexpansion coefficients** in radial (α_R) and tangential (α_T) directions were evaluated by means of the same procedure as in the previous experimental study (Angst and Malo 2012a). The fitted coefficients for the present study are

presented in Table A.2 together with the results from the previous study. The comparison reveals two issues: First, according to both studies different hygroexpansion coefficients apply for the wetting and the drying case, whereby the coefficients are larger in the wetting case. The ratio between the coefficients in radial and tangential directions, however, is similar, being about 1:2. Secondly, the coefficients within one group (wetting or drying) are similar in both studies, although these were determined on different specimens using different climate variations.

Table A.2 Hygroexpansion coefficients

Hygroexpansion coefficients	Wetting	Drying
Present study	$\alpha_R = 0.17$, $\alpha_T = 0.34$	$\alpha_R = 0.14$, $\alpha_T = 0.28$
Previous study (Angst and Malo 2012a)	$\alpha_R = 0.15$, $\alpha_T = 0.32$	$\alpha_R = 0.14$, $\alpha_T = 0.26$

Summary and conclusions

The test results presented above, involving more extreme climate variations than those of the main experiments reported in this thesis, represent an additional data set, which might – for example – be used as a basis for numerical simulations of moisture induced stresses in glulam. Due to the more extreme climate variations applied in the present study compared to previous studies, certain effects were amplified and could thus be detected:

- An effect of moisture content on modulus of elasticity was found, namely that the MOE increases with decreasing MC. This is in agreement with the literature. This effect was not detected or negligible compared to other effects when smaller, however more realistic climate variations were applied.

- The screw reinforcement was found to increase the tensile stresses up to critical stresses (above characteristic tensile strength) at the cross section border during drying exposure. This effect was less pronounced when smaller climate variations were applied, so that the tensile stresses did not reach critical levels.

Moreover, the present experiments confirmed results from the previous study (Angst and Malo 2012a), namely that the hygroexpansion coefficients in cross-

grain directions are different for wetting and for drying. During wetting, larger hygroexpansion coefficients apply.

References

Angst V, Malo KA (2012a) The effect of climate variations on glulam - an experimental study. European Journal of Wood and Wood Products DOI 10.1007/s00107-012-0594-y

Angst V, Malo KA (2012b) Effect of self-tapping screws on moisture induced stresses in glulam. Submitted to Engineering Structures

Dinwoodie JM (2000) Timber - Its nature and behaviour (2nd ed.). E & FN SPON, London and New York

prEN 14080 (2011) Timber structures - Glued laminated timber and glued solid timber. European committee for standardization, Brussels

Ranta-Maunus A (2003) Effects of climate and climate variations on strength. In: Timber engineering. Thelandersson S, Larsen HJ (eds), John Wiley & Sons Ltd, Chichester, England, pp 153-167

APPENDIX B

Additional test results:
Glulam specimens subjected to cyclic climate variations between 90 – 50 – 90% RH

APPENDIX B

Additional test results: Glulam specimens subjected to cyclic climate variations between 90 – 50 – 90% RH

Test program

In this appendix, additional test results on reinforced (using SPAX screw) and unreinforced glulam specimens ($W*H*L$ = 90*270*90 mm^3) subjected to cyclic climate variations (one-dimensional) are presented and discussed. In contrast to other studies, e.g. (Jönsson 2004), the cyclic climate variations in the present case were not selected to be symmetric (for example a beam conditioned at 60% RH and cycling between 80 and 40% RH). For the present study, the glulam beams were not seasoned in a certain RH, but rather used in the condition they were at delivery from the manufacture, which corresponded to approximately 60% RH. Specimens were cut from the beams and stored in a closed box, in order to obtain a uniform moisture content (MC) distribution across the cross section width, before being subjected to wetting (90% RH) and drying (50% RH) cycles with 7 days interval. In this manner, the wetting cycles involved a larger climate gradient than the drying cycles.

The experimental procedure for determining restrained strain, released strain, and MC corresponds to the one described in detail in Angst and Malo (2012a), where single climate changes were studied. The slightly adapted procedure in the case of reinforced specimens is presented in Angst and Malo (2012b). The test program is summarised in Table B.1.

Table B.1 Test program

Test series (measurements)	Seasoned in	Exposed to	Parallel specimens	Testing time (days)
Restrained strain, released strain, MC	~60% RH	Cyclic: 90% and 50% RH	3 unreinforced / 3 reinforced	7^{w}, 14^{dr}, 21^{w}, 28^{dr}, 35^{w}, 42^{dr}

$^{w, dr}$ denote if the specimens are at the end of a wetting (w) or drying (dr) cycle at test time

Results and discussion

In the following, the results from the described experiments are presented and discussed. Except for the moisture content, the results were assumed to be symmetric, thus the values from the same distance from the cross section centre (slices 1/9, slices 2/8, slices 3/7, slices 4/6) obtained from the cutting procedure described in Angst and Malo (2012a) were considered together. In this way, the mean values and the standard deviations were based on 6 measured values per slice.

Fig. B.1 shows the **moisture content** in the different slices of the specimens after cycling between 90 and 50% RH. The distribution is fairly symmetric and the standard deviations are minimal, almost not visible at all. It can be noticed that the cycles mainly affect the outer two to three slices of the specimen (slices 1/9, 2/8, 3/7), whereas the inner parts are significantly less affected by the moisture variations. This same observation was already done by Jönsson (2004), who applied a cyclic climate change on unreinforced glulam specimens, starting with 60% RH and cycling between 40% and 80% RH with 7 days interval. Please also note that the MC in the inner parts of the specimen keeps increasing after a wetting cycle although the specimen is subjected to a drying cycle. Thus, there is a continuously increasing trend in MC in the cross section centre. This is not surprising since the difference from the original state (conditioned at 60% RH) to the wetting exposure (90% RH) is larger than the one to the drying exposure (50% RH).

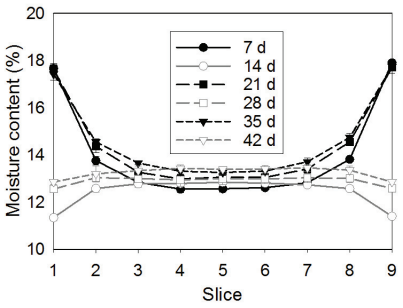

Fig. B.1 Mean moisture content distribution during cycling

Fig. B.2 shows the **restrained strain distribution** measured at the specimen surface after a) wetting cycles (7, 21, and 35 d) and b) drying cycles (14, 28, 42 d). The standard deviations are not depicted for reason of clarity but are considerable

ranging from 0.0002 up to 0.0012. The restrained swelling strains measured after wetting cycles exhibit a similar pattern as the strains in specimens exposed to single wetting changes (Angst and Malo 2012a, b): The reinforcing screw prevents to a certain degree the deformation of the glulam specimen. The strains measured after drying cycles in the present experiments differ from the strains in specimens exposed to single drying changes of earlier studies reported in this thesis (Angst and Malo 2012a, b). Due to the relatively small MC gradients during drying cycles and the increasing MC trend in the cross section centre (Fig. B.1), the strains are always positive, which means the specimens are swelling over time. However, the reinforcing screw has the same effect as during wetting cycles; namely inhibiting the dimensional changes in the timber.

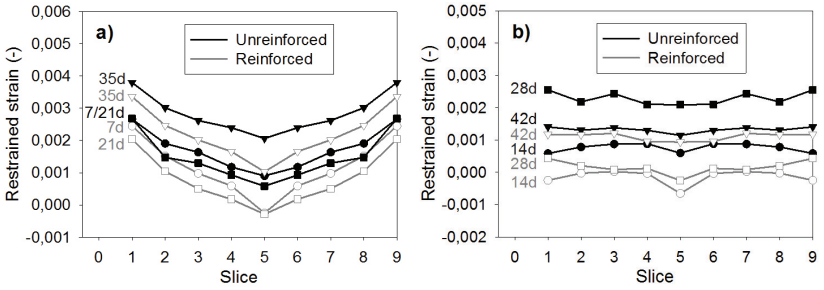

Fig. B.2 Mean restrained strains after a) wetting cycles and b) drying cycles

Fig. B.3 shows the **released strain distributions** after cyclic climate change. The standard deviations are again not depicted, but were below 0.0011 after wetting cycles (a) and below 0.0007 after drying cycles (b). In reinforced specimens the strains could not be evaluated in the inner slices (slices 4, 5, 6) due to the presence of the screw. The released strains are in the following used to calculate the internal stresses, in the same manner as previously reported (Angst and Malo 2012a).

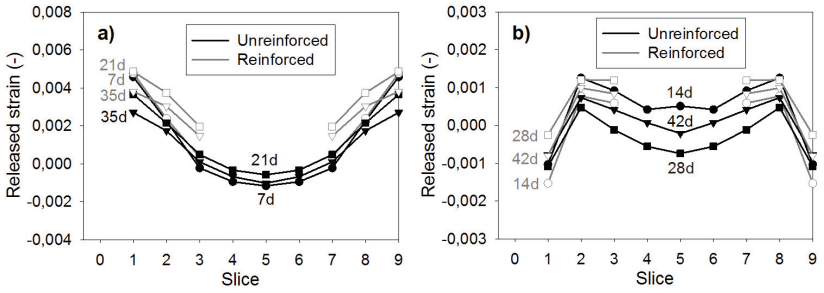

Fig. B.3 Mean released strains after a) wetting cycles and b) drying cycles

Fig. B.4 presents the internal stress distribution, calculated by means of the released strains (Fig. B.3) and the MOE's from Angst and Malo (2012a). Note that the mean values and the standard deviations are based on 6 measured strains and 24 measured MOE values per slice. The tensile stresses arising after both wetting and drying cycles are generally below 0.5 MPa, which is the characteristic tensile strength of glulam perpendicular to grain according to prEN 14080 (2011). The stresses are smaller than corresponding stresses after single wetting exposures, for example Angst and Malo (2012a). It is believed that due to the short cycles, no large stresses develop and that longer cycles would yield pronouncedly higher stresses, which is in accordance with Aicher and Dill-Langer (1997).

Due to the increasing trend in MC in the specimens, the stresses after drying cycles (Fig. B.4b) show a particular distribution: In the cross section centre, the stresses are tensile stresses (at 28 and 42 d), which is normally the case after wetting cycles, while at the cross section border, the stresses are also tensile stresses, this being according to the case after drying cycles. Thus, the main effect of the present drying cycles is to decrease the stresses in the centre; the cycles are not long enough (or the difference from the seasoned state (60% RH) to the drying climate (50% RH) is not high enough) for the stresses to become compressive stresses.

While the screw reinforcement clearly decreases the arising tensile stresses in the cross section centre, the effect of the reinforcing screw at the border is not clearly visible. After wetting cycles (Fig. B.4a), the reinforced specimens exhibit slightly larger (compressive) stresses at the cross section border, whereas after drying cycles (Fig. B.4b), the stresses in reinforced and unreinforced specimens can hardly be discerned.

Finally, as was already noticed by Jönsson (2004), time and number of cycles do not seem to affect the stress distribution in any specific direction, which means that there is no cumulative effect of repeated moisture cycling.

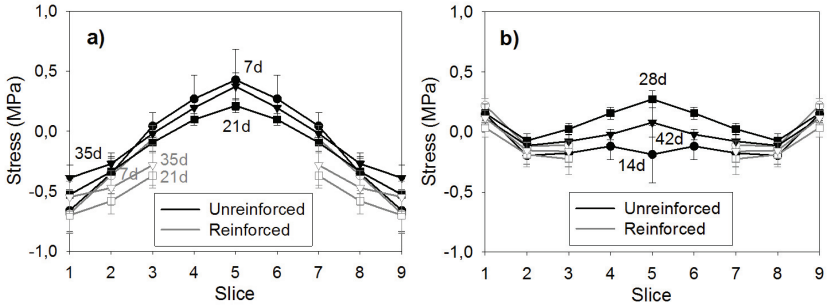

Fig. B.4 Mean internal stress after a) wetting cycles and b) drying cycles (symbols = mean values over cross section height, whiskers = standard deviations)

Summary and conclusions

The following conclusions are drawn from the test results presented above involving "skewed" cyclic climate variations (seasoned at 60% RH, wetting at 90% RH, drying at 50% RH):

- The short cycles of 7 day intervals result in rather small tensile stresses, which are generally below the characteristic tensile strength of glulam perpendicular to grain
- Owing to the skewed cyclic climate variations of the present case, the central parts of the specimens are always in a "wetting phase". The MC increases continuously although the specimens are repeatedly subjected to drying, and the stresses in the specimen centre are also tensile stresses after drying cycles
- The stresses are – as in the case of single climate changes – larger after wetting cycles than after drying cycles. This is also in agreement with other studies involving "symmetric" cyclic climate variations (Aicher and Dill-Langer 1997; Jönsson 2004)
- In correspondence to previous findings (Jönsson 2004), no cumulative effect of repeated moisture cycling was found

References

Aicher S, Dill-Langer G (1997) Climate induced stresses perpendicular to the grain in glulam. Otto-Graf-Journal 8:209-231

Angst V, Malo KA (2012a) The effect of climate variations on glulam - an experimental study. European Journal of Wood and Wood Products DOI 10.1007/s00107-012-0594-y

Angst V, Malo KA (2012b) Effect of self-tapping screws on moisture induced stresses in glulam. Submitted to Engineering Structures

prEN 14080 (2011) Timber structures - Glued laminated timber and glued solid timber. European committee for standardization, Brussels

Jönsson J (2004) Internal stresses in the cross-grain direction in glulam induced by climate variations. Holzforschung 58:154-159

DEPARTMENT OF STRUCTURAL ENGINEERING
NORWEGIAN UNIVERSITY OF SCIENCE AND TECHNOLOGY

N–7491 TRONDHEIM, NORWAY
Telephone: +47 73 59 47 00 Telefax: +47 73 59 47 01

"Reliability Analysis of Structural Systems using Nonlinear Finite Element Methods",
C. A. Holm, 1990:23, ISBN 82-7119-178-0.

"Uniform Stratified Flow Interaction with a Submerged Horizontal Cylinder",
Ø. Arntsen, 1990:32, ISBN 82-7119-188-8.

"Large Displacement Analysis of Flexible and Rigid Systems Considering Displacement-Dependent Loads and Nonlinear Constraints",
K. M. Mathisen, 1990:33, ISBN 82-7119-189-6.

"Solid Mechanics and Material Models including Large Deformations",
E. Levold, 1990:56, ISBN 82-7119-214-0, ISSN 0802-3271.

"Inelastic Deformation Capacity of Flexurally-Loaded Aluminium Alloy Structures",
T. Welo, 1990:62, ISBN 82-7119-220-5, ISSN 0802-3271.

"Visualization of Results from Mechanical Engineering Analysis",
K. Aamnes, 1990:63, ISBN 82-7119-221-3, ISSN 0802-3271.

"Object-Oriented Product Modeling for Structural Design",
S. I. Dale, 1991:6, ISBN 82-7119-258-2, ISSN 0802-3271.

"Parallel Techniques for Solving Finite Element Problems on Transputer Networks",
T. H. Hansen, 1991:19, ISBN 82-7119-273-6, ISSN 0802-3271.

"Statistical Description and Estimation of Ocean Drift Ice Environments",
R. Korsnes, 1991:24, ISBN 82-7119-278-7, ISSN 0802-3271.

“Properties of concrete related to fatigue damage: with emphasis on high strength concrete”,
G. Petkovic, 1991:35, ISBN 82-7119-290-6, ISSN 0802-3271.

"Turbidity Current Modelling",
B. Brørs, 1991:38, ISBN 82-7119-293-0, ISSN 0802-3271.

"Zero-Slump Concrete: Rheology, Degree of Compaction and Strength. Effects of Fillers as Part Cement-Replacement",
C. Sørensen, 1992:8, ISBN 82-7119-357-0, ISSN 0802-3271.

"Nonlinear Analysis of Reinforced Concrete Structures Exposed to Transient Loading",
K. V. Høiseth, 1992:15, ISBN 82-7119-364-3, ISSN 0802-3271.

"Finite Element Formulations and Solution Algorithms for Buckling and Collapse Analysis of Thin Shells",
R. O. Bjærum, 1992:30, ISBN 82-7119-380-5, ISSN 0802-3271.

"Response Statistics of Nonlinear Dynamic Systems",
J. M. Johnsen, 1992:42, ISBN 82-7119-393-7, ISSN 0802-3271.

"Digital Models in Engineering. A Study on why and how engineers build and operate digital models for decisison support",
J. Høyte, 1992:75, ISBN 82-7119-429-1, ISSN 0802-3271.

"Sparse Solution of Finite Element Equations",
A. C. Damhaug, 1992:76, ISBN 82-7119-430-5, ISSN 0802-3271.

"Some Aspects of Floating Ice Related to Sea Surface Operations in the Barents Sea",
S. Løset, 1992:95, ISBN 82-7119-452-6, ISSN 0802-3271.

"Modelling of Cyclic Plasticity with Application to Steel and Aluminium Structures",
O. S. Hopperstad, 1993:7, ISBN 82-7119-461-5, ISSN 0802-3271.

"The Free Formulation: Linear Theory and Extensions with Applications to Tetrahedral Elements with Rotational Freedoms",
G. Skeie, 1993:17, ISBN 82-7119-472-0, ISSN 0802-3271.

"Høyfast betongs motstand mot piggdekkslitasje. Analyse av resultater fra prøving i Veisliter'n",
T. Tveter, 1993:62, ISBN 82-7119-522-0, ISSN 0802-3271.

"A Nonlinear Finite Element Based on Free Formulation Theory for Analysis of Sandwich Structures",
O. Aamlid, 1993:72, ISBN 82-7119-534-4, ISSN 0802-3271.

"The Effect of Curing Temperature and Silica Fume on Chloride Migration and Pore Structure of High Strength Concrete",
C. J. Hauck, 1993:90, ISBN 82-7119-553-0, ISSN 0802-3271.

"Failure of Concrete under Compressive Strain Gradients",
G. Markeset, 1993:110, ISBN 82-7119-575-1, ISSN 0802-3271.

"An experimental study of internal tidal amphidromes in Vestfjorden",
J. H. Nilsen, 1994:39, ISBN 82-7119-640-5, ISSN 0802-3271.

"Structural analysis of oil wells with emphasis on conductor design",
H. Larsen, 1994:46, ISBN 82-7119-648-0, ISSN 0802-3271.

"Adaptive methods for non-linear finite element analysis of shell structures",
K. M. Okstad, 1994:66, ISBN 82-7119-670-7, ISSN 0802-3271.

"On constitutive modelling in nonlinear analysis of concrete structures",
O. Fyrileiv, 1994:115, ISBN 82-7119-725-8, ISSN 0802-3271.

"Fluctuating wind load and response of a line-like engineering structure with emphasis on motion-induced wind forces",
J. Bogunovic Jakobsen, 1995:62, ISBN 82-7119-809-2, ISSN 0802-3271.

"An experimental study of beam-columns subjected to combined torsion, bending and axial actions",
A. Aalberg, 1995:66, ISBN 82-7119-813-0, ISSN 0802-3271.

"Scaling and cracking in unsealed freeze/thaw testing of Portland cement and silica fume concretes",
S. Jacobsen, 1995:101, ISBN 82-7119-851-3, ISSN 0802-3271.

"Damping of water waves by submerged vegetation. A case study of laminaria hyperborea",
A. M. Dubi, 1995:108, ISBN 82-7119-859-9, ISSN 0802-3271.

"The dynamics of a slope current in the Barents Sea",
Sheng Li, 1995:109, ISBN 82-7119-860-2, ISSN 0802-3271.

"Modellering av delmaterialenes betydning for betongens konsistens",
Ernst Mørtsell, 1996:12, ISBN 82-7119-894-7, ISSN 0802-3271.

"Bending of thin-walled aluminium extrusions",
Birgit Søvik Opheim, 1996:60, ISBN 82-7119-947-1, ISSN 0802-3271.

"Material modelling of aluminium for crashworthiness analysis",
Torodd Berstad, 1996:89, ISBN 82-7119-980-3, ISSN 0802-3271.

"Estimation of structural parameters from response measurements on submerged floating tunnels",
Rolf Magne Larssen, 1996:119, ISBN 82-471-0014-2, ISSN 0802-3271.

“Numerical modelling of plain and reinforced concrete by damage mechanics”,
Mario A. Polanco-Loria, 1997:20, ISBN 82-471-0049-5, ISSN 0802-3271.

“Nonlinear random vibrations - numerical analysis by path integration methods”,
Vibeke Moe, 1997:26, ISBN 82-471-0056-8, ISSN 0802-3271.

“Numerical prediction of vortex-induced vibration by the finite element method”,
Joar Martin Dalheim, 1997:63, ISBN 82-471-0096-7, ISSN 0802-3271.

“Time domain calculations of buffeting response for wind sensitive structures”,
Ketil Aas-Jakobsen, 1997:148, ISBN 82-471-0189-0, ISSN 0802-3271.

"A numerical study of flow about fixed and flexibly mounted circular cylinders",
Trond Stokka Meling, 1998:48, ISBN 82-471-0244-7, ISSN 0802-3271.

“Estimation of chloride penetration into concrete bridges in coastal areas”,
Per Egil Steen, 1998:89, ISBN 82-471-0290-0, ISSN 0802-3271.

“Stress-resultant material models for reinforced concrete plates and shells”,
Jan Arve Øverli, 1998:95, ISBN 82-471-0297-8, ISSN 0802-3271.

“Chloride binding in concrete. Effect of surrounding environment and concrete composition”,
Claus Kenneth Larsen, 1998:101, ISBN 82-471-0337-0, ISSN 0802-3271.

“Rotational capacity of aluminium alloy beams”,
Lars A. Moen, 1999:1, ISBN 82-471-0365-6, ISSN 0802-3271.

“Stretch Bending of Aluminium Extrusions”,
Arild H. Clausen, 1999:29, ISBN 82-471-0396-6, ISSN 0802-3271.

“Aluminium and Steel Beams under Concentrated Loading”,
Tore Tryland, 1999:30, ISBN 82-471-0397-4, ISSN 0802-3271.

"Engineering Models of Elastoplasticity and Fracture for Aluminium Alloys",
Odd-Geir Lademo, 1999:39, ISBN 82-471-0406-7, ISSN 0802-3271.

"Kapasitet og duktilitet av dybelforbindelser i trekonstruksjoner",
Jan Siem, 1999:46, ISBN 82-471-0414-8, ISSN 0802-3271.

“Etablering av distribuert ingeniørarbeid; Teknologiske og organisatoriske erfaringer fra en norsk ingeniørbedrift”,
Lars Line, 1999:52, ISBN 82-471-0420-2, ISSN 0802-3271.

“Estimation of Earthquake-Induced Response”,
Símon Ólafsson, 1999:73, ISBN 82-471-0443-1, ISSN 0802-3271.

“Coastal Concrete Bridges: Moisture State, Chloride Permeability and Aging Effects”
Ragnhild Holen Relling, 1999:74, ISBN 82-471-0445-8, ISSN 0802-3271.

”Capacity Assessment of Titanium Pipes Subjected to Bending and External Pressure”,
Arve Bjørset, 1999:100, ISBN 82-471-0473-3, ISSN 0802-3271.

“Validation of Numerical Collapse Behaviour of Thin-Walled Corrugated Panels”,
Håvar Ilstad, 1999:101, ISBN 82-471-0474-1, ISSN 0802-3271.

“Strength and Ductility of Welded Structures in Aluminium Alloys”,
Miroslaw Matusiak, 1999:113, ISBN 82-471-0487-3, ISSN 0802-3271.

“Thermal Dilation and Autogenous Deformation as Driving Forces to Self-Induced Stresses in High Performance Concrete”,
Øyvind Bjøntegaard, 1999:121, ISBN 82-7984-002-8, ISSN 0802-3271.

“Some Aspects of Ski Base Sliding Friction and Ski Base Structure”,
Dag Anders Moldestad, 1999:137, ISBN 82-7984-019-2, ISSN 0802-3271.

"Electrode reactions and corrosion resistance for steel in mortar and concrete",
Roy Antonsen, 2000:10, ISBN 82-7984-030-3, ISSN 0802-3271.

"Hydro-Physical Conditions in Kelp Forests and the Effect on Wave Damping and Dune Erosion. A case study on Laminaria Hyperborea",
Stig Magnar Løvås, 2000:28, ISBN 82-7984-050-8, ISSN 0802-3271.

"Random Vibration and the Path Integral Method",
Christian Skaug, 2000:39, ISBN 82-7984-061-3, ISSN 0802-3271.

"Buckling and geometrical nonlinear beam-type analyses of timber structures",
Trond Even Eggen, 2000:56, ISBN 82-7984-081-8, ISSN 0802-3271.

”Structural Crashworthiness of Aluminium Foam-Based Components”,
Arve Grønsund Hanssen, 2000:76, ISBN 82-7984-102-4, ISSN 0809-103X.

“Measurements and simulations of the consolidation in first-year sea ice ridges, and some aspects of mechanical behaviour”,
Knut V. Høyland, 2000:94, ISBN 82-7984-121-0, ISSN 0809-103X.

”Kinematics in Regular and Irregular Waves based on a Lagrangian Formulation”,
Svein Helge Gjøsund, 2000-86, ISBN 82-7984-112-1, ISSN 0809-103X.

”Self-Induced Cracking Problems in Hardening Concrete Structures”,
Daniela Bosnjak, 2000-121, ISBN 82-7984-151-2, ISSN 0809-103X.

"Ballistic Penetration and Perforation of Steel Plates",
Tore Børvik, 2000:124, ISBN 82-7984-154-7, ISSN 0809-103X.

"Freeze-Thaw resistance of Concrete. Effect of: Curing Conditions, Moisture Exchange and Materials",
Terje Finnerup Rønning, 2001:14, ISBN 82-7984-165-2, ISSN 0809-103X

Structural behaviour of post tensioned concrete structures. Flat slab. Slabs on ground",
Steinar Trygstad, 2001:52, ISBN 82-471-5314-9, ISSN 0809-103X.

"Slipforming of Vertical Concrete Structures. Friction between concrete and slipform panel",
Kjell Tore Fosså, 2001:61, ISBN 82-471-5325-4, ISSN 0809-103X.

"Some numerical methods for the simulation of laminar and turbulent incompressible flows",
Jens Holmen, 2002:6, ISBN 82-471-5396-3, ISSN 0809-103X.

“Improved Fatigue Performance of Threaded Drillstring Connections by Cold Rolling”,
Steinar Kristoffersen, 2002:11, ISBN: 82-421-5402-1, ISSN 0809-103X.

"Deformations in Concrete Cantilever Bridges: Observations and Theoretical Modelling",
Peter F. Takâcs, 2002:23, ISBN 82-471-5415-3, ISSN 0809-103X.

"Stiffened aluminium plates subjected to impact loading",
Hilde Giæver Hildrum, 2002:69, ISBN 82-471-5467-6, ISSN 0809-103X.

"Full- and model scale study of wind effects on a medium-rise building in a built up area",
Jónas Thór Snæbjørnsson, 2002:95, ISBN82-471-5495-1, ISSN 0809-103X.

"Evaluation of Concepts for Loading of Hydrocarbons in Ice-infested water",
Arnor Jensen, 2002:114, ISBN 82-417-5506-0, ISSN 0809-103X.

"Numerical and Physical Modelling of Oil Spreading in Broken Ice",
Janne K. Økland Gjøsteen, 2002:130, ISBN 82-471-5523-0, ISSN 0809-103X.

"Diagnosis and protection of corroding steel in concrete",
Franz Pruckner, 20002:140, ISBN 82-471-5555-4, ISSN 0809-103X.

"Tensile and Compressive Creep of Young Concrete: Testing and Modelling",
Dawood Atrushi, 2003:17, ISBN 82-471-5565-6, ISSN 0809-103X.

"Rheology of Particle Suspensions. Fresh Concrete, Mortar and Cement Paste with Various Types of Lignosulfonates",
Jon Elvar Wallevik, 2003:18, ISBN 82-471-5566-4, ISSN 0809-103X.

"Oblique Loading of Aluminium Crash Components",
Aase Reyes, 2003:15, ISBN 82-471-5562-1, ISSN 0809-103X.

"Utilization of Ethiopian Natural Pozzolans",
Surafel Ketema Desta, 2003:26, ISSN 82-471-5574-5, ISSN:0809-103X.

"Behaviour and strength prediction of reinforced concrete structures with discontinuity regions",
Helge Brå, 2004:11, ISBN 82-471-6222-9, ISSN 1503-8181.

"High-strength steel plates subjected to projectile impact. An experimental and numerical study",
Sumita Dey, 2004:38, ISBN 82-471-6282-2 (printed version), ISBN 82-471-6281-4 (electronic version), ISSN 1503-8181.

"Alkali-reactive and inert fillers in concrete. Rheology of fresh mixtures and expansive reactions."
Bård M. Pedersen, 2004:92, ISBN 82-471-6401-9 (printed version), ISBN 82-471-6400-0 (electronic version), ISSN 1503-8181.

"On the Shear Capacity of Steel Girders with Large Web Openings".
Nils Christian Hagen, 2005:9 ISBN 82-471-6878-2 (printed version), ISBN 82-471-6877-4 (electronic version), ISSN 1503-8181.

”Behaviour of aluminium extrusions subjected to axial loading”.
Østen Jensen, 2005:7, ISBN 82-471-6873-1 (printed version), ISBN 82-471-6872-3 (electronic version), ISSN 1503-8181.

”Thermal Aspects of corrosion of Steel in Concrete”.
Jan-Magnus Østvik, 2005:5, ISBN 82-471-6869-3 (printed version), ISBN 82-471-6868 (electronic version), ISSN 1503-8181.

”Mechanical and adaptive behaviour of bone in relation to hip replacement.” A study of bone remodelling and bone grafting.
Sébastien Muller, 2005:34, ISBN 82-471-6933-9 (printed version), ISBN 82-471-6932-0 (electronic version), ISSN 1503-8181.

“Analysis of geometrical nonlinearities with applications to timber structures”.
Lars Wollebæk, 2005:74, ISBN 82-471-7050-5 (printed version), ISBN 82-471-7019-1 (electronic version), ISSN 1503-8181.

“Pedestrian induced lateral vibrations of slender footbridges”,
Anders Rönnquist, 2005:102, ISBN 82-471-7082-5 (printed version), ISBN 82-471-7081-7 (electronic version), ISSN 1503-8181.

“Initial Strength Development of Fly Ash and Limestone Blended Cements at Various Temperatures Predicted by Ultrasonic Pulse Velocity”,
Tom Ivar Fredvik, 2005:112, ISBN 82-471-7105-8 (printed version), ISBN 82-471-7103-1 (electronic version), ISSN 1503-8181.

“Behaviour and modelling of thin-walled cast components”,
Cato Dørum, 2005:128, ISBN 82-471-7140-6 (printed version), ISBN 82-471-7139-2 (electronic version), ISSN 1503-8181.

“Behaviour and modelling of selfpiercing riveted connections”,
Raffaele Porcaro, 2005:165, ISBN 82-471-7219-4 (printed version), ISBN 82-471-7218-6 (electronic version), ISSN 1503-8181.

”Behaviour and Modelling og Aluminium Plates subjected to Compressive Load”,
Lars Rønning, 2005:154, ISBN 82-471-7169-1 (printed version), ISBN 82-471-7195-3 (electronic version), ISSN 1503-8181.

”Bumper beam-longitudinal system subjected to offset impact loading”,
Satyanarayana Kokkula, 2005:193, ISBN 82-471-7280-1 (printed version), ISBN 82-471-7279-8 (electronic version), ISSN 1503-8181.

“Control of Chloride Penetration into Concrete Structures at Early Age”,
Guofei Liu, 2006:46, ISBN 82-471-7838-9 (printed version), ISBN 82-471-7837-0 (electronic version), ISSN 1503-8181.

“Modelling of Welded Thin-Walled Aluminium Structures”,
Ting Wang, 2006:78, ISBN 82-471-7907-5 (printed version), ISBN 82-471-7906-7 (electronic version), ISSN 1503-8181.

”Time-variant reliability of dynamic systems by importance sampling and probabilistic analysis of ice loads”,
Anna Ivanova Olsen, 2006:139, ISBN 82-471-8041-3 (printed version), ISBN 82-471-8040-5 (electronic version), ISSN 1503-8181.

“Fatigue life prediction of an aluminium alloy automotive component using finite element analysis of surface topography”.
Sigmund Kyrre Ås, 2006:25, ISBN 82-471-7791-9 (printed version), ISBN 82-471-7791-9 (electronic version), ISSN 1503-8181.

”Constitutive models of elastoplasticity and fracture for aluminium alloys under strain path change”,
Dasharatha Achani, 2006:76, ISBN 82-471-7903-2 (printed version), ISBN 82-471-7902-4 (electronic version), ISSN 1503-8181.

“Simulations of 2D dynamic brittle fracture by the Element-free Galerkin method and linear fracture mechanics”,
Tommy Karlsson, 2006:125, ISBN 82-471-8011-1 (printed version), ISBN 82-471-8010-3 (electronic version), ISSN 1503-8181.

“Penetration and Perforation of Granite Targets by Hard Projectiles”,
Chong Chiang Seah, 2006:188, ISBN 82-471-8150-9 (printed version), ISBN 82-471-8149-5 (electronic version), ISSN 1503-8181.

“Deformations, strain capacity and cracking of concrete in plastic and early hardening phases”,
Tor Arne Hammer, 2007:234, ISBN 978-82-471-5191-4 (printed version), ISBN 978-82-471-5207-2 (electronic version), ISSN 1503-8181.

“Crashworthiness of dual-phase high-strength steel: Material and Component behaviour”,
Venkatapathi Tarigopula, 2007:230, ISBN 82-471-5076-4 (printed version), ISBN 82-471-5093-1 (electronic version), ISSN 1503-8181.

“Fibre reinforcement in load carrying concrete structures”,
Åse Lyslo Døssland, 2008:50, ISBN 978-82-471-6910-0 (printed version), ISBN 978-82-471-6924-7 (electronic version), ISSN 1503-8181.

“Low-velocity penetration of aluminium plates”,
Frode Grytten, 2008:46, ISBN 978-82-471-6826-4 (printed version), ISBN 978-82-471-6843-1 (electronic version), ISSN 1503-8181.

“Robustness studies of structures subjected to large deformations”,
Ørjan Fyllingen, 2008:24, ISBN 978-82-471-6339-9 (printed version), ISBN 978-82-471-6342-9 (electronic version), ISSN 1503-8181.

"Constitutive modelling of morsellised bone",
Knut Birger Lunde, 2008:92, ISBN 978-82-471-7829-4 (printed version), ISBN 978-82-471-7832-4 (electronic version), ISSN 1503-8181.

"Experimental Investigations of Wind Loading on a Suspension Bridge Girder",
Bjørn Isaksen, 2008:131, ISBN 978-82-471-8656-5 (printed version), ISBN 978-82-471-8673-2 (electronic version), ISSN 1503-8181.

"Cracking Risk of Concrete Structures in The Hardening Phase",
Guomin Ji, 2008:198, ISBN 978-82-471-1079-9 (printed version), ISBN 978-82-471-1080-5 (electronic version), ISSN 1503-8181.

"Modelling and numerical analysis of the porcine and human mitral apparatus",
Victorien Emile Prot, 2008:249, ISBN 978-82-471-1192-5 (printed version), ISBN 978-82-471-1193-2 (electronic version), ISSN 1503-8181.

"Strength analysis of net structures",
Heidi Moe, 2009:48, ISBN 978-82-471-1468-1 (printed version), ISBN 978-82-471-1469-8 (electronic version), ISSN1503-8181.

"Numerical analysis of ductile fracture in surface cracked shells",
Espen Berg, 2009:80, ISBN 978-82-471-1537-4 (printed version), ISBN 978-82-471-1538-1 (electronic version), ISSN 1503-8181.

"Subject specific finite element analysis of bone – for evaluation of the healing of a leg lengthening and evaluation of femoral stem design",
Sune Hansborg Pettersen, 2009:99, ISBN 978-82-471-1579-4 (printed version), ISBN 978-82-471-1580-0 (electronic version), ISSN 1503-8181.

"Evaluation of fracture parameters for notched multi-layered structures",
Lingyun Shang, 2009:137, ISBN 978-82-471-1662-3 (printed version), ISBN 978-82-471-1663-0 (electronic version), ISSN 1503-8181.

"Modelling of Dynamic Material Behaviour and Fracture of Aluminium Alloys for Structural Applications"
Yan Chen, 2009:69, ISBN 978-82-471-1515-2 (printed version), ISBN 978-82 471-1516-9 (electronic version), ISSN 1503-8181.

"Nanomechanics of polymer and composite particles"
Jianying He 2009:213, ISBN 978-82-471-1828-3 (printed version), ISBN 978-82-471-1829-0 (electronic version), ISSN 1503-8181.

"Mechanical properties of clear wood from Norway spruce"
Kristian Berbom Dahl 2009:250, ISBN 978-82-471-1911-2 (printed version) ISBN 978-82-471-1912-9 (electronic version), ISSN 1503-8181.

"Modeling of the degradation of TiB_2 mechanical properties by residual stresses and liquid Al penetration along grain boundaries"
Micol Pezzotta 2009:254, ISBN 978-82-471-1923-5 (printed version) ISBN 978-82-471-1924-2 (electronic version) ISSN 1503-8181.

"Effect of welding residual stress on fracture"
Xiabo Ren 2010:77, ISBN 978-82-471-2115-3 (printed version) ISBN 978-82-471-2116-0 (electronic version), ISSN 1503-8181.

"Pan-based carbon fiber as anode material in cathodic protection system for concrete structures" Mahdi Chini 2010:122, ISBN 978-82-471-2210-5 (printed version) ISBN 978-82-471-2213-6 (electronic version), ISSN 1503-8181.

"Structural Behaviour of deteriorated and retrofitted concrete structures" Irina Vasililjeva Sæther 2010:171, ISBN 978-82-471-2315-7 (printed version) ISBN 978-82-471-2316-4 (electronic version) ISSN 1503-8181.

"Prediction of local snow loads on roofs" Vivian Meløysund 2010:247, ISBN 978-82-471-2490-1 (printed version) ISBN 978-82-471-2491-8 (electronic version) ISSN 1503-8181.

"Behaviour and modelling of polymers for crash applications" Virgile Delhaye 2010:251, ISBN 978-82-471-2501-4 (printed version) ISBN 978-82-471-2502-1 (electronic version) ISSN 1503-8181.

"Blended cement with reducted CO_2 emission – Utilizing the Fly Ash-Limestone Synergy", Klaartje De Weerdt 2011:32, ISBN 978-82-471-2584-7 (printed version) ISBN 978-82-471-2584-4 (electronic version) ISSN 1503-8181.

"Chloride induced reinforcement corrosion in concrete" Concept of critical chloride content – methods and mechanisms. Ueli Angst 2011:113, ISBN 978-82-471-2769-9 (printed version) ISBN 978-82-471-2763-6 (electronic version) ISSN 1503-8181.

"A thermo-electric-Mechanical study of the carbon anode and contact interface for Energy savings in the production of aluminium". Dag Herman Andersen 2011:157, ISBN 978-82-471-2859-6 (printed version) ISBN 978-82-471-2860-2 (electronic version) ISSN 1503-8181.

"Structural Capacity of Anchorage Ties in Masonry Veneer Walls Subjected toEarthquake". The implications of Eurocode 8 and Eurocode 6 on a typical Norwegain veneer wall. Ahmed Mohamed Yousry Hamed 2011:181, ISBN 978-82-471-2911-1 (printed version) ISBN 978-82-471-2912-8 (electronic ver.) ISSN 1503-8181.

"Work-hardening behaviour in age-hardenable Al-Zn-Mg(-Cu) alloys". Ida Westermann , 2011:247, ISBN 978-82-471-3056-8 (printed ver.) ISBN 978-82-471-3057-5 (electronic ver.) ISSN 1503-8181.

"Behaviour and modelling of selfpiercing riveted connections using aluminium rivets". Nguyen-Hieu Hoang, 2011:266, ISBN 978-82-471-3097-1 (printed ver.) ISBN 978-82-471-3099-5 (electronic ver.) ISSN 1503-8181. ISSN 1503-8181.

“Fibre reinforced concrete”. Sindre Sandbakk, 2011:297, ISBN 978-82-471-3167-1 (printed ver.) ISBN 978-82-471-3168-8 (electronic ver) ISSN 1503:8181.

“Dynamic behaviour of cablesupported bridges subjected to strong natural wind”. Ole Andre Øiseth, 2011:315, ISBN 978-82-471-3209-8 (printed ver.) ISBN 978-82-471-3210-4 (electronic ver.) ISSN 1503-8181.

“Constitutive modeling of solargrade silicon materials” Julien Cochard, 2011:307, ISBN 978-82-471-3189-3 (printed ver). ISBN 978-82-471-3190-9 (electronic ver.) ISSN 1503-8181.

“Constitutive behavior and fracture of shape memory alloys” Jim Stian Olsen, 2012:57, ISBN 978-82-471-3382-8 (printed ver.) ISBN 978-82-471-3383-5 (electronic ver.) ISSN 1503-8181.

“Field measurements in mechanical testing using close-range photogrammetry and digital image analysis” Egil Fagerholt, 2012:95, ISBN 978-82-471-3466-5 (printed ver.) ISBN 978-82-471-3467-2 (electronic ver.) ISSN 1503-8181.

“Towards a better understanding of the ultimate behaviour of lightweight aggregate concrete in compression and bending”, Håvard Nedrelid, 2012:123, ISBN 978-82-471-3527-3 (printed ver.) ISBN 978-82-471-3528-0 (electronic ver.) ISSN 1503-8181.

“Numerical simulations of blood flow in the left side of the heart” Sigrid Kaarstad Dahl, 2012:135, ISBN 978-82-471-3553-2 (printed ver.) ISBN 978-82-471-3555-6 (electronic ver.) ISSN 1503-8181.